INFORMATION TO USERS

This manuscript has been reproduced from the microfilm master. UMI films the text directly from the original or copy submitted. Thus, some thesis and dissertation copies are in typewriter face, while others may be from any type of computer printer.

The quality of this reproduction is dependent upon the quality of the copy submitted. Broken or indistinct print, colored or poor quality illustrations and photographs, print bleedthrough, substandard margins, and improper alignment can adversely affect reproduction.

In the unlikely event that the author did not send UMI a complete manuscript and there are missing pages, these will be noted. Also, if unauthorized copyright material had to be removed, a note will indicate the deletion.

Oversize materials (e.g., maps, drawings, charts) are reproduced by sectioning the original, beginning at the upper left-hand corner and continuing from left to right in equal sections with small overlaps. Each original is also photographed in one exposure and is included in reduced form at the back of the book.

Photographs included in the original manuscript have been reproduced xerographically in this copy. Higher quality 6" x 9" black and white photographic prints are available for any photographs or illustrations appearing in this copy for an additional charge. Contact UMI directly to order.

UMI

A Bell & Howell Information Company
300 North Zeeb Road, Ann Arbor MI 48106-1346 USA
313/761-4700 800/521-0600

VIBRATIONAL CIRCULAR DICHROISM OF GRAMICIDIN: CONFORMATIONAL STUDIES IN LIPID BILAYER AND ORGANIC SOLVENT.

BY

ISMAILU O. AGBAJE

A dissertation submitted to the Graduate Faculty in Biochemistry in partial fulfillment of the requirements for the degree of Doctor of Philosophy, The City University of New York.

1996

This manuscript has been read and accepted for the Graduate Faculty in Biochemistry in satisfaction of the dissertation requirement for the degree of Doctor of Philosophy.

July 29, 96
Date

Chair of Examining Committee

August 5, 1996
Date

Executive Officer

Supervisory Committee

The City University of New York

ABSTRACT

VIBRATIONAL CIRCULAR DICHROISM: CONFORMATIONAL STUDIES OF GRAMICIDIN IN LIPID BILAYER AND ORGANIC SOLVENT

By

Ismailu O. Agbaje

Adviser: Professor Max Diem

In this dissertation we report the first vibrational circular dichroism of gramicidin (GA) in a model lipid bilayer, dimyristoylphosphatidylcholine (DMPC), as well as in an organic solvent (pyridine). Our findings reveal that gramicidin is inserted into the bilayer as an extended left-handed $\beta^{6.3}$-helix, which is believed to be the ion conducting dimer that is arranged in an N- to -N-termini conformation. In pyridine, gramicidin adopts a left-handed, intertwined double stranded $\beta^{5.6}$-helix. This may be a minor form of the membrane-bound ion conducting gramicidin channels. Our observations support several other spectroscopic conformational studies of GA.

Acknowledgement

I would like to express my gratitude to Dr. Max Diem, my mentor, for his fatherly guidance through out the many years that I have spent in his laboratory both as an undergraduate and as a graduate student. Without his tutelage many of my undertakings would have been impossible. Many thanks to my MBRS and MARC "parents" : Dr. Lipke, Dr. Rudner and Dr. Lavalle. These great people made my future brighter than ever, through their encouragement, guidance and immeasurable support. For this I will be for ever grateful.

Many thanks to my wife for her encouraging words, love and understanding. I would like to thank my parents and siblings for putting up with me through all these years. I greatly appreciate your love and support.

I would also like to give thanks to my colleagues past and present without exception. Special thanks to Dr. Sheryl Birke, Luis Chiriboga and Ali Kocak, for their friendship and support. Many thanks to Dr. Tsao and Dr. Ping, for their time in some of the enlightening discussions I have shared during my studies in this laboratory. A very special thanks to Dr. Zakim for many of his fatherly advise on matters of medical profession and suggestions in scientific writings.

Most important of all, I would like to give thanks to God for making it all possible.

DEDICATED TO MY GRANDPARENTS.

PREFACE

Proteins are central in the actions of biological processes. Important biomolecules such as enzymes, immunoglobulin, contractile molecules in muscle and the like are proteins. It is of great importance to elucidate their structures for a better understanding of biological processes. They function as enzymes which catalyze many biochemical reactions. Proteins serve as regulators of these reactions, both directly as components of enzymes and indirectly in the form of hormones as well as receptors for those hormones. Ion channels, and biomolecule transporters are made of proteins. Proteins such as rhodopsin in the retina of the eye, acquire sensory information for vision, and immunoglobulins are essential for biological defense in higher animals. Proteins interact with nucleic acids for the expression of, and the duplication of genetic information. Clearly then, proteins are of considerable importance in the conduction and propagation of life. This is one of the paramount reasons that many active research endeavors are devoted to understanding protein's structures and functions.

Many techniques over the years have centered on the understanding of structure of proteins in an effort to elucidate the mechanisms of protein activities. Chemical techniques such as sequencing, Edman by degration and C- and N-terminal identification have been employed to determine of primary sequences of proteins. Application of theoretical models, such as Chou-Fasman scheme, to information derived from primary structures has been used to predict secondary and tertiary structures of proteins. Physical methods like X-ray crystallography have revealed information on protein structures through the study of protein crystals. Although these techniques have yielded a wealth of information with regard to the structure of several proteins, there is still a need for further understanding of the nature of proteins in their natural environment.

Techniques that are applicable to solution studies of proteins are in demand. Since biomolecular interactions and recognition occur in solution phase in biological systems, physical methods to determine directly the solution phase structures of protein are of prime importance in modern biophysical research. Among all the spectroscopic techniques available, nuclear magnetic resonance (NMR) spectroscopy has clearly emerged as the most powerful solution structural tool. NMR often yields as detailed structural information as crystallography for biological molecules, such as peptides of up to about 150 amino acids. NMR spectroscopy has been used to study solution dynamics of protein. Information such as protein-protein interaction and protein foldings have been derived from NMR spectroscopy. However, these studies are limited to small proteins, and are not applicable to reactions that are complete within 10^{-6} sec, or less. Hence, the need for other techniques that can elucidate larger molecules, and perhaps on a faster time scale.

Circular dichroism (CD) is the differential absorption exhibited by a system for left- versus right-circularly polarized light. In order to demonstrate CD activity, a system must contain an asymmetric center, which is coupled in some manner to the chromophore giving rise to the absorption, or be dissymmetric. Pioneering efforts from this research field have sought to establish a set of CD basis spectra for three principal secondary states of proteins: α-helix, β-sheet, and random coil. However, inability to conclusively identify pure prototype conformational states of polypeptides for analysis of protein structure, together with a recognition that CD from aromatic side chains can interfere with analysis of CD in the region of peptide backbone transitions accessible to standard instruments (185-230 nm), has led to further development of the CD approach in recent years. Furthermore, a related chiroptical technique of potential for studying protein secondary structure has since begun to emerge.

Infrared vibrational circular dichroism (VCD) is a relatively new spectroscpic technique in which differential absorption of left and right circularly polarized light and vibrational transitions are monitored in the infrared (IR) region. Therefore, it can be viewed as an extension of IR spectroscopy. Yet it differs from conventional IR absorption spectroscopy, wherein the exciting radiation is unpolarized or linearly polarized, in that circularly polarized light is used to provide an additional degree of structural sensitivity, namely that toward the handedness, helicity, or dissymmetry of a molecular system. VCD has the potential to overcome the limitations ascribed to the methods mentioned above. One need not degrade or remove the protein, before the secondary structure can be determined. Also, VCD has a faster time scale (10^{-15} - 10^{-11} sec) than NMR techniques. Moreover, it is sensitive to micro quantities and is gaining wide application in biophysical research areas. Therefore, it is an ideal tool to monitor conformation and conformational changes in biomolecules.

Conformational sensitivity of VCD can be visualized to originate from the dipolar coupling of (achiral) IR transitions in analogy to the coupling of electronic transitions that gives rise to electronic CD. Thus the exciton theory invoked for the interpretation of CD spectra may be used to interpret VCD as well. Because the transition moments in vibrations such as the carbonyl stretching mode at ~1650 cm^{-1} (6 μm) are smaller than their electronic counterparts, such as $\pi^* \leftarrow$ n or $\pi^* \leftarrow \pi$ transitions, the dipolar coupling extends over shorter distances in VCD than in CD. Consequently, VCD is a superior technique to monitor short-range structural motifs, such as various turns in peptides or short DNA sequences. In addition, the better spectral resolution of IR transitions, as compared with the often very broad and unstructured electronic transitions in the ultraviolet (UV) range, allows a better and more detailed assignment of spectral features.

VCD has been observed for peptides in the spectral range from 3500 to ~ 1200 cm^{-1} (2.8-8 μm) in a number of vibrational transitions. In this thesis we shall concentrate on VCD results obtained for the amide I vibration, which is the carbonyl stretching motion of the amide moiety. This vibration occurs between 1630 and 1700 cm^{-1} and has a dipole transition moment of ~0.29 D. Conformationally dependent VCD spectral features in aqueous and non-aqueous solutions are relatively easily accessible for this band.

This thesis consists of two parts. In the first part of this thesis, VCD is applied to the study of poly-L-tyrosine, a model polypeptide, which is known to adopt distinct, defined secondary conformations as a function of its solution environment and temperature. The second part involves the first study of the application of VCD to a protein integrated in a model biomembrane. Also, we observed conformational changes of this peptide (gramicidin), as it functions (ion channel for K^+ and Na^-) in a model biomembrane (dimyristoylphosphatidyl-choline(DMPC)). This work was done to contribute to VCD as a viable technique for probing secondary conformations of polypeptides in solution. Our endeavors reveal some very interesting results.

TABLE OF CONTENTS

CHAPTER ONE

INTRODUCTION

This chapter is meant to provide a historical perspective of optical activity and to introduce the basic principles needed for appreciation of this phenonmenon. The layout herein is a hybrid formulation of major texts found in this field, in particular, the text by Erying and Cadwell, and Velluz et al. The first part consists of the discovery of optical activity to circular dicroism. For further illustration of this concept, the later part of this chapter makes use of some related basic equations.

I. FROM ROTATORY POWER TO CIRCULAR DICHROISM

A. Optical Rotation

The first manifestation of optical activity was pointed out by Arago[1] in 1811, during his study of the action of a quartz plate on polarized light. Several years later, Biot[2] showed that this phenomenon was not confined to crystalline substances. Solutions of certain natural products also possessed the property of rotating the plane of polarization of plane-polarized light. Biot studied the physical laws of the phenomenon in detail and showed, in particular, that the angle of rotation varies linearly with the thickness of the solution through which the beam of light passes, as well as with the concentration of the active product. Furthermore, he showed the angle of rotation varied with the wavelength.

Optical rotary power was rapidly found to be an essential characteristic of many organic substances, but Pasteur's discover of the optical resolution of racemic tartrates[3]

represented the most significant advance. Apart from showing the importance for organic synthesis with the possibility of separating racemates into active enantiomers constitutes, Pasteur was able to interpret the observed hemihedry of crystals and correlate their macroscopic asymmetry with the asymmetry of the molecule itself, thus initiating the science of optical isomerism. As a corollary, this exceptional scientist clearly deduced that the rotary power was connected with the existence of non-superimposable asymmetry in the molecule. In Pasteur's time, the concept of interatomic linkages was only in its primary stages and it was difficult to investigate this principle of asymmetry. Nonetheless, Pasteur intuitively visualized the tetrahedral carbon atom. He had in fact observed that, when the hemihedral facets of tartrate crystal are protracted, tetrahedrons are obtained, the orientation of which depend upon the sign of the optical activity of the tartrate.

The concept of a carbon atom situated at the center of a tetrahedron with its valence bonds directed towards the apices was not verified until the results of work by Le Bel[4] and van't Hoff [5] appeared in 1874. If four different substituents are attached to the carbon atom, the mirror image of the structure is not superimposable with the original; the molecule now possesses rotary power. The concept of the asymmetric carbon atom was thus deduced.

For the first time, optical activity was no longer associated with the molecule as a whole but rather with a definite center therein. In particular, it was now possible to ascertain the correct number of isomers and the variations in rotary power from one isomer to another in the case of a molecule containing several asymmetric centers. Furthermore, the reduction in the number of optical isomers due to internal compensation could be determined.

The theory of the asymmetric carbon atom was developed up to a point where it was next thought that the presence of at least one such carbon atom in the molecule was necessary to give rise to optical activity. We now know that this is not true. Certain molecules, such as biphenyl derivatives for example, can be optically resolved. In order to explain these phenomena, we have to return to Pasteur's concept of molecular dissymmetry and ascribe optical activity to any molecule whose mirror image is not

superimposable with the original. To be precise, it should be added that Le Bel had recognized this fact in his publication, which covered not only molecules containing carbon but also molecules encountered in inorganic chemistry. Since these ideas were expressed in an abstract style, they had been forgotten in favor of Van't Hoff's concepts, which were easier to understand.

The discovery of optical activity had thus allowed the conclusion to be made that two-dimensional formulae are insufficient to account for the properties of molecules and opened up a new chapter of chemistry -- that of stereochemistry.

The concept of molecules in three dimensions was certainly fundamental, but it was no less important to define for each individual case the configuration of the molecule, that is, the position in space of each atom. Amongst the problems of configuration presented by each synthesis of new substances, we can cite in particular the cases of hydroxy acids, amino acids, and especially sugars. Many publications on this subject have appeared, but it would seem appropriate to mention here one article of interest which was published by Klyne[6] several years ago and which contains numerous references.

It should be emphasized that rotary power in itself does not allow the configuration of a given product to be defined. The structure is deduced by analogy with molecules whose stereochemistry has already been determined relative to basic models (glyceraldehyde or serine) by means of chemical degradations, which are frequently very laborious. However, it has been possible to lay down certain rules. It should suffice to quote one of the oldest and most important of these, *viz*. Freudenberg's displacement rule[7]. According to this rule, if two similar asymmetric molecules A and B are altered in the same way to give A' and B', the differences of molecular rotation A-A' and B-B' will have the same sign. This and similar rules facilitate the establishment of relative configurations of asymmetric centers when degradations are difficult or impossible.

Similarly, attempts have been made to find empirical rules which would permit *a priori* calculations of the rotary power of a given structure. Of these works, that of Wallis [8] and Brewster[9] should be quoted as well as a criticism by Kauzmann *et al.*[10] concerning the way in which the contributions of the different groups are considered to be

directly additive. These authors propose a method of computation based upon the interaction of pairs of groups and upon the additivity of these interactions.

It must be stressed that these rules are to be applied with great caution, since they are not valid in all cases. It frequently happens that a modification made sufficiently close to a center of asymmetry profoundly affects the conclusions that are drawn. This phenomenon has been defined explicitly by Freudenberg and is called the vicinal effect, but it is always rather difficult to predict it with certainty.

Finally, simple application of the rules does not permit the determination of absolute configuration. In particular, there was no fundamental reason for conferring a positive sign to D-glyceraldehyde according to Fisher's representation[11] rather than a negative one. To solve the problem, either a different method had to be used or the sign of the rotary power of one of the configurations had to be calculated. Thus, Kuhn[12] applied a method of calculation for one of the configurations of 2-butanol and found that Fisher's hypothesis was correct; but the simplifying hypotheses necessarily used made the result uncertain. It was not until 1951 that Bijvoet[13] employing an x-ray diffraction method, was able to show definitely that Fisher's choice was in accordance with fact. The problem of absolute configuration could thus be considered as solved for molecules which could be related to basic models.

B. Rotary Dispersion

In spite of its undeniable contribution to the development of stereochemistry, the determination of rotary power with light from the sodium D line or even from blue and green lines of the mercury arc represents a very imperfect tool. The wavelengths of these lines generally lie far from the absorption regions of the constituent groups in the molecule and are only very slightly influenced by the asymmetric characteristics of these groups.

It has been known for a long time that rotary power varies with wavelength and Biot[14] pointed out that rotary dispersion was a more interesting characteristic of a

substance than a simple measurement at a given wavelength. However, Cotton was the first to study rotatory dispersion in detail within the actual regions of absorption of chromophores and this as early as 1896[15]. It is known that in this wavelength region the curve describing rotary power as a function of λ is not plain but possesses an S-form which by its sign, amplitude, and appearance is characteristic of the chromophore and of its asymmetry. Each chromophore -- and by this is meant all the bonds in the molecule -- will give rise to such an S-curve in its region of absorption if it is asymmetric. Outside this region, the rotary power varies in a uniform manner and decreases constantly in absolute value with increasing distance from the absorption band.

At any given wavelength, the measured rotary power is the sum of the rotary powers of each of the active chromophores. The most important contribution to this sum is made by the active chromophore, whose absorption wavelength is nearest to the wavelength at which the measurement is made. However, this preponderance diminishes as one goes toward longer wavelengths. For most optically active organic substances, the absorptions lie in the far ultraviolet; and for this reason, measurements using sodium D light are not very useful in most cases. Nevertheless, until the 1960's chemists employed measurements of rotary power in the visible region almost exclusively. However, since its discovery the phenomenon of dispersion has been studied continually. In particular, in addition to the work of Cotton, that of Levene, Pickard, Kenyon, Lowry, Kuhn, and Rupe[16] should be quoted; however, these authors dealt more with fundamental studies of optical rotation than with its application to structural determination.

The situation is explained by the very considerable difficulties presented by the measurement of rotary power in the ultraviolet region. Formerly, determinations were very tedious and required a trained staff. However, this technical problem would not seem to explain fully the chemist's reticence toward this method. If the determination of the rotary dispersion problems, the experimental difficulties would have been accepted and the method would have been widely applied. However, this is not the case, primarily because a large number of chromophores remained outside of the scope of measurement and

because the very significant increase in rotary power with decreasing wavelength usually did not justify making delicate measurements in the far ultraviolet. On the other hand, in the case of molecules possessing a measurable chromophore it was necessary to work by analogy and therefore to set up empirical rules based on the examination of numerous products. Here again, the difficult nature of the measurements and especially the time required to carry them out certainly did not stimulate further development of the method.

In the years that followed, the description of photoelectric polarimeters for use in the ultraviolet[17], followed more recently by that of recording spectropolarimeters[18], has completely modified the aspects of the problem. It became a simple matter to trace a dispersion curve, and soon it was possible to combine a large number of results and thence deduce rules of structural analysis. Impetus has been given principally by Djerassi's school with his work on keto steroids[19]. These methods have since been widely employed, principally in the field of steroids and terpenes.

The degree of success has been astonishing. This is due to the fact that, although operating on the same principle of analogy as was used for structural analysis based on rotary power at the sodium D line, rotary dispersion offers numerous advantages. First of all, the immediate environment of the chromophore is of prime importance (Freudenberg's vicinal effect), thus reducing the complexity of the problem in structures with numerous asymmetric centers, such as steroids and terpenes. The formation of a chromophore in successive parts of the molecular skeleton by simple chemical reactions generally permits a study of the different ring junctions. Furthermore, complete knowledge of the Cotton curve, including its amplitude, sign, and fine structure, allows far more complete characterization of the asymmetry induced by the environment upon a given chromophore. Thus, it is fairly easy to distinguish a 3-A/B-*trans*-ketone from an 11-ketone by studying dispersion curves, whereas the increment of rotation in sodium D light with respect to the parent steroid without the keto group would be practically the same in the two cases. Moreover, assuming that the analogies have been established, examination of the curve usually suffices to solve the problem. This is not the case when sodium D light is used, for calculation on the basis of the difference between the substance being studied and the

parent compound without the chromophore is necessary. It frequently happens, however, that the parent substance cannot be prepared owing to lack of starting materials or because of difficulties in its chemical synthesis. Thus, rotary dispersion constitutes an immensely more elegant tool for the chemist than ordinary polarimetric analysis, and the method has allowed rules of much more general applicability to be established.

Although rotary dispersion represents a significant advance over classical polarimetric analysis, it nevertheless has certain intrinsic defects. For example, the continuous background due to the chromophores, which absorb in the more distant ultraviolet is always superimposed upon the Cotton effect of a chromophore. Since the measurements are generally conducted in the ultraviolet, this background can sometimes be disturbing and can conceal the S-curve of the chromophore. When fine structure is present, the resultant shape of the curve makes the analysis of each contribution a delicate matter.

C. Circular Dichroism

Circular dichroism does not have the disadvantages mentioned above. The phenomenon of CD was studied by Cotton[15] at the same time as rotary dispersion, and this famous physicist had shown that each optically active material absorbed left and right circularly polarized light to different extents. If ε_L and ε_R are the molecular coefficients of absorption for the left and right polarized forms respectively, the difference $\varepsilon_L - \varepsilon_R$ is a measure of the intensity of circular dichroism. This difference, which we have represented by $\Delta\varepsilon$, varies with wavelength and can be positive or negative The form of the curve $\Delta\varepsilon = f(\lambda)$ for a simple optical transition is a bell-shaped one quite similar to that of curves found in spectroscopy with ordinary light. This is normal, since $\Delta\varepsilon$ represents the difference between two absorption curves. Moreover, $\Delta\varepsilon$ as well as ε_L and ε_R only have significant values in a narrow region in the proximity of the absorption maximum of the

chromophore under examination. The form of the curve lends itself better to the interpretation of fine structures than does the S-curve of rotary dispersion.

In allowing an easier and sometimes more effective analysis of asymmetric structures, circular dichroism does not invalidate the general rules, but it does give them a new aspect. Circular dichroism and rotary dispersion are, in fact, two manifestations of one and the same phenomenon, *viz.* the interaction between polarized light and asymmetric molecular structure.

For some time, circular dichroism remained less developed than rotary dispersion. This delay was due to the complexity of the apparatus required to make measurement and to difficulties in the technique of measurement, which are even greater than in the case of rotary dispersion. Of the pioneer work in the field of circular dichroism, that of Kuhn is especially worthy of mention, particularly from the point of view of his theoretical study of the phenomenon[20].

The degrees of complexity of the initial measurements is due to the fact that, in nearly all cases, a secondary phenomenon was utilized, namely the transformation of plane-polarized light into elliptically polarized light during the passage of the beam through the active material in the region of its absorption. By analyzing the basic phenomenon, *i.e.*, the difference in absorption between the two types of circularly polarized light, researchers have been able to devise a relatively simple apparatus that permits measurement of circular dichroism as easily as the recording of absorption curves with a spectrophotometer[21]. Within a short time, many data were collected, which led to a better understanding of some results of rotary dispersion[21].

D. Molecular Interpretation

So far the empirical use of the phenomenon of optical activity for structural determination has been considered. This point of view is the most interesting to the

chemist, but nevertheless a theoretical explanation of the phenomenon related to the structure of the molecule has long been sought.

Following the work of Lorentz on the propagation of electromagnetic waves in matter, the classical theories of optical activity were developed principally by Born, De Mallemann, and Kuhn. Parallel to these, a quantum theory was worked out, first by Rosenfield and later by Condon. These theories led to a general formulation of optical activity, but usually they have no practical application, because too many simplifications have to be introduced into the classical theories as well as into the quantum theories. A general review of these methods is to be found in a book by Mathieu published in 1946[22]. Stated briefly, the molecule is divided into groups of isotropic and anisotropic oscillators, and the perturbations caused by coupling between the main oscillator and the neighboring oscillators is calculated.

One method in particular should be mentioned here. This is Condons' "one electron" theory, as developed by Eyring, Gorin, Kauzmann, and Walter[22]. These authors no longer consider coupled of oscillators, but rather a single electron -- that of the chromophore -- oscillating in the asymmetric electrostatic field induced by neighboring atoms. This theory can be more readily visualized.

Even in this simplified form, the calculation of a given problem proves to be difficult. On application to simple examples, it generally leads to the correct sign; but it must always be kept in mind that the result is largely dependent on the approximations and on the spatial location of the groups. Kirkwood has shown this effectively for 2-butanol, in which, according to the choice of model, large deviations are obtained in the computed results[23].

One of the chief difficulties involved in applying molecular theories of rotary power to a concrete case lies in the symmetric nature of the principal chromophore in almost every instance. The optical activity is the result of the perturbation introduced by neighboring groups. It is thus to a certain extent a second order phenomenon which is consequently more difficult to evaluate. Furthermore, as a first approximation, only the interaction between the chromophore and neighboring groups is calculated and the sum of

the effects worked out. Generally, however, the sign of each contribution is not the same for all of the groups; the over-all effect is therefore an algebraic sum which often nearly balances out. It can easily be understood that errors can have significant effect on the absolute value of the final result and frequently even on the sign.

However, the molecular theories of the phenomenon have led to a better understanding of the observed facts and have provided an explanation of empirical rules, often even permitting prediction of their limitations. These theories are continually being improved, and mention should be made here especially of the work of Moffitt and Moscowitz[24], whose results will be discussed in a following chapter.

II. CONFORMATIONAL STUDIES

A. Introduction to Optical Activity

In 1812, Jean Baptiste Biot [25] repeated an experiment first performed by his colleague, Francois Arago, in 1811 [26]. Plane polarized white light, produced by reflection off a glass plate, was passed through quartz. The light was polarized perpendicular to the symmetry axis (optic axis) of the crystal. The light passing through the quartz was examined by observing it though a piece of calcite. It was observed that when the calcite was rotated, different color appeared. Biot, unlike Arago, interpreted the effect. He said that the appearance of colors was due to rotation of the plane of polarization about the axis of travel. Furthermore, the angle of rotation depends upon the wavelength of light used. This effect is known today as optical rotary dispersion. Biot also discovered that quartz crystals occur in two forms, the physical properties of which are similar except in one respect: each form rotates light in a direction opposite to that of the other form. We now call these two forms of quartz left handed and right handed. A compound which rotates light clockwise (when viewed looking towards the source of light), is called dextrorotatory; compounds rotating plane polarized light in a counterclockwise direction are said to be levorotatory.

Biot continued his experiments using liquids in which he immersed the quartz. He then discovered that liquids themselves can be optically active. Among the liquids he examined were turpentine, lemon oil, alcohol solutions of camphor and aqueous solutions of sugar and tartaric acid. Because some of the liquids, such as lemon oil, were found naturally in one form and were oriented randomly in the liquid state, Biot reasoned that optical activity is a property of the individual molecules. To test this theory, he heated turpentine and attempted to measure the optical rotation of the vapor. He observed that isolated gas phase molecules do indeed rotate plane polarized light [27]. Biot, through his

measurements to determine the optical rotation of quartz, found that optical rotation is inversely proportional to the square of the wavelength of light passed through a given path length of quartz. Drude modified this law and equation 1.1 bears his name:

$$\theta = \sum_j \frac{A_j}{(\lambda^2 - \lambda_j^2)} \qquad 1.1$$

A_j is a constant, λ_j is the wavelength of an absorption, and λ is the wavelength of incident light. Even modern theories of optical rotation in transparent media have this form.

Augustin Fresnel put forth the first theory of optical rotation. This followed his discovery of circularly polarized light. A more detailed discussion of circular polarization is given in chapter 3; here, only general concepts are summarized. The tip of an electric field vector lying in a plane perpendicular to the direction of propagation traces out a helix as time passes (Fig. 1). When viewed along the propagation direction, the helix appears as a circle (Fig. 2). Fresnel reasoned that linearly polarized light can be thought of as the sum of left and right circularly polarized beams of equal amplitude propagating coherently. The orientation of the plane of polarization depends upon the relative phases of the two components. The phase difference is, in turn, due to a velocity difference between the two circular components in an optically active medium. If, at a given instant, the electric field vectors of both circularly polarized components are parallel to the plane of polarization of the incident light, then at the same point in time, electric field vectors at some point z=l in the medium are inclined at angles $\theta^R = -2\pi cl/\lambda v^R$ and $\theta^L = 2\pi cl/\lambda v^L$ respectively, to the plane of polarization. Here, c represents the velocity of light, λ is the wavelength, and v is

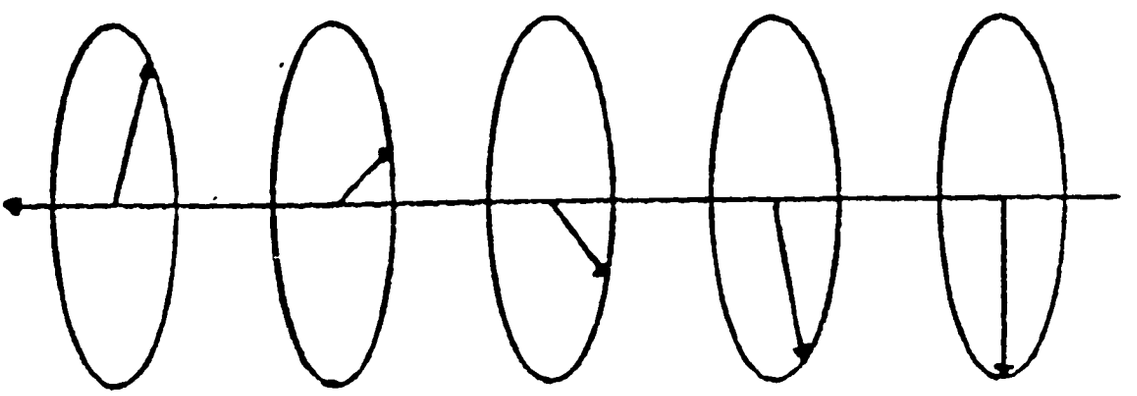

Figure 1. Circular polarizaton of light.

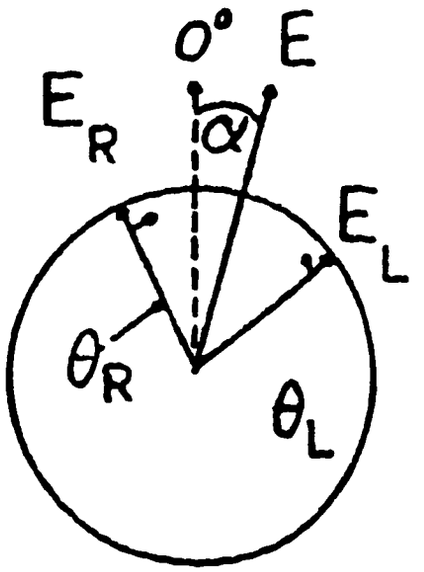

Figure 2. View of a circularly polarized beam of light along the direction of propagation.

the velocity of propagation. R and L denote circular polarization states. The angle of rotation is:

$$\alpha = 1/2\ \theta^R + \theta^L = (\pi cl/\lambda)(\lambda\ \{1/v^L - 1/v^R\}) \qquad 1.2$$

Here, l represents the path length of the sample. The above equation is valid in transparent media. Since n = c/v, where n is the refractive index,

$$\alpha = \pi\lambda/(n^L - n^R) \qquad 1.3$$

The refractive index is a complex quantity; that is, it can be described by a number containing a real part and an imaginary part. The real part of the refractive index describes the index of optical rotation and the optical rotary dispersion. The imaginary part describes the absorption.

Because absorption and refractive index are so closely related, it was reasoned that optically active samples should absorb left and right handed light differently. This effect, called circular dichroism (CD), was first observed by Haidinger [28] in 1847 in amethyst crystals.

In 1848, Pasteur used the term dissymetric to describe crystals of tartrate salts he had been studying. Dissymmetric compounds are not necessarily asymmetric; the former can possess rotational symmetry axes but no planes or centers of symmetry. He performed the first optical resolution of a racemic compound, a tartrate (Mitscherlich's salt), into its component mirror images (enantiomers) and observed that each one rotated light in the opposite direction. Thus, Pasteur was the first to recognize that crystals which are not superimposable on their mirror images exhibit optical rotation [29].

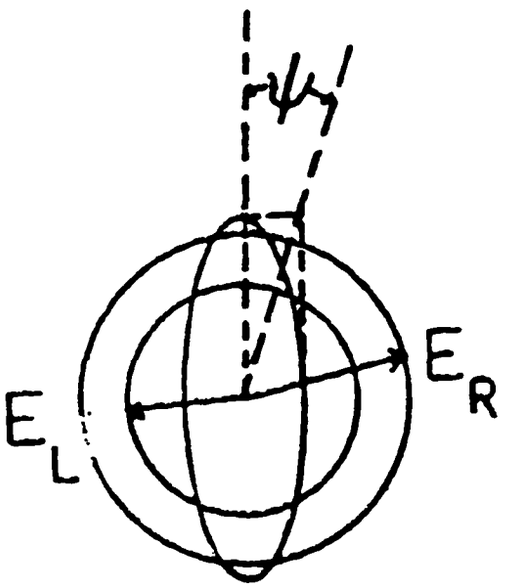

Figure 3. Elliptically polarized light viewed along the propagation direction.

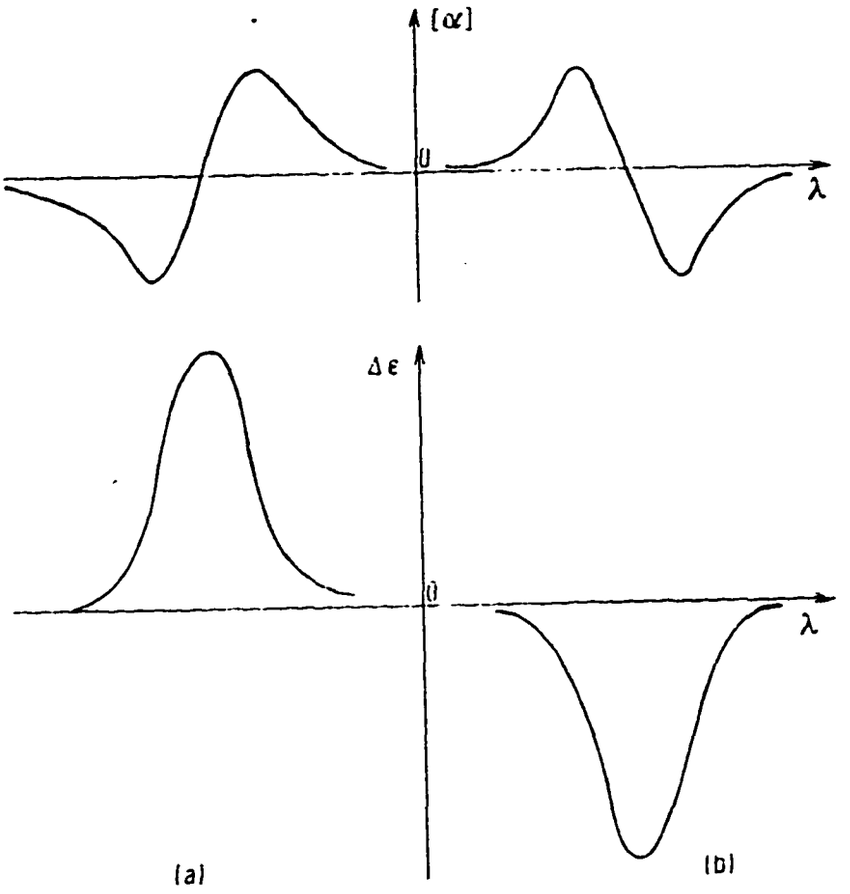

Figure 4. Optical rotatory dispersion curves (above) and circular dichroism (CD) curves (below) for : a.) dextrorotatory chromophore, b.) a levorotatory chromophore.

Furthermore, he attributed optical activity of quartz to dissymmetry of the crystal lattice. This was confirmed by fusing the quartz, causing optical activity to disappear. He attributed the optical activity of organic liquids and solutions to dissymmetry in the molecular framework.

Cotton [30], in 1895, observed CD in solutions of copper and chromium tartrate. If left and right handed light is absorbed differently by the sample, a linearly polarized incident beam will emerge from the sample with elliptical polarization. Elliptically polarized light is obtained when left and right circular components of different amplitude are added vectorial. The amplitude difference arises due to preferential absorption of one of the circular components (Fig. 3). A parameter, called the ellipticity ψ, is used to describe elliptically polarized light. It is defined as:

$$\tan \psi = (E_R - E_L)/ (E_R + E_L) \qquad 1.4$$

The amplitude attenuation of a light beam by absorption in a medium of refractive index n and path length l is given by:

$$E = E_o^{(2\pi nl)} \qquad 1.5$$

R and L, as usual, denote right and left polarization states and E denotes the electric field vector. E_0 is the incident electric field strength. For differential absorption, the ellipticity is given by:

$$\tan \psi = \tanh (\pi l/\lambda)(n_L - n_R)) \qquad 1.6$$

Both circular dichroism and optical rotation are functions of the wavelength of light passing through the medium. The type of curves these functions exhibit are shown in Figure 4. The ellipticity maximum coincides with the inflection point of the rotary

dispersion curve and is monosignate. Ideally, the inflection point of the ORD curve coincides with the CD maximum. The CD may, of course, be positive or negative. At wavelengths far from an absorption maximum, ORD is given by the Drude equation; this must be modified at absorption maxima. Absorption bands close together yield CD and ORD curves which are complicated surperpositions of the curves of each separate band.

Optical rotation measurements are presented as the specific rotation, defined as:

$$[\alpha] = \alpha V / mL \qquad 1.7$$

where α is the measured optical rotation in degrees, V is the volume containing a given mass m of optically active material, and L is the path length in decimeters. CD spectra are displayed as the difference in molar extinction coefficients versus wavelength.

A dimensionless factor, g, called the dissymmetry factor was introduced by Kuhn [31]. It is given by:

$$g = (\varepsilon_L - \varepsilon_R) / (\varepsilon_R + \varepsilon_L) \qquad 1.8$$

The epsilons are the extinction coefficients for each polarization state at a given wavelength. Note that the constants occurring in the equations for absolute absorption measurements drop out. Furthermore, in the case of identical coupled oscillators, g, is a factor of molecular geometry only.

UV and visible CD bands can be related to the stereochemistry of the molecular skeleton, because CD depends upon the spatial distribution of electronic states over the nuclear framework of the molecule. The sign and magnitude of Cotton effects were first related to molecular structure using the famous "octant rule", devised by Moffitt, Woodward, Moscowitz, Klyne, and Djerassi in 1961 [32]. In this study, the carbonyl

group in steroids was the absorbing "probe." The symmetry of the carbonyl (C=O) group, originally C_{2v} is lowered by asymmetric perturbation due to the molecular skeleton. Thus, it exhibits CD and ORD. Three nodal planes, two of which are the symmetry planes of the C_{2v} point group and the third being a nodal plane through and perpendicular to the C=O bond axis, split the area surrounding the C=O group into octants. The electronic CD and ORD were correlated with the position (octant) the perturbing group occupied. Furthermore, changes in the magnitude and sign of Cotton effects as the perturber moved from one octant to the other were predicted.

Although ORD and CD effects, collectively known as the Cotton effect, have been known for some time, experiments designed to measure them were not applied until the 1950's, when photomultiplier tubes were developed. Before that time, visible and UV spectra were recorded on photographic plates. The introduction of electro-optic modulators, used to create circular polarization and switch between polarization states, in the 1960's, made measurement of UV/visible CD and ORD routine.

B. Introduction to Optical Activity Theory

Optical activity can be explained using not only the technique of quantum mechanical perturbation theory, but also in terms of multipole moments induced in molecules when they interact with radiation. Several types of quantities are encountered

when discussing the above mentioned moments. Those having a magnitude, but not associated with any direction in space, such as temperature, are scalars. Vectors differ from scalars in that they have a direction associated with a magnitude. Velocity is a familiar example of a vector. The magnitude of a vector quantity can be specified only if at least two dimensions, corresponding to directions in space, are given. Molecular polarizabilities are tensor quantities. Unless otherwise noted, quantities given in this section with two or more subscripts are tensors. Spatial directions are given by the subscripts i, j, and k. These should not be confused with the unit vectors along the x, y and z axes, respectively. When used as subscripts, the three letter can designate any axis in the coordinate system. A repeated subscript signifies a summation over that particular index. Such notation is known as the Einstein summation convention for tensors. For example, the electric polarizability tensor relates the induced dipole of a molecule to the applied electric field:

$$\mu_i = \alpha_{ij} E_j \qquad 1.9$$

The physical significance of this equation is that the directions of the influence of E and the response are not necessarily the same; i.e., the induced dipole does not necessarily lie in the same direction as the vector E because the polarizability, μ, is anisotropic. Thus, the induced dipole moment along the x axis of a molecule can be written:

$$\mu_X = \alpha_{ij} E_j \qquad 1.10$$

where the summation is carried out over j, j = i, j, k, and i = x. The Einstein convention simplifies this expression further by omitting the summation symbol, this being understood because of the presence of the repeated subscript. Thus, the summation is shorthand for

the following expression:

$$\mu_X = \alpha_{xx}E_x + \alpha_{xy}E_y + \alpha_{xy}E_z \qquad 1.11$$

If an electromagnetic wave propagates through a nonmagnetic, transparent, anisotropic medium [33],

$$D_i = \varepsilon_{ik} E_k \qquad 1.12$$

and

$$H_i = (\hat{I} /\mu_o) B_i \qquad 1.13$$

The tensor $\hat{I}$ is the permittivity of the medium and all components are positive. E and B are the electric and magnetic fields, respectively, of the wave in free space and D and H are the corresponding fields in the medium. Maxwell's equations for a wave of frequency ω are:

$$\mu i\omega H = c\nabla E \qquad 1.14$$

and

$$\mu i\omega D = -c\nabla H \qquad 1.15$$

Vector superscripts have been omitted from D, E, and H for simplicity. The lower case i denotes an imaginary quantity. The speed of light is given by c. For a plane polarized beam, H/c = k x E and D/c = -k x H. k is a propagation vector pointing in the direction of travel. A vector n is defined by:

$$k = \omega n/c \qquad 1.16$$

The magnitude of n is equal to the refractive index of the medium. H and D can be written as H = n x E and D = -n x H. Then, D = n x E x n = n^2E-(n·E)n. If the

components of vector D in the above equation are equated with 1.11, three linear equations, one for each component of E, are finally obtained:

$$n^2 = E_i - n_i n_k = \varepsilon_{ik} E_k \qquad 1.17$$

D can be written in terms of a bulk polarization P and a quadropole polarization Q:

$$D_i = \varepsilon_o E_i + P_i - (1/3)\, \nabla_j Q_{ij} \qquad 1.18$$

The bulk polarizations can, in turn, be related to the polarizations of the constituent molecules by:

$$P_i = N\mu_i \qquad 1.19$$

$$Q_{ij} = N\theta_{ij} \qquad 1.20$$

N is the number density of molecules. The oscillating multipole moments μ and θ are, in general, complex. They are given by [34]:

$$\mu_i = \alpha_{ij}\,(E_j) + (1/3)A_{i,jk}\,(E_{jk}) + G_{ij}\,(B_j) + \ldots\ldots \qquad 1.21$$

$$\theta_{ij} = a_{k,ij}\,(E_k) + d_{k,ij}(B_k) + \ldots\ldots \qquad 1.22$$

Equation 1.21 gives the induced electric dipole moment of the molecule; 1.22 describes the induced electric quadropole moment. In addition to these, magnetic dipole moments can also be induced. These are given by:

$$m_i = \chi_{ij}\,(B_j) + g_{ji}\,(E_j) + (1/3)\, D_{i,jk}E_{jk} + \ldots \qquad 1.23$$

These quantities g, a, and d are, in general, complex. They are given by:

$$g_{ij} = G_{ij} + iG_{ij'}\,, \qquad 1.24a$$

$$a_{i,jk} = A_{i,jk} + iA_{i,jk'} \qquad 1.24b$$

$$d_{i,jk} = D_{i,jk} + iD_{i,jk} \qquad 1.24c$$

The quantities G, G', A and A' are known as the dynamic molecular property tensors. The derivatives of these tensors with respect to the normal coordinate give directly the intensities observed in Raman Optical Activity (ROA). G involves interference between the electric dipole and magnetic dipole matrix elements and is given by:

$$G_{ij} = (2/h)\,\Sigma\,(\omega_{jn} / \omega_{jn}^2 - \omega^2)\,\mathrm{Re}(\langle n|\mu_i|j\rangle\,\langle j|m_j|n\rangle) \qquad 1.25$$

The sum is taken over all j not equal to n. Re denotes the real part of the expression. ω is the frequency of radiation interacting with the molecule. The expression for G' is almost identical to this one, except that the imaginary, rather than the real part of the expression is evaluated. G' is negative. The expressions for A and A' take the same general form as those for G and G', respectively. The difference is that A involves interference between the electric dipole and electric quadropole. In order to obtain expressions for optical activity in terms of the dynamic molecular property tensors, a new tensor must be defined. This tensor is given by:

$$\xi_{ijk} = (1/c)\,[(1/3)\,i\omega\,(A_{i,jk} - a_{j,ik}) + \varepsilon_{jik}\,G_{ij} + \varepsilon_{jki}\,g_{kj}] \qquad 1.26$$

The ε represents the Levi-Civita tensor. It has a value of 1 if the subscripts can be brought into the form ijk by a cyclic permutation of the subscripts. If such a form can be obtained only by non-cyclic permutation, the tensor takes on a value of -1. Repeated subscripts imply a zero value for the tensor.

Using this expression, equation 1.16 can be written in the form:

$$[(n^2 - 1)\delta_{ij} - \mu_o c^2 N\,(\alpha_{ij} + n_k\,\xi_{ijk} + \ldots)]\,E_k = 0 \qquad 1.27$$

Axes are now specified as i = x , j = y, and k = z. The direction of propagation is

along the z axis. The equations for x and y axis components circularly polarized light can be used in the above equation to yield two equations for the refractive index which can be combined. Since the refractive index is a complex quantity, the real and imaginary parts can be separated. The separate parts can then be substituted into the phenomenological equations for optical rotation and circular dichroism given earlier to yield:

$$\Delta\theta \approx -(1/2)\omega\mu_o lN[-c\alpha_{xy}(f) + (1/3)\,\omega(A_{x,yz}(f) - A_{y,xz}(f)) + G'_{xx}(f) + G'_{yy}(f)] \quad 1.28$$

$$\Delta\eta \approx -(1/2)\omega\mu_o lN[-c\alpha_{xy}(g) + (1/3)\,\psi(A_{x,yz}(g) - A_{y,xz}(g)) + G'_{xx}(g) + G'_{yy}(g)] \quad 1.29$$

The letters f and g represent dispersion and absorption lineshape functions, respectively. It was mentioned at the beginning of this section that the medium is anisotropic.

In an isotropic medium, the average of the tensor components over all space must be taken. When this is done, the quadropole terms drop out and the following equations are obtained.

$$\Delta\theta \approx -(1/3)\omega\mu_o lN\, G'_{ii}(f) \quad 1.30$$

and

$$\Delta\eta \approx -(1/3)\omega\mu_o lN\, G'_{ii}(g) \quad 1.31$$

The first of these two equations is the Rosenfield equation.

C. Comparison Of Spectroscopic Techniques For The Determination Of The Solution Conformation Of Biomolecules

The present understanding of processes in modern biology and medicine has resulted from a detailed knowledge of the structure of biomolecules and the structural changes accompanying interactions of biomolecules. To date, X-ray crystallography has probably revealed more structural information of biomolecules than all other physical techniques combined. The results of these structural studies have revolutionized biology, although crystallographic results strictly apply to solid crystalline phases only. However, deductions about solution phase structures have been made from the structures in the solid phase, and compared with solution structures obtained spectroscopically or via other techniques.

While x-ray crystallography can provide precise conformational details of protein secondary structure from available single crystals, there is considerable interest in other spectroscopic techniques that are able to yield information regarding the solution phase conformation of proteins. Circular dicroism (CD) in electronic transitions is the most extensively developed of these techniques, having evolved steadily since the late 1960s [1-5]. In addition, IR [41] and Raman [42-46] spectroscopy, and more recently, Fourier transform IR (FTIR) spectroscopy [45-47] have been used to predict quantitatively the conformational composition of protein secondary structure. Even though a great deal of progress has been achieved using these spectroscopic methods, further advancement is

needed to provide the desired level of information. To date, these techniques have been shown to yield results that are generally consistent with the results of x-ray studies, but little has been done to investigate the structure of proteins for which no x-ray data exist or to uncover differences between protein conformation in solution compared to the crystalline state.

NMR spectroscopy has yielded considerable structural information, but the results often suggest no discernible solution structure for small systems, such as a tri- or tetra-peptides. This is due to the flexibility and structural variance displayed by these sample systems. However, the lack of interactions between parts of the molecule, which normally are detected via Nuclear Overhauser enhancements and refined into molecular structures during NMR structural determinations, should not be interpreted as a lack of a solution structure. It is the slow time scale of NMR, coupled with the rapidly interconverting conformations, which weakens these effects to the point that they no longer can be detected with certainty. Structural techniques that operate on a much faster time scale (e.g. UV-CD spectroscopy, or forms of vibrational spectroscopy) demonstrate that there is a preferred class of solution conformers even in small peptide systems.

Thus, it is sensible to supplement the available resonance spectroscopic methods with other methods, which sample molecular conformation via different interactions and at different spatial and temporal resolution. By virtue of their origin, chiropractical techniques have played an enormously important role in the derivation and establishment of solution structures. Electronic CD (ECD) has been used very successfully to establish solution conformation of nucleic acids and peptides. In a macromolecule with a fixed

structure, such as a helix, repeating units that incorporate an electronic transition are arranged in fixed geometric patterns. The coupling of these transitions yields CD features which not only allow a qualitative identification of a secondary structure, but also reveal quantitative information about the angles between the interacting transitions. In the exciton model, to be discussed in more detail in later on in chapter two, the rotational strength created by the coupling of interacting transitions depends on expressions of the form:

$$R \propto [T_{ij} \cdot \mu_i \times \mu_j] \qquad 1.32$$

where μ_i and μ_j are the interacting dipole transition moments, and T_{ij} are the distances between the dipoles. The conformational sensitivity of CD and (VCD) results from the vector cross product in equation 1.32, as will be discussed below.

Thus, CD spectroscopy is a very sensitive tool to monitor conformational changes between well-defined solution structures. However, the interpretation of UV-CD spectra is often complicated by the broadness of the peaks. This is particularly true in the case of nucleotides, where the electronic transitions of the bases are superimposed, and where the exact nature and direction of the dipole transition moments, the coupling of which give rise to the observed CD spectra, are not well established. In peptides, two transitions ($\pi^* \leftarrow n$ and $\pi^* \leftarrow \pi$) occur and overlap in the region where the exciton CD is observed, thus, complicating the interpretation of spectra. Furthermore, electronic transitions are often not sensitive toward small chemical changes in molecules, unless the chemical

modification involves the electronic chromophore, and lack the structural sensitivity of other spectroscopic techniques.

Vibrational spectroscopy per se is not a very good quantitative probe of molecular conformation either, although it has been used quite successfully as a qualitative probe. To date, most of these efforts have utilized the frequency shift of certain vibrations, such as the peptide amide I and III vibrations, and certain B or Z-form specific Raman bands in nucleic acids, as markers for secondary structure. These methods are feasible because normal modes of vibrations are sensitive to subtle changes in the surroundings of the probe groups. Best results are obtained for large, well defined shifts alone to monitor secondary conformation is somewhat ambiguous and will not yield conformational angles directly and quantitatively.

The combination of the principles of vibrational spectroscopy with those of optical activity leads to new spectroscopic techniques in VOA, infrared CD (VCD) and Raman optical activity (ROA), just as there are two techniques in conventional vibrational spectroscopy. In VOA, the enormous sensitivity of chiroptical techniques towards the relative orientation of interacting groups is coupled with the advantages of vibrational spectroscopy, namely transitions, that are narrow, well resolved and reasonably sensitive to structural variations (the vibrational "fingerprints"). Therefore, VOA was viewed for a long time as an ideal new tool for investigating the conformation of biological molecules, and the observation of optical activity in vibrational transitions was first attempted (unsuccessfully) over five decades ago. Theoretical predictions were published about the magnitudes and conformational sensitivity of vibrational optical activity even before its

experimental verification.

Among the two techniques of VOA, VCD was the first to be utilized to solve problems of real biophysical and biostructural significance. Mostly due to insufficient instrumental sensitivity, these studies were not possible until the mid- to late 1980s, when VCD was first applied to study the conformation of homo-polyamino acids in aqueous and non-aqueous media.

The conformational sensitivity of VCD in the amide I region of peptides can be thought of as being due to the dipolar coupling of the C=O stretching vibrations of the peptide linkages according to equation 1.32. The coupling of these transitions produces distinct VCD and infrared absorption spectra, to be discussed later in detail: the VCD patterns are known as positive and negative couplets, and the infrared spectra show multiplet structures. These spectral features will permit a quantitative determination of dihedral angles between the coupled oscillators. This point was, in fact, recognized prior to the experimental verification of VCD; signs and intensities of coupled oscillator VCD were calculated for poly-amino acids, and the amide A and I VCD was predicted [51].

Similarly, the C=O stretching dipole transition moments of the bases in helical DNA and RNA couple, and give rise to distinct, conformation dependent VCD signals between 1550 and 1750 cm^{-1}. Since these modes are localized on groups which are achiral, the VCD is nearly entirely due to the dissymmetric coupling of these transitions according to equation 1.32, which is sensitive to the geometry between the groups. Since VCD is a form of vibrational spectroscopy, it probes DNA and peptide structures at a very fast time scale, and with a conformational specificity that is unavailable by any other

experimental means.

These vibrations discussed so far occur in the 6 μm spectral region in the mid-infrared; however, most vibrational modes in a molecule will exhibit VCD, and other vibrations in the 12 μm, as well as the 3.5 to 2.5 μm range, have shown interesting VCD results. In this thesis, only the 6 μm region (the C=O stretching vibration) will be discussed. To observe VCD in this spectral region, a chiroptical instrument with infrared optics (with materials such as CaF_2) was utilized.

CHAPTER TWO

INFRARED VIBRATIONAL CIRCULAR DICHROISM (VCD) OF POLY-L-TYROSINE IN THE AMIDE I AND AMIDE III SPECTRAL REGION

The focus of this chapter rests on the comparison of observed VCD spectra of a model peptide (poly-l-tyrosine) with those computed for several secondary structures in the amide I region, using the extended coupled oscillator formalism (ECO). Also, we present a preliminary conformational studies of this homopolypeptide in the amide III region in an effort to establish this region for conformational analysis. The author contributed to these studies through data collection and the calculation of computed structures.

INTRODUCTION:

The peptide backbone exists in a number of distinct and well-known conformations, determined by the value of the ϕ and ψ angles [19]. Among the most common of these conformations is the right-handed α-helix, which shows distinct CD features described by Holzwarth and Doty [9] and Greenfield and Fasman [7]. The aforementioned angles ϕ and ψ associated with the right-handed α-helix fall into a broad minimum energy region in the Ramachandran plot for peptides, centered about -55°, -55°. Many α-helical model peptides can be induced to undergo a phase transition by varying the acidity or the ionic strength of the solvent. Poly(L-lysine), for example, exists in an α-helical form at a pH above 10.6. When the medium is acidified, a distinct phase transition to another conformer occurs, which exhibits CD spectra that are smaller in amplitude than those of the α-helix, and are inverted in sign. This conformation has been referred to as the "random coil" form.

The first conformation-dependent VCD spectra of polyamino acids were reported by Yasui and Keiderling [26,27] for poly(L-tyrosine) (PLT) in DMSO, and nearly simultaneously by Keiderling's and Nafie's groups for poly(L-lysine) (PLL) in aqueous solution [15,26,27]. This last study showed unequivocally that a true random conformation, obtained by denaturation of PLL, shows minimal VCD signals in the amide I' region. On the basis of the sign pattern of the observed VCD couplet, this publication also suggested that the "random coil" conformation was actually a left-handed helical structure.

VCD has been reviewed a number of times recently (see reference 10), and it is an ideal tool to study the conformation of polypeptides in solution phase. Like in CD, most of the observed signals in polypeptides are due to the dipolar coupling of the transition moments localized on the peptide linkages. Unlike CD, in which there are at least two overlapping transitions ($\pi^* \leftarrow$ n and $\pi^* \leftarrow \pi$) forming the exciton manifold in the 180-230-nm region, the wavelength range in VCD can be selected such that only one transition contributes. Furthermore, the bandwidth of a typical vibrational band is about the same as the exciton splitting. Thus, relatively sharp and distinct VCD spectra are obtained.

Vibrational transition moments are smaller than the electronic counterparts in the amide moiety. Thus, the coupling in VCD, extends over shorter distances than in electronic CD, and, therefore, VCD is sensitive to structural order which extends over shorter distances than that responsible for the electronic CD. Finally, the direction of the dipole transition moment is less ambiguous in VCD than in CD, and is nearly parallel to the direction of the C-O bond of the amide I vibration. This simplifies the computational procedures, which can be adapted readily from procedures derived for electronic exciton interactions by Tinoco [24].

Thus, VCD is a powerful method to quantitatively determine the conformation of peptides in solution. Efforts from this research group have previously solved the solution structure of a small peptide, $(L\text{-}Ala)_3$, in aqueous solution via the vibrational exciton approach [11]. In this section, we present computational results for the α-helical conformation to establish that the "extended coupled oscillator" (ECO) formalism, which we have applied successfully to the computation of VCD spectra of DNA, also is applicable to model peptides. Original VCD intensity calculations for helical polymers were carried out before experimental data were available [2,3,21]. Some aspects of experimental and prior theoretical results were discussed by Lipp and Nafie [12]. The work presented here represents the first attempt to directly compare observed and computed VCD data for the α-helical conformation and so evaluate the validity of the model chosen.

We also present calculated VCD spectral results for some known left-handed structures and compare these results to the experimental data for the "random coil" conformation. These studies suggest that this "random coil" conformer is either one of two left-handed helices for which the calculated VCD spectra are virtually indistinguishable. One of these structures falls into the range of left-handed α-helicity, with conformational angles $\phi = 60°$ and $\psi = 30°$, and with about three residues per turn. The other possible structure lies in the broad energy minimum centered around $\phi = 120°$ and $\psi = 120°$. In this region, the pleated sheet structures and various known left-handed helical structures (with $\phi \sim -100°$ and ψ between 100° and 130°) occur. Both these

structures reproduce the VCD spectra observed for the so-called random-coil conformation nearly equally well.

In addition, we present a preliminary VCD measurements of poly-l-tyrosine in the amide III region (1200-1350 cm^{-1}). The reason for doing so is the long recognized sensitivity of the amide III region, in infrared and Raman spectroscopies, toward the conformation of peptides. We anticipated that the amide III would show conformational sensitivity in VCD as well. Although this presumption turned out to be correct, difficulties arise with the amide III region. The motion of atoms in amide III is not as well defined, for example, as it is in the amide I vibration, which is predominantly a C=O stretching motion.

In this study, we report the first detailed VCD spectra of PLT in the amide III region. This sample system was selected since its secondary conformation, in non-aqueous solution, is well established from prior CD and VCD studies. PLT exists, in acidic solution as a well defined *α*-helix, and in neutral solution in a conformation which is often referred to as "random coil." We report here the first amide III results of the phase transition between these two forms, and a tentative interpretation of the amide III VCD in terms of the vibrational analysis performed earlier.

MATERIALS AND METHODS

A. Data Acquisition

All the data presented for the amide I region were obtained from one of the two dispersive instruments constructed and optimized by our research group (VC-II). VCII is specifically constructed for data acquisition in the amide I region of IR spectrum. VCII has a peak performance at 6 μm. Its high sensitivity at this wavelength is due to a high sensitivity HgCdTe detector, with a maximum D* of 9×10^{10}cmHz$^{1/2}$/w, and an optical system, which is optimized for 6 μm. For the preliminary studies of poly-l-tyrosine in the amide III region, VCI was used for data aquisition. Though less sensitive than VCII, VCI has a broader range of data aquisition.

Although both instruments give reproducible VCD spectra, if a solvent baseline is subtracted from the raw VCD data, in the following study the baseline was derived by averaging the VCD spectra of poly-L-tyrosine and poly-D-tyrosine (pDT). The baseline derived in this manner was subtracted from the spectra of pLT. This method of background subtraction was employed, since the amide III VCD is an entirely unmapped area, and comparison of D- and L-enantiomers gives the most reliable VCD data.

Commercially purchased poly-L- and poly-D-tyrosine were dissolved in DMSO (neutral media) and DMSO/TFA 20% by volume (acid environment) for studies of the amide I region. For the amide III region DMSO-d_6 (neutral media) and trichloroacetic acid (TCA)-acidified DMSO-d_6 (acidic environment) were used as solvents. Poly-L and poly-D-tyrosines were of 50 to 500 chain length, and were used after freeze-drying to remove indeterminate amounts of water contaminating the samples. DMSO was distilled over CaH_2 to remove water. Water in the sample or the solvent must be removed to prevent loss of signal intensity due water's absorption in the range of our study. The instruments must be kept free of water vapor as well. This is done by running dry air through the

instruments for the duration of data acquisition. The data collected were then compared to theoretically predicted data calculated using the coupled oscillator's formalism.

B. Sample Preparation

Sample concentrations were between 15 and 50mg of peptide in DMSO and DMSO/TFA (20% by volume). All samples were contained in cells consisting of 32-mm-diameter CaF_2 windows with teflon spacers of appropriate thickness between 15 and 50 μm. The total sample volume required was between 15 and 30 μL. All results are reported in units of ε (liter per mole per centimeter) per residue.

For acidic solutions, DMSO was acidified by adding 20% by volume trifluoroacetic acid (TFA) for the studies in the amide I region. The TFA was not completely dry; thus, the IR absorption spectra of samples containing this acid show various water peaks in the 1600-1700 cm^{-1} region. Data collected are then compared to those derived by calculation *via* extended couple oscillator (ECO)

In the second study, acidification of DMSO was accomplished by adding 20% (by volume) dichloroacetic acid (DCA) for studies in the amide I region, and trichloroacetic acid (TCA) in the amide III region. The use of trichloroacetic acid for studies in the amide III region is necessitated by the opaqueness of DCA between 1200 and 1300 cm^{-1} due to the presence of the C-H deformation mode in dichloracetic acid. Here we established that TCA induces a similar phase transition in pLT by comparing the amide I spectra obtained after adding DCA and TCA to solutions of pLT in DMSO.

C. Computational Procedures

Infrared absorption and VCD intensity calculations were carried out via the degenerate extended coupled oscillator (DECO) formalism, which is based on Tinoco's exciton description of the rotary power of polymers [24]. In this formalism, the rotational strengths for each of the *k* exciton components of an *n*-mer of coupled transitions can be written as [4].

$$R_k = -(\pi \nu_0 / c) \sum_{i=1}^{n} \sum_{j1}^{n} C_{ik} C_{jk} (\mathbf{T_{ij}} \cdot \mu_i \times \mu_j) \qquad 2.1$$

Here, μ_i and μ_j are the interacting dipole moments, separated by vector T_{ij}, ν_0 is the frequency of the uncoupled transition, and *c* the velocity of light. The c_{ij} are the eigenvector components of the dipole-dipole interaction matrix V_{ij}.

$$V_{ij} = \frac{\mu_i \cdot \mu_j}{T_{ij}^3} - 3\frac{(\mu_i \cdot T_{ij})(\mu_j \cdot T_{ij})}{T_{ij}^5} \qquad 2.2$$

Each of the terms in the summation in eq 2.1 is equivalent to a coupled oscillator expression for a simple coupled dimer. The summation is over all pairwise interactions, weighted by the eigenvector coefficients. Inclusion of all coupling interactions is particularly important in peptide helices, where the coupling energy between carbonyl group *i* and *i*+3 is still relatively large [21].

The DECO expression in eq 2.1 above formally appears similar to the fixed charge equation derived by Schellman [17]. However, eq 2.1 is accurate within the exciton formalism and relies only on observable quantities, such as the dipole transition moment and geometric parameters.

The infrared absorption intensities can be obtained from the dipole strengths, *D*, defined by

$$\mathbf{D_k} = \sum_{i=1}^{n} c_{ik}^2 \, \mu_i^2 + 2 \sum_{i=1}^{n} \sum_{j>i}^{n} c_{ik} c_{ij} (\mu_1 \cdot \mu_2) \qquad 2.3$$

The computations are carried out as follows. Structures for various peptide conformations were generated using the program MacroModel [22], running on a Micro VAX/Evans & Sutherland PS 390 Graphics workstation or later, using Hyperchem running on Pentium processor in a personal computer. MacroModel permits the creation of peptide structures using predetermined conformational angles for right- and left-handed α-helices, as well as for a number of other common structures. Alternatively, the ϕ and ψ angles may be input manually to create less common structures. Amino acid sequence may be specified; however, in this study, homooligopeptides with chain lengths of between 8 and 30 residues were specified. No energy minimization of the structures was performed, since it is important for the following VCD calculations that the structures are the ones actually specified via the input parameters. Originally, tyrosine residues were used to construct the atomic coordinates. However, since no energy minimization was performed, alanine residues were used for the final calculations, because only the backbone structure was desired, which is virtually identical for $(L\text{-}Ala)_8$ and $(L\text{-}Tyr)_8$. Both models gave identical results in the VCD exciton calculations, because the nature of the side chain has no effect on the VCD exciton calculations.

The Cartesian coordinates of all atoms of the peptides were fed into the DECO program, written in our laboratory, which selects the carbonyl C and O atoms, and attaches transition dipole moments along the C=O bond. The dipole transition moment for an amide I vibration was taken to be m = 0.29 D = 0.29 x 10^{-18} esu cm, in agreement with the work by Snir et al. [21] and our own previous peptide VCD data.

The rotational and dipole strengths were converted to spectra by overlaying Gaussian, Lorentzian, or mixed band shapes. In the results reported here, 100% Gaussian band shapes with a half-width (at half-heights) of 9 cm^{-1} were used. The resulting spectra are converted to ε units and normalized with respect to the number of residues in the computed structures.

DISCUSSION

A. Experimental and Computational Studies in Amide I Region

Figure 1 shows the infrared absorption and VCD spectra of poly-L-tyrosine in the amide I region, in both the α-helix and the "random coil" conformer. These spectral results have been reported previously by Yasui and Keiderling [26,27], and similar features, with similar $\Delta\varepsilon / \varepsilon$ values, were observed for other polyamino acids as well. Thus, one can conclude that these features are due to the secondary structure of the peptide under investigation, and are independent of the nature of the side group.

The inversion of the VCD features between the helical and the "random coil" structures is readily apparent. The magnitude of the "random coil" VCD, which is only slightly smaller than that of the α-helical form, suggests that the "random coil" has short range order similar to that found in the α-helix, but presumably with opposite handedness. In a number of previous investigations, (see, for example, Sengupta and Krimm,[20]) the possibility for a relatively ordered state of this "random coil" conformation was proposed. We have calculated the expected VCD for some of these proposed conformations, and have compared calculated spectra to the observed VCD of the "random coil".

First, the computational procedures were calibrated by reproducing the spectra observed for the α-helix conformation. The structural parameters of this conformation are well established. However, the question arises whether or not the conformation observed at concentrations typically used for VCD studies is the same as the one observed in CD studies by Wen and Woody [25]. We have varied the concentration by half an order of magnitude, and have not observed any changes in the VCD features when the acid (TFA) concentration is constant. However, at low concentrations of acid, the observed VCD spectra depend on the sample concentrations: at low PLT concentration the random coil is observed, whereas high sample concentrations favor a transition to the α-helical form. Thus, at the concentration shown , PLT exhibits VCD features similar to those observed for other α-helical peptides, and we are certain that we are dealing with an α-helical peptide.

Using carbonyl coordinates created by MacroModel or Hyperchem and the computational procedures discussed above, we obtained calculated spectra for the α-helix form shown in Figure 2. These calculations use the correct coordinates of the carbonyl groups, and dipole transition directions along the C=O bond direction. Our computational results contain both the helical contributions as well as the Moffit terms[18].

The results agree reasonably well with the previous calculations by Schellman and coworkers [21]. However, our computations are smaller by a factor of five than those reported previously, and thus, are closer to the experimental values. However, the calculations by Schellman's group used a different approach within the exciton formalism than our calculations. Nevertheless, it is gratifying to see that many of the features agree very well between the two models: the interaction energies between peptide linkages, i, i+1, i+2, i+3 used by Schellman, based on the empirical data by Miyazawa and Blout [13], are identical in sign and very close in magnitude to ours based on dipole-dipole interaction energies alone (cf. Eq. 2.2). Furthermore, the sign and intensity patterns of the calculated spectra using the two models agree well. The calculated results predict a conservative couplet for the α-helical conformation; yet the observed results reveal that the integrated negative peak is larger than the positive one by a factor of 1.2. (In the spectra of the "random coil" conformation, *vide infra*, the negative lobe is larger by a factor of 1.5.) Thus, it is clear that exciton interactions cannot explain the observed optical activity completely. Other factors contribute to the observed VCD. We have shown before that an uncoupled amide I' vibration in dipeptides composed of L-amino acids exhibits negative VCD intensity [16]. Thus, the negative bias of the observed VCD spectra in PLT could result from optical activity induced in the C=O chromophore by the chirality of the amino acid residues, or from other factors such as charge flow between oscillators.

Inspection of the eigenvectors reveals that nearly all negative VCD intensity is due to the component polarized parallel to the helix axis, as predicted by Snir [21]. However, the strong infrared absorption intensity calculated for this peak appears at higher frequency than the zero crossing of the VCD spectra, whereas the observed IR spectrum has its absorption maximum under the positive part of the VCD couplet. This is a quite

serious discrepancy. Within the exciton formalism, there is no explanation for this discrepancy, but possible causes, involving vibrational interactions, will be discussed below.

We used a much shorter peptide sequence (an octamer) for our computations, whereas Schellman used a 36-mer. We find that the spectral features produced with an octamer are virtually indistinguishable from those of a longer polymer. Indeed, when the polymer length exceeds about 12, the spectral amplitudes appear to decrease slightly, due to cancellation of many positive and negative contributions. This observation is not true for the rotational strengths R_k, when no band when no band shape effect are taken into account. The values of the dominant terms R_k in fact, approach a value nearly independent of the chain length, which is given by the coupling interaction. Our computed results are about a factor of two stronger than the observed ones, independent of the peptide length and band shape parameters.

The computed features shown in Figure 2 are obtained, as previously in the case of computed DNA VCD, with no adjustable parameters. To facilitate a comparison with the work of Schellman and coworkers, we utilized 100% Gaussian band envelopes in these computations, although we have found previously that 50:50 Gaussian:Lorenzian mixtures give slightly better fits to the observed spectra. As mentioned before, the dipole strength of the amide I transition, and its unperturbed vibrational frequency were taken from our previous peptide studies [11], and agree well with Schellman's data. These parameters were not allowed to vary to reproduce the α-helix spectral features.

The calculated VCD spectrum is nearly exactly a factor of two smaller than the observed one, whereas the calculated absorption spectrum is slightly larger than the experimental data. In addition, the calculated infrared absorption spectrum is significantly narrower than the observed one. We believe that these three discrepancies all arise from the same problem. In our calculations, only dipole-dipole coupling between the aimde I vibrations was considered. In reality, one expects vibrational coupling (through the vibrational force field) to contribute significantly to the interaction between the dipoles, and, thus, increase the splitting between the exciton components. This, in fact, will reduce

the cancellation of positive and negative exciton components, increasing the magnitude of the VCD spectra and the half-width of the absorption spectra. It also could affect the computed peak positions. The same arguments had to be made before when the VCD spectra of $(L\text{-}Ala)_3$ were fitted with computational data [11]. In this case, the computed splitting between the coupled oscillator components was much smaller than the observed splitting, which reduced the VCD computed intensities.

We have initiated calculations that take into account the force field effects on the computed VCD spectra. This procedure involves calculating the normal modes of the peptide backbone explicitly, in a fashion similar to the calculations reported by Moore and Krimm [14]. The potential energy matrix is then augmented by the dipole-dipole interaction energies described in eq. 2.2. The aim of these calculations is to use the complete vibrational eigenvectors to compute the VCD intensities according to Eq. 2.1. This procedure, in principle, should account for the observed differences in VCD band shapes for α-helical peptides between amide I and amide I' vibrations, *i.e.*, upon deuteration of the amide proton. These calculations are well underway and preliminary results indicate that the splitting between the exciton components is, indeed, significantly larger when the vibrational coupling is taken into account. Furthermore, a better understanding of the splitting and ordering of the exciton components is expected to emerge. An improper ordering of the eigenvalues and eigenvectors in the pure exciton calculations could, conceivably, be responsible for the improper position of the absorbance maximum relative to the VCD zero-crossing in the calculated spectra presented. However, these calculations are significantly more complicated, and depend on many more parameters than the simple vibrational exciton calculations presented so far. Thus, they will not be useful for some time until all parameters are optimized. In the meantime, the vibrational exciton model, which has severe limitations, offers the only practical method of computing VCD intensities for a molecule of this magnitude. In light of the shortcomings of the ECO model, the agreement between observed and calculated VCD spectra for the α -helix amide I region (cf. Figure 6) is excellent.

The computation presented so far established the limits of reliability of the computational procedures for a well established peptide conformation. Next, computed VCD results for possible left handed structures will be presented. Previously, CD and vibrational arguments have been presented [20,23], suggesting that the "random coil" conformation might be an extended left handed helical structure. Thus, we calculated VCD intensities for a number of left handed structures in order to establish whether or not these structures exhibit computed VCD features similar to the ones observed. However, we did not attempt to analytically fit computed *vs.* observed spectra by varying the angles ϕ and ψ systematically, since such a fitting procedure is extremely complicated, given the varying sign and magnitude of the exciton splitting, intensity cancellations, etc.

Instead, we computed VCD intensities for a number of conformers in the vicinity of energy minima in the Ramachandran plot. The region with ϕ = -110 and ψ = 120°, close to the pleated sheet conformation described by Creighton [1], produced structures with good agreement with the observed spectra. In addition, the region around the left-handed α-helix (60°, 50°) yielded similar agreement. In both cases, it was found that the conformations with more residues per turn (for example, with ϕ and ψ values of 60° and 75°, respectively) reproduced the spectra less satisfactorily than more extended structures with less than three residues per turn.

The criteria used to select the best fit were as follows. We searched for a conformation where the computed spectrum was about 50 to 70% of the observed ones, since one may assume that the vibrational coupling is too low for the "random coil" conformer as well, and since the α-helical structure yielded too low computed spectra by a similar amount. In addition, the crossover point in the VCD spectra (observed at 1661 cm^{-1} for α-helical and 1674 cm^{-1} for the "random coil" conformation) was used as a criterion. Finally, the overall intensity pattern and the band shapes were required to be as close as possible to the observed ones.

The computed VCD spectra of two conformers fulfilling these requirements are shown in figure 3. One of these structures has the conformational angles ϕ = 60° and ψ = 30°. This conformer falls at the very edge of a conformational energy minimum in the

Ramachandran plot, and has a ϕ angle similar to that of the left-handed α-helix, but is more extended. This structure is stabilized by internal hydrogen bonds similar to that found in a right-handed α-helix. Calculated VCD spectra for a number of structures in the vicinity of the left-handed α-helix were very similar to each other, and increased in magnitude as the number of residues per turn increased.

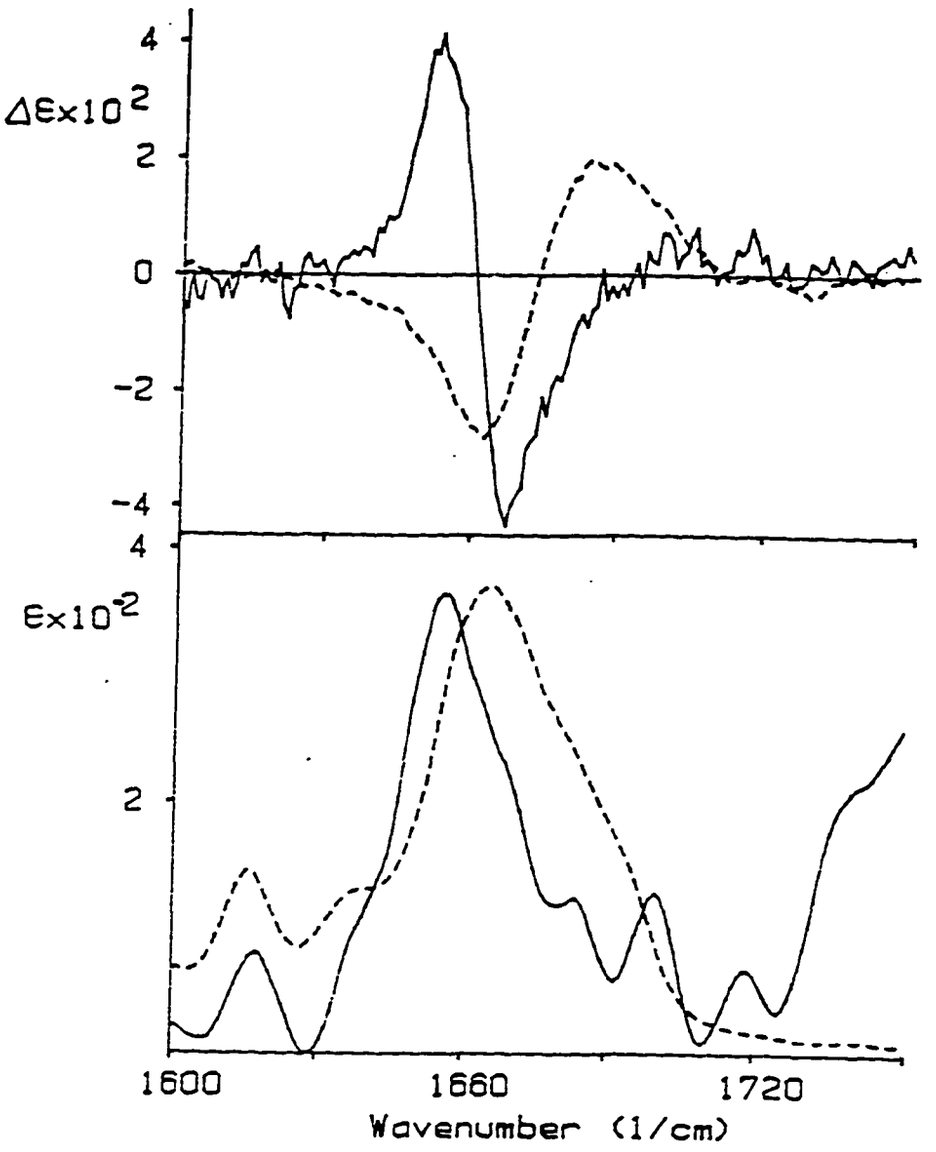

Figure 1. Observed infrared VCD (top) and Absorption spectra (bottom) of poly- L-tyrosine. Solid trace :DMSO:TFA (20% by volume) ; Sample concentration: 42mg/mL, pathlength: 15 μm ;
Dashed trace: DMSO; Sample concentration; 23 mg/mL, pathlength: 15μm.

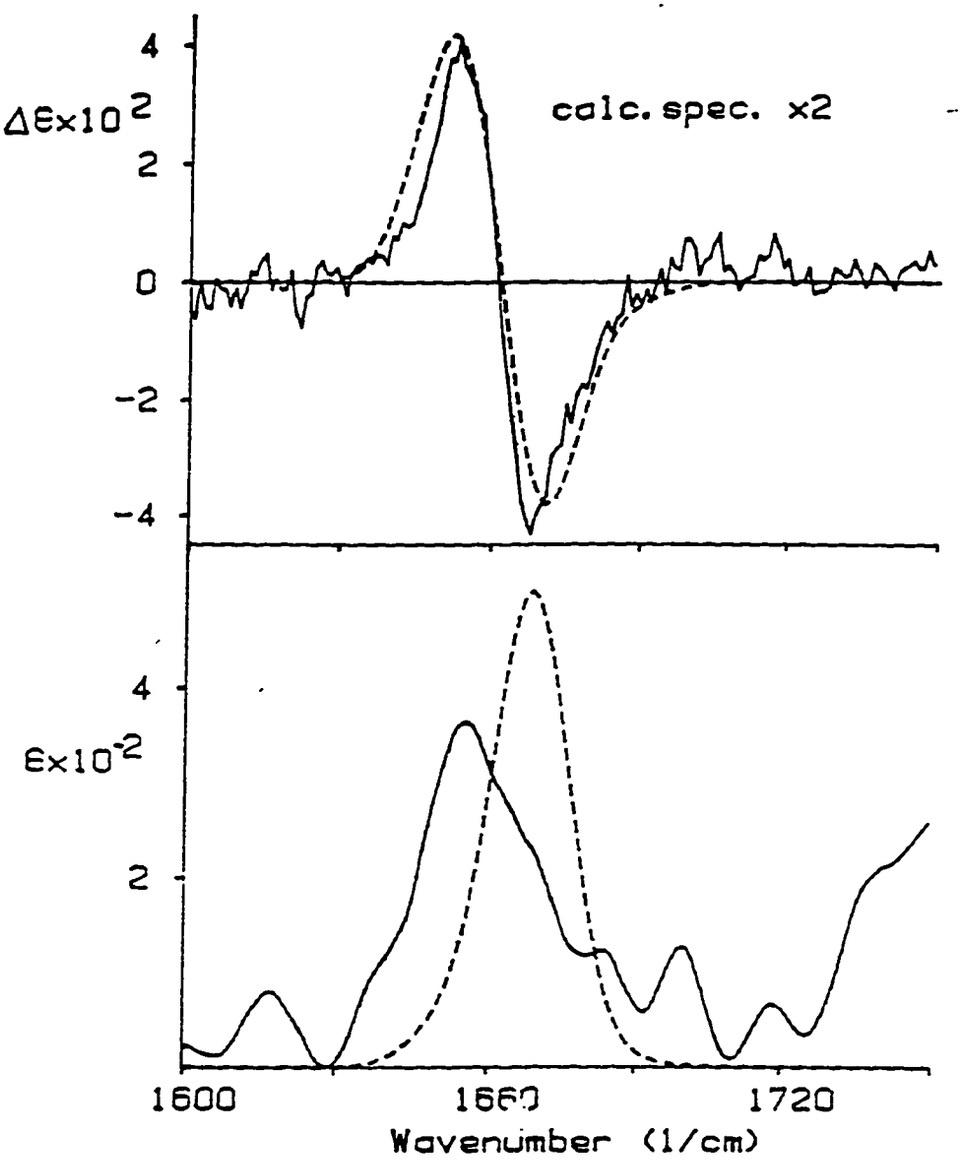

Figure 2. Observed (solid traces) and computed (dashed traces) of α-helical poly-l-tyrosine; Experimental conditions: same as in figure 1; Computational conditions: octamer, $\phi = 52°$, $\psi = 53°$.

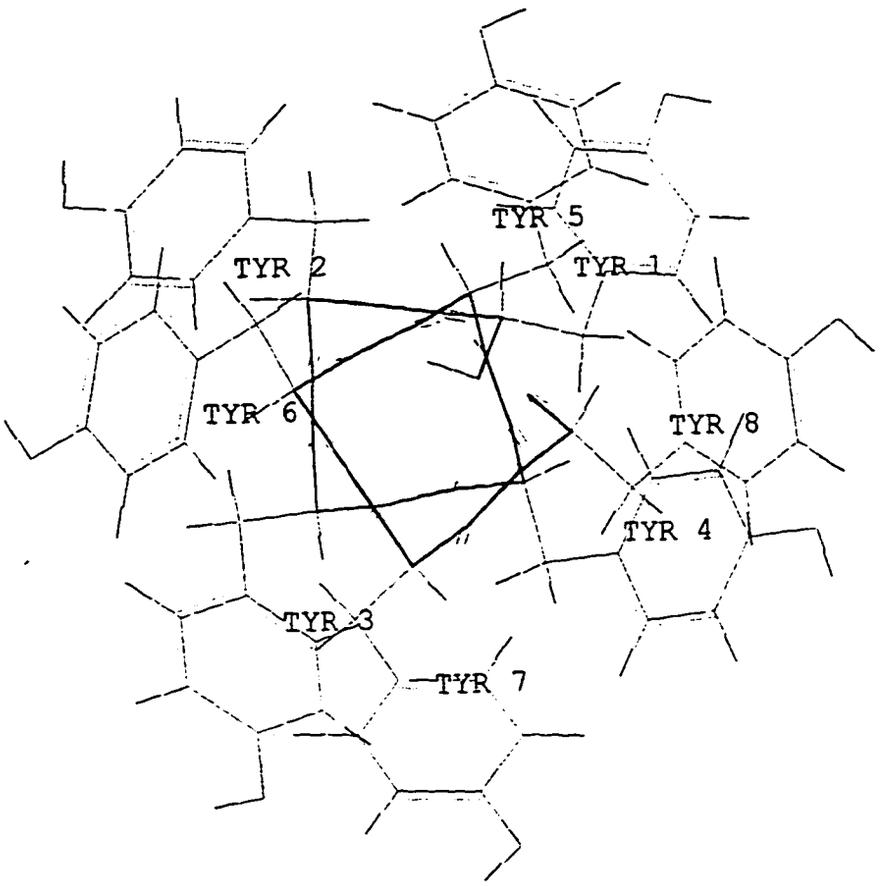

Figure 2a. Computed structure: octamer, $\phi = 52°$, $\psi = 53°$

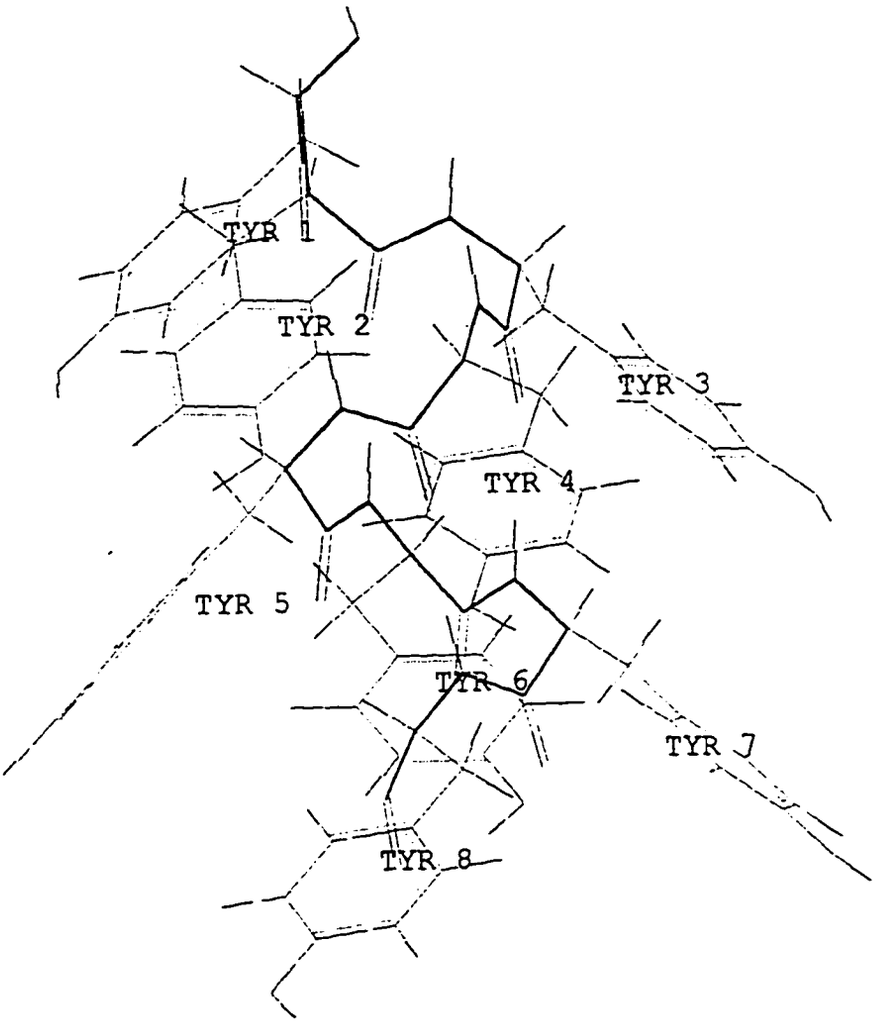

Figure 2b. Sideview representation of figure 2a.

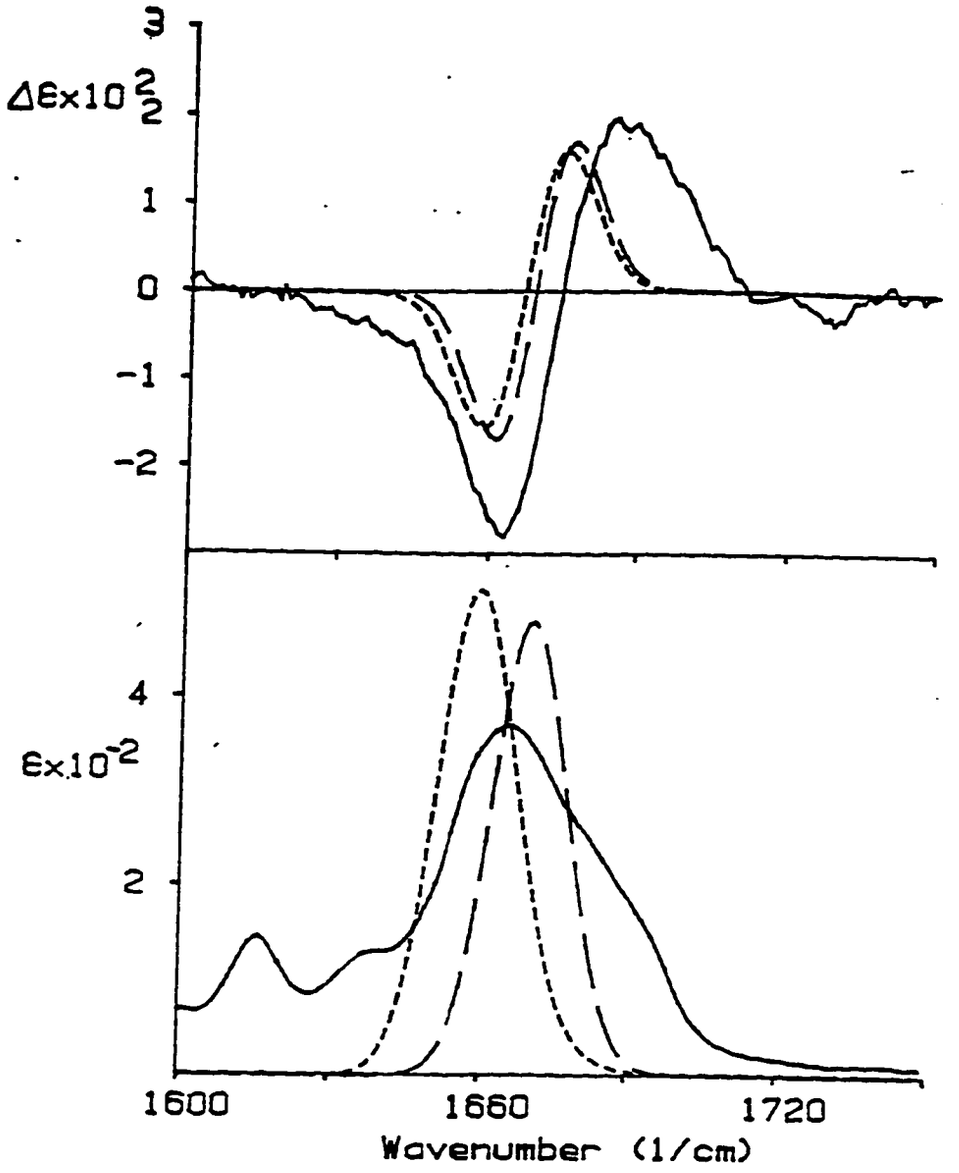

Figure 3. Observed (solid traces) and computed (dashed traces) of "random coil" poly-l-tyrosine. Experimental conditions: same as figure 1. Computation conditions: short dashes: octamer, ϕ =60°, ψ = 30° ;
long dashes : octermer, ϕ = 110° , ψ = 120°

The other structure, which fits the observed spectra well is qualitatively similar to the extended left-handed structure with 2.5 residues per turn as suggested by Krimm [20] for the "random coil" conformation. Our calculations suggest a structure with ϕ and ψ angles of -110° and 120°, respectively. This structure is very close to the dividing boundary between left and right handed structures in the Ramachandran map (see, for example, Dickerson and Geis, [4]). Indeed, changing the conformational angles by a few degrees switches the sign patterns of the computed VCD features. This structure does not have intramolecular hydrogen bonds, and is even further extended than the extended helix (EH) postulated by Krimm.

The fit between the VCD spectra computed for these two conformers and the observed spectra is about equally good. The extended structure has a zero crossing somewhat closer to the observed one. The rotational strengths calculated for the extended structure are much larger (by a factor of three) than those calculated for the left-handed α-helix; however, the splitting is much smaller in the extended structure, and cancellation reduces the intensities to levels similar to those calculated for the left-handed α-helix.

Based on the VCD data alone, we cannot decide between the two computed structures. However, there are a few facts that make us believe that the extended structure is more likely to describe the "random coil" conformation best. First, prior CD and vibrational studies by Krimm and his coworkers favor the extended form. Second, the left-handed α-helix has a hydrogen bonding pattern similar to that of the right-handed α-helix; thus, it is not intuitively clear why acidification of a DMSO solution should favor one conformer over the other. Finally, a left-handed α-helix has not been found *via* crystallographic techniques, whereas the extended left handed helical form falls into a broad region of many established structural motifs in peptides.

We conclude that the ECO formalism may be used to compute VCD features of homo-oligo peptides in the amide I region. Although a solution structure of the peptide conformation generally referred to as the "random coil" cannot yet be derived unambiguously from VCD data, we have shown that several left-handed helices exhibit VCD spectra similar to the one observed. This result suggests that the "random coil"

conformation has high order on the VCD interaction length, which may be judged from the coupling energies to be at least five residues. Among two conformers which fit the observed VCD features, we favor the one which is similar to the extended helix described by Krimm and coworkers [20].

B. Preliminary Study in the Amide III Region

DATA AND DISCUSSION:

Here we present the first amide III VCD conformational analysis of the secondary structure for a polypeptide as a function of its solution environment. In DMSO solution, acidified by DCA, PLT exists in left handed *α*-helix, identified by a typical CD pattern in the 195 to 230 nm region. This conformation exhibits a positive/negative VCD couplet (from lower to higher wavenumber) in the amide I region, shown in Figure 1.

In neutral DMSO solution, PLT shows a large negative/positive couplet in the amide I region, which is typical for the so-called "random coil" conformation (Figure 4). In this figure, the corresponding amide II VCD results are shown as well. At neutral pH, the amide III region exhibits three distinct peaks, as is expected from the previous studies on the exact nature of the amide III vibration (Figure 5). The triad of peaks between 1270 and 1350 cm^{-1} has been observed in a number of peptides and peptide models. Depending on the conformation, clear couplets are observed between any two or three members of the triad.

The solution of PLT in neutral DMSO-d_6 shows large positive/negative/negative amide III VCD. Upon increasing the acidity of the solution, the infrared absorption spectra show a coalescence of the two high frequency peaks at 1330 and 1390 cm^{-1} (figure 5) .

The amplitude features of VCD spectra diminished gradually with increasing acid concentration, and are inverted at 20% TCA.

The sign observed for PLT in neutral solution, namely positive/negative/negative, is similar to the amide III VCD observed for $(L\text{-}Ala)_3$ in aqueous solutions. $(L\text{-}Ala)_3$ was shown by VCD studies in the amide I region, as well as recent 2-D NMR studies, to possess a distinct solution conformation, stabilized by a zwitterionic interaction of the charged and groups. The molecular conformation of $(L\text{-}Ala)_3$, as determined by VCD, is best described as a "left-handed bridge" structure. Thus, we may conclude that the VCD of the amide III region of PLT, in neutral DMSO, is left handed as well. Similar conclusions on the nature of the "random coil conformation" of peptides have been reached by other techniques.

The dotted trace in Fig. 5 represents the amide III signal of α-helix. It shows no discernable VCD peaks that may be attributed to α-helical structure. Using Resonance Raman spectroscopy, Asher and co-coworkers [29] showed that amide III absorption peaks are not specific for the coupling of C_α-H bending mode and amide III mode. Further, they reported that peptides, as well as compounds that contain no C_α or C_N clearly exhibit bands in the amide III region. The VCD spectrum in figure 5 supports their observations. Therefore, it appears that α-helical amide III signals are not observable in vibrational spectroscopy.

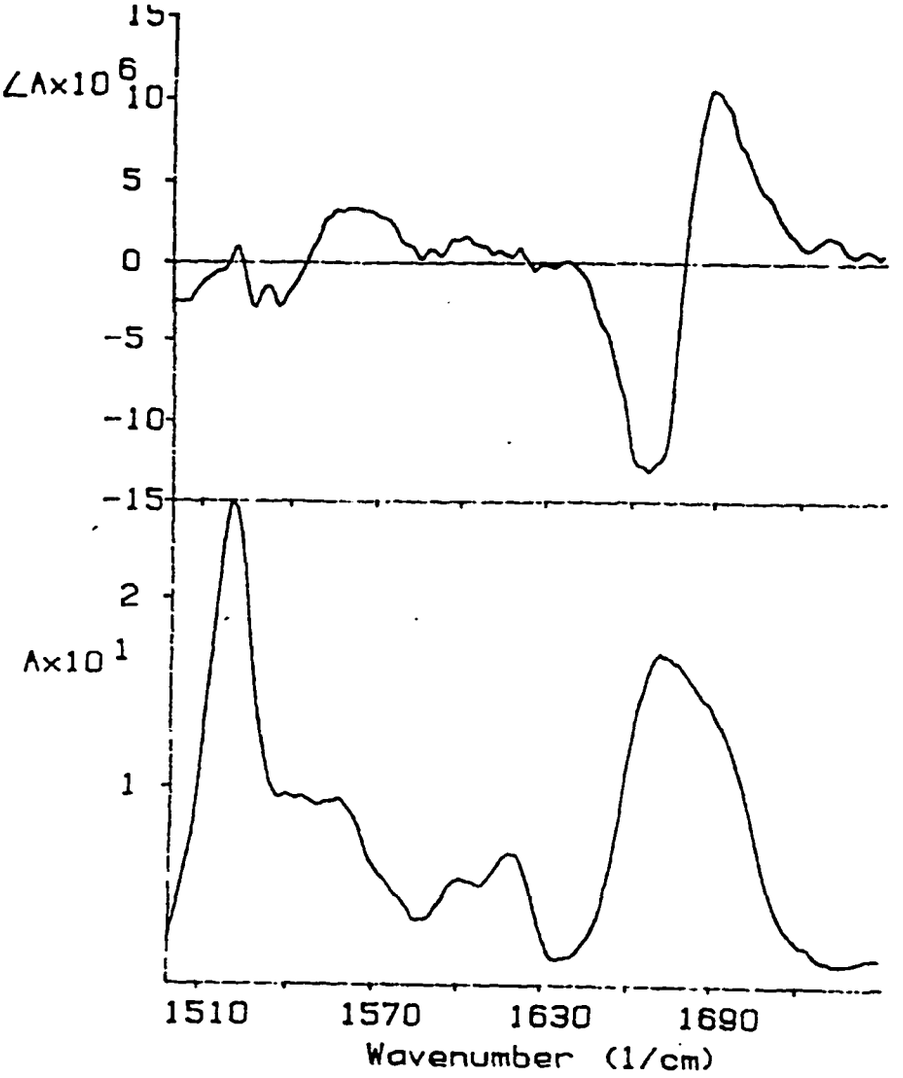

Figure 4. VCD (top) and IR absorption spectra of the "random coil" structure of poly-L-tyrosine in DMSO in the amide I / amide II region.

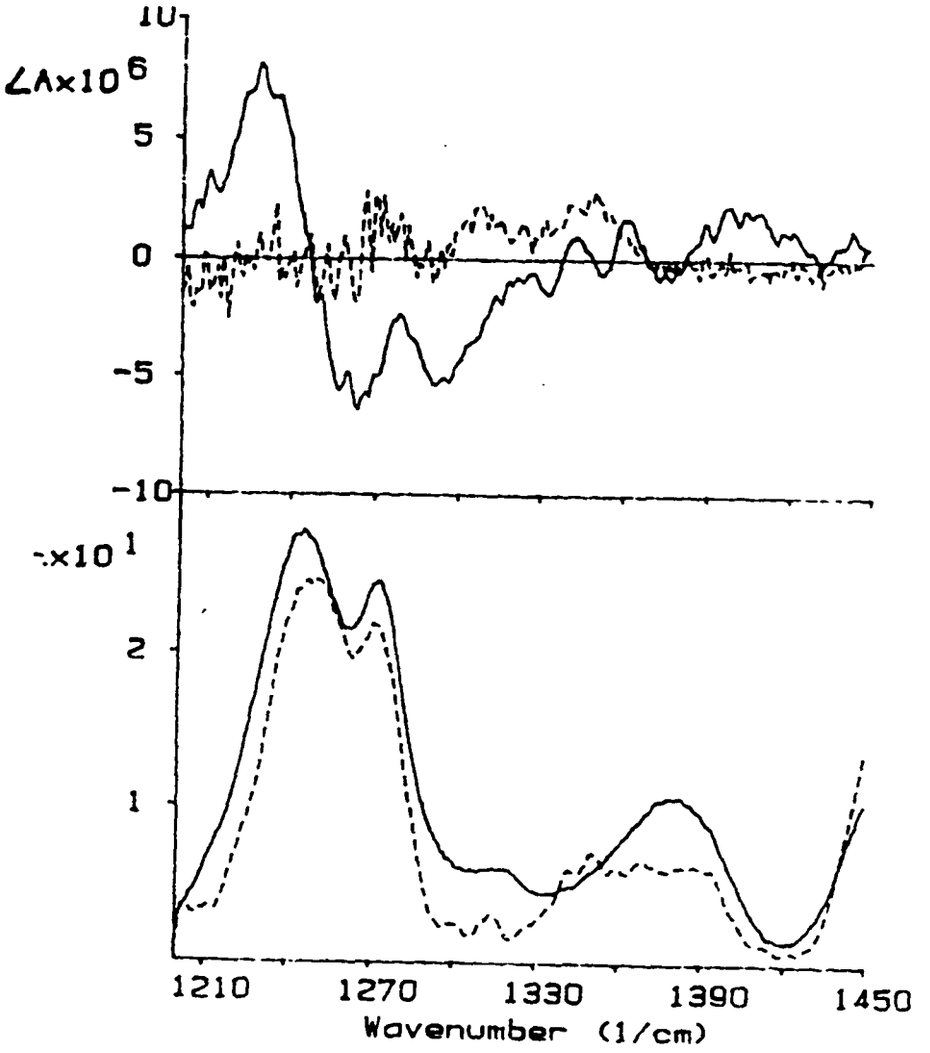

Figure 5. VCD (top) and IR absorption spectra (bottom) of the PLT in neutral DMSO. in amide III. Solid trace; "random coil." Dashed trace; α-helix.

CHAPTER THREE

VIBRA TIONAL CIRCULAR DICHROISM OF GRAMICIDIN: CONFORMATION IN LIPID BILAYER AND ORGANIC SOLVENT

In this chapter we present the first vibrational circular dichroism of gramicidin (GA) in a model lipid bilayer, dimyristoylphosphatidylcholine (DMPC), as well as in an organic solvent (pyridine). Our findings reveal that gramicidin is inserted into the bilayer as an extended left-handed helical structure, which is believed to be the ion conducting dimer that is arranged in an N- to -N-termini conformation. In pyridine, gramicidin adopts a left-handed helical structure, which has been shown to consist of a population of intertwined double helical structure. This may be a minor form of the membrane-bound ion conducting gramicidin channels. Our observations support several other spectroscopic conformational studies of GA.

INTRODUCTION:

Gramicidin (80% gramicidin A, 5% gramicidin B, and 15% gramicidin C) is a channel-forming ionophore from *bacillus brevis* that permits the passage of protons and alkali cations but is blocked by Ca^{2-}. It is a 15-residue, linear, hydrophobic polypeptide of alternating L- and D-residues that is chemically blocked at its amino terminus by formylation. It is blocked at the carboxyl terminus by an amide bond with ethanolamine:

HCO-L-VAL^{1}-GLY^{2}-L-ALA^{3}-D-LEU^{4}-L-ALA^{5}-D-VAL^{6}-L-VAL^{7}-D-VAL^{8}-L-TRP^{9}-D-LEU^{10}-L-TRP^{11}-D-LEU^{12}-L-TRP^{13}-D-LEU^{14}-L-TRP^{15}-NH_2CH_2-CH_2OH.

In gramicidin B and C, the tryptophan at position 11 is replaced by phenylalanine and tyrosine residues, respectively. NMR and X-ray crystallographic evidence indicate that gramicidins dimerize in a head-to-head fashion to form a trans-membrane channel (Fig 3-1). This observation is corroborated by observation that two gramicidin A molecules are covalently cross-linked to form a functional ion channel.

The gramicidin conformation is not α helical, because α-helices lack a central channel and can not consist of alternating L and D residues [3]. Urry [91] has proposed that Gramicidin A forms a novel helix that he named the β-helix because it resembles a rolled-up, parallel β-sheet. Successive N-H groups in the backbone of this model alternately point up and down the helix to form hydrogen bonds with backbone carbonyl groups. As a consequence of alternating D and L residues, the side chains of the β-helix hangs on its periphery to form channels with the required hydrophobic exterior. The polar backbone groups line the central channel and thereby facilitate the passage of ions. This model is consistent with results of spectroscopic and NMR measurement on gramicidin in lipid bilayers.

Although gramicidin has been used widely as a model for the hydrophobic part of intrinsic membrane proteins, we are using it to model integrated membrane proteins. Recently, it has been shown by circular dichroism [2], NMR spectroscopy [2,4,5,6], and high performance liquid chromatography [66] that gramicidin can adopt various

conformational states in hydrated phospholipid bilayers. A number of factors may determine the conformation that the gramicidin molecule ultimately adopts in phospholipid dispersion, such as the peptide/lipid ratio, the solvent used to cosolubilize the phospholipid and gramicidin, the incubation time and temperature [2,4,5,6]. Trifluoroethanol was originally suggested as a good cosolubilization solvent because of the monomeric nature of gramicidin in trifluoroethanol (TFE) solution [7]. In fact, it has been shown that when gramicidin is added to diacylphosphatidylcholine model membranes from a solution in TFE, it is incorporated directly in the $\beta^{6.3}$ conformation [8] ($\beta^{6.3}$ is a β-helical conformation with 6.3 residues per turn). By contrast, when gramicidin is incorporated from solvents such as chloroform or ethanol, in which it tends to form various, intertwined dimers, the channel structures are slow to appear [4,5]. In our study we used TFE as the cosolubilization solvent, because gramicidin adopts the $\beta^{6.3}$-helix conformer when it is solvated by TFE. Moreover, it is incorporated into the model membrane in this conformation [1], if cosolubilized in TFE.

Vibrational spectroscopy is well-suited for the study of lipid-protein interactions, since it allows the investigation of the conformation of phospholipid molecules at different levels in the lipid bilayers. More importantly, it provides direct information of the conformations of proteins in the bilayers. A number of groups have investigated the interaction between gramicidin and bilayer phospholipid bilayers, [4,9,10,11,12]. Bouchard et al.[1] used FTIR to demonstrate that the conformation adopted by gramicidin in the membrane is dependent on the cosolubilization solvent. Only when TFE is used does gramicidin adopt the β-helix conformation in dimyristoyl-phosphocholine (DMPC) model membrane.

We adapted the findings of Bouchard et al.[1], and take them a step further. We prepared gramicidin-DMPC system as described by Bouchard et al.[1]. Our absorption spectra are identical in shape and in frequency of the peak's maximum.

GENERAL BACKGROUND [1, 2]

A. Conformation of Gramicidin

Gramicidin can adopt a variety of conformations. Due to the alternating sequence of L and D amino acid residues the peptide forms β-type of helices with a hydrogen bonding pattern in the backbone similar to that in β-sheets [34-36]. In these β-helices the amino acid residues are pointing outwards and the carbonyl moieties are alternately pointing upwards and downwards in the interior of the helix, providing the helices with a hydrophilic pore. The helices may be right or left-handed, they can differ in the number of amino acid residues per turn and hence in length and diameter, and in the orientation of their side chains [34,36,37]. Individual molecules can fold into single-stranded helices that are stabilized by intramolecular hydrogen bonding and may associate end to end with additional stabilization of the dimer by intermolecular hydrogen-bonding [35,37,38]. Double-stranded helices can be formed as well, in which the two strands run either parallel or antiparallel and in which the dimer is stabilized by intermolecular hydrogen-bonding only [36]. The physical properties of these different structures of gramicidin have been reviewed recently [39,54]. Examples of the backbone configuration of two different conformations are shown in Fig.3-1.

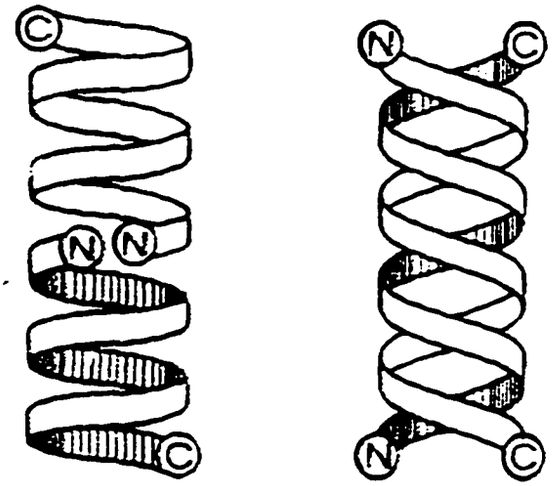

Figure 1. Schematic representation of the backbone configuration of a single-stranded N-N terminal helical dimer of gramicidin and a double-stranded anti-parallel helical dimer.

B. Crystal Structure of Gramicidin

In general the most unambiguous approach to establish the three-dimensional structure of peptides and proteins in solution or in a membrane bound form is by X-ray diffraction studies on single crystals. Although many such studies on gramicidin crystals have been reported in the past [41-48], it was not until recently that two groups simultaneously succeeded in solving two different crystal structures at high resolution [49,50].

Wallace and Ravikumar [49] prepared crystals of gramicidin and Cs^+ from methanolic solution. The crystal structure they obtained was a left-handed antiparallel dimer with 6.4 amino acid residues per turn, held together by 28 intermolecular hydrogen-bonds. This folding motif produces a pore with a diameter of 4.9 A and a length of 26 A with nearly flat surfaces at the ends of the pore. Side to side contacts between dimers were not extensive, the dimers were rather found to stack up end to end, forming contiguous tubes. This same group reported that cocrystals of gramicidin in a lipid displayed completely different properties, but they have not yet succeeded in solving the three-dimensional structure of gramicidin in these complexes [45,58, 40].

Langs [50] prepared gramicidin crystals from a benzene-ethanol mixture in the absence of ions and lipid. In these crystals too, gramicidin was present as a left handed, antiparallel, double helical dimer, held together by 28 intermolecular hydrogen bonds. However, the dimensions of the pore were quite different from those reported by Wallace and Ravikumar [49]. Both strands had 5.6 amino acid residues per turn, leading to an overall length of the dimer of 31 A and an average inner diameter of the pore of 4.8 A. The tyrptophans appeared to be orthogonally stacked in pairs of two, resulting in a structure in which the 8 indole rings of 8 tryptophans were clustered in three distinct regions, which protruded from the periphery of the probe. This would permit arrangement of long chain lipids parallel to the outer surface of the pore between the protruding tryptophan regions. The chains could then act as splines to constrain helical twist deformations of the pore. More recently, Lands and coworkers [51] elucidated the structure of gramicidin crystals prepared from methanol solution in the absence of ions,

and reported it to be an antiparallel double helical dimer, nearly identical to the one in crystals obtained from ethanolic solution, with the same length but with a larger average inner diameter of 5.09 A [51].

These different types of antiparallel dimers all appear to have suitable properties to form transmembrane ion-conducting channels in bilayers. The length is in the order of magnitude of the hydrophobic part of a lipid bilayer, the pore diameter is large enough to allow passage of small cations and the hydrophobic amino acids at the outside of the pore can interact favorably with the lipid acyl chains. Also a theoretical study on the properties of this antiparallel dimer suggested that it can act as a channel [52]. However, the antiparallal double helical dimer is at the most only a minor ion-conducting form in black lipid membranes, that occurs only under highly specific conditions [61-63].

In the sections that follow we will provide the first VCD conformational studies of gramicidin in an organic solvent and a model membrane environment.

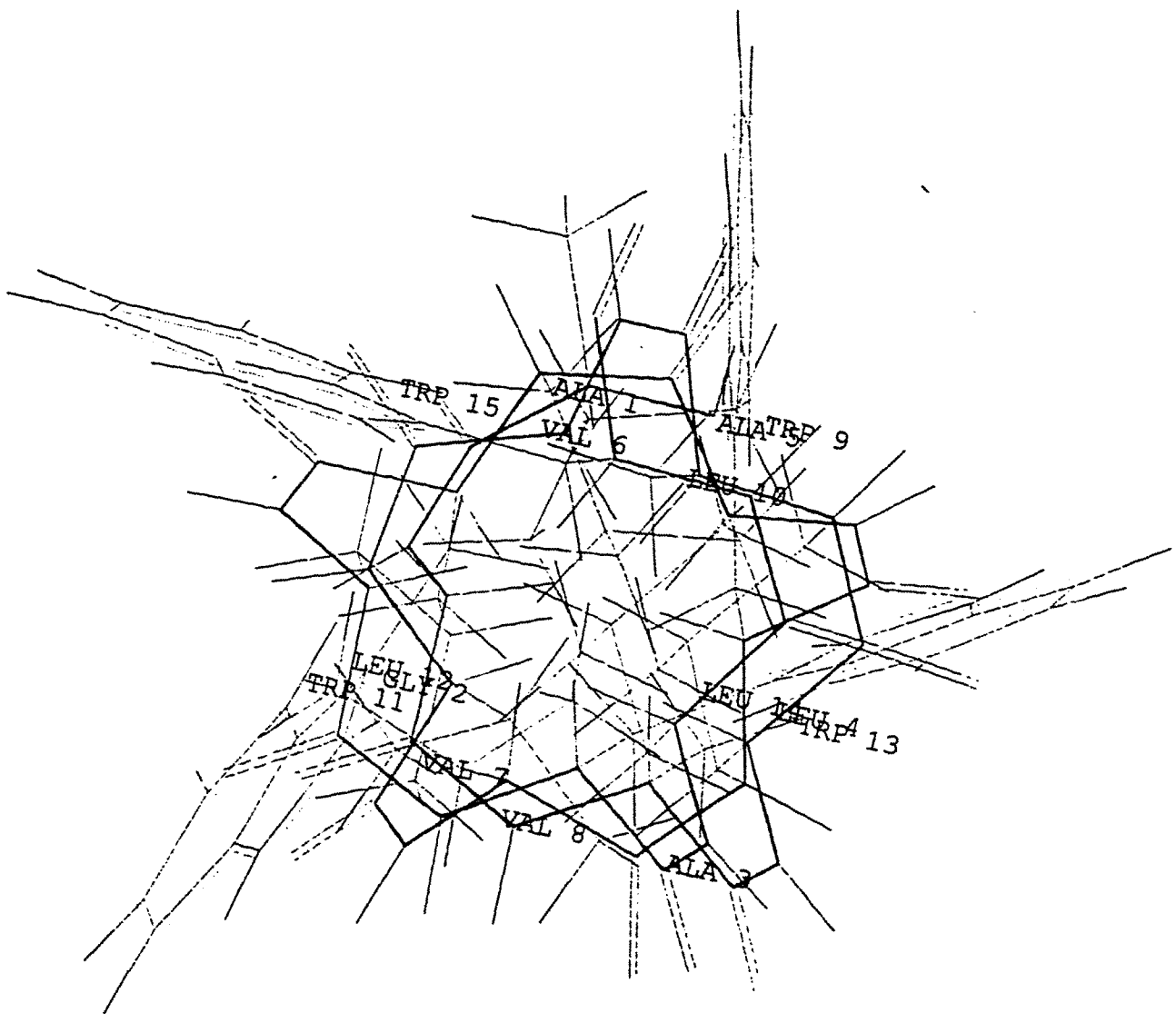

Figure 2. Axial view of a gramicidin (crystal) molecule. Constructed using Hyperchem and crystal data [49].

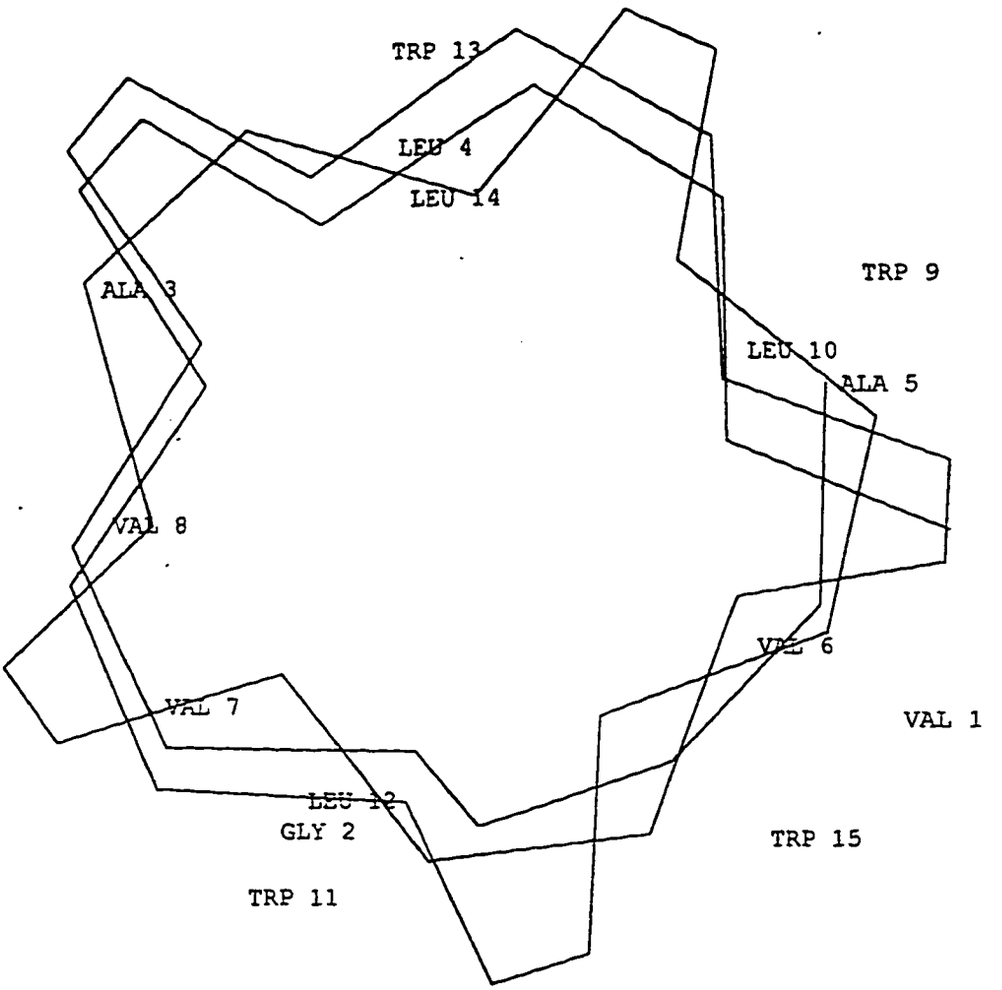

Fig.2a Backbone structure of figure 2.

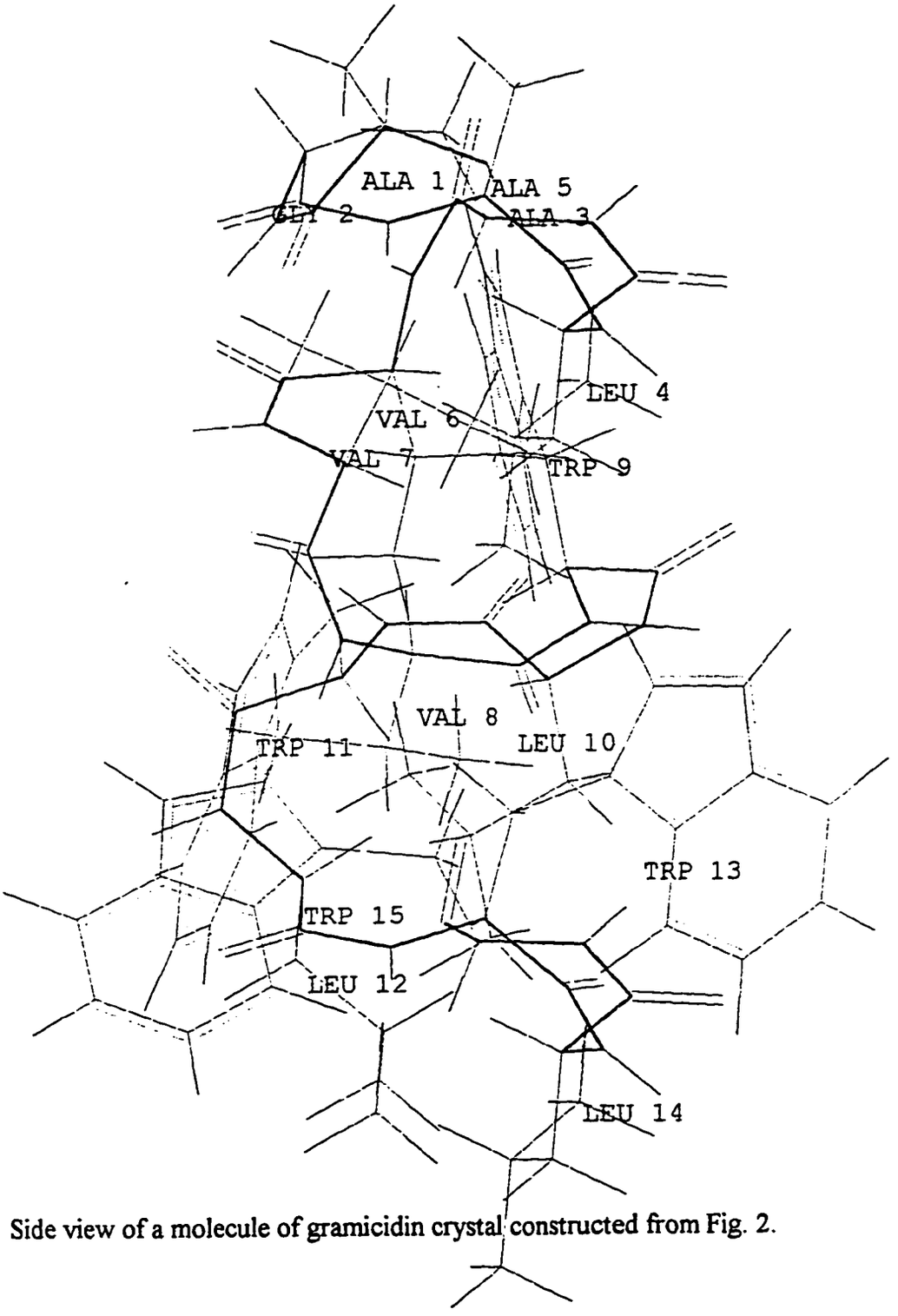

Figure 3 Side view of a molecule of gramicidin crystal constructed from Fig. 2.

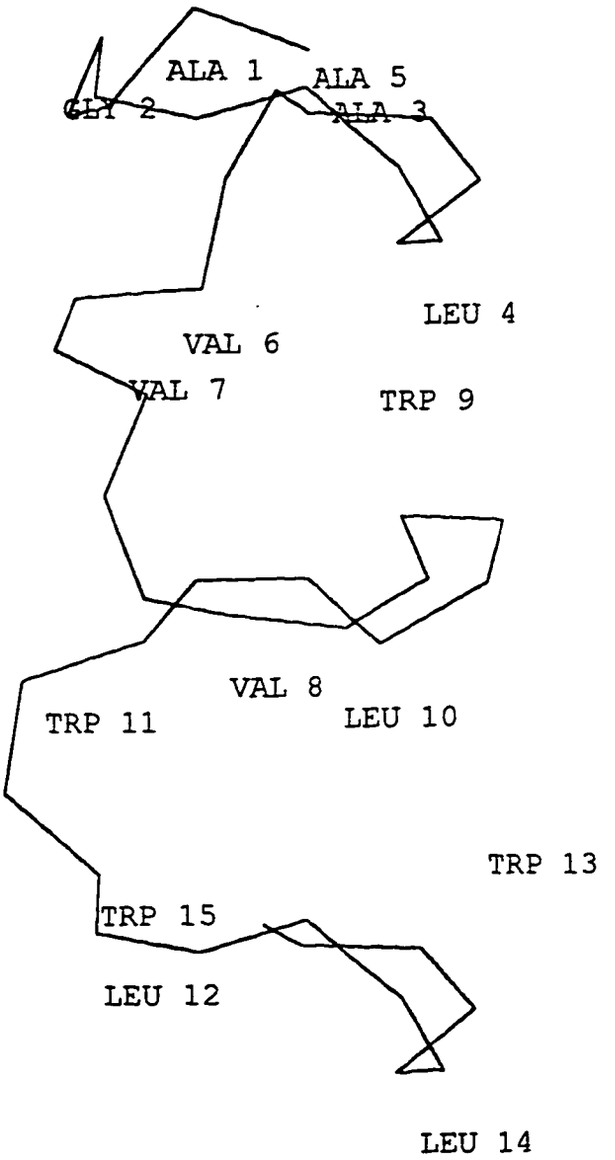

Figure 3a Backbone structure of figure 3.

MATERIALS AND METHODS.

Gramicidin and DMPC were obtained from Sigma Co. (St. Louis, MO) and used without any further purification. Trifluoroethanol (TFE) and pyridine were purchased from Aldrich Chemical Co. (Milwaukee, WI). The salts used in the preparation of buffers were of analytical grade.

Preparation of samples.

Samples of DMPC/gramicidin were prepared in approximately a 10:1 mole ratio by co-dissolving appropriate amounts of peptide and lipid in TFE.. Samples were incubated at 52 ° C for 1 to 4hrs and shaken on a vortex mixer at least a few times during the incubation cycle. After the incubation, the organic solvents were evaporated under vacuum overnight to insure complete removal of solvents. The samples were then hydrated with a Na_2HPO_4 or K_2HPO_4 (100mM) buffer at pH 7.0, prepared in D_2O, and submitted to several cyles of heating (50-52°C)-vortex shaking-cooling (20°C). For the solvent study a solution of 5 mg/mL was made.

VCD measurement.

All infrared and absorption spectra were recorded on a dipersive VCD instrument, optimized in the amide I region, the design and performance of which have been described in detail elsewhere [92,93]. The samples were loaded between CaF_2 windows at a path length of 50 μm. Spectra shown are the average of 10-20 scans at 40°C. Baselines obtained under identical conditions for solution containing buffer and DMPC or pyrimidine were subtracted from the sample VCD of DMPC/gramicidin and pyrimidine/gramicidin, respectively.

A. VCD of Gramicidin in Organic Solvent

Background [1,2]:

Conformational behavior in organic solvents

The conformations of gramicidin in organic solvents have been studied extensively with a variety of (bio)physical techniques, including nuclear magnetic resonance (NMR) [37,53-59], circular dichroism (CD) [36,44,45,60-63], infra-red (IR) and Raman spectroscopy [36,61,62,64,65], high performance liquid chromatography (HPLC) [61,66-85], thin layer chromatography (TLC) [80] and fluorescence techniques [61,63]. Urry and coworkers [62] first demonstrated the conformation to be solvent dependent. Subsequent studies by Veatch and coworkers [50,63] gave detailed insight into the complexity of the conformational behavior of gramicidin. From one organic solvent these authors were able to isolate several distinct but interconvertable conformational species of gramicidin [36], all of which were proposed to be intertwined double helical dimers. The distribution of conformations, the kinetics of interconversion from one conformation into another and the dimerization constant all were found to depend strongly on solvent polarity and peptide concentration [63]. With increasing solvent polarity an increase in monomer-dimer ratio was found and a decrease of the rate of interconversion. The percentage of dimers increased with increasing gramicidin concentration.

Four interconvertable species were found in ethanol. After separation of this by thin layer chromatography (TLC), they could be isolated with a "minimum interconversion" protocol using dioxane or ethylacetate, in which the rate of interconversion was extremely slow [36]. The major species was postulated to be a double helix with antiparallel β hydrogen-bonding and could be obtained by crystallization from ethanol. Using the same protocol, Arseniev and coworkers [53] identified and characterized these species by two-dimensional NMR techniques, as two left-handed parallel helical structures, one left-handed anti-parallel helices, and one right-handed parallel; all had 5.6 residues per turn. All were found to be double helical dimers with a handedness and hydrogen-bonding pattern, as proposed earlier by Veatch and Blout [63].

These species were denoted 1, 2, 3, and 4 in order of increasing mobility on TLC by Veatch and Blout [63]. It was concluded that species 1, 2 and 4 are probably helical structures with largely parallel-β hydrogen bonding; species 1 and 2 have a handedness opposite that of species 4. Species 3 has largely antiparallel-β hydrogen bonding. However, Sychev et al [61], via a detailed experiment and analysis, proposed that these species are indeed anti-parallel with species 1-3 exhibiting left helical sense as opposed to the right-handednes of species 4.

From dimerization constants [63] a change to dominantly monomeric conformation can be expected at very low concentrations, i.e., below the 10-100 μM range. This is in agreement with size-exclusion HPLC studies. Using 40 μM solutions of gramicidin in ethanol, the majority of gramicidin molecules are present as double helical dimers with a substantial amount of monomer also present [66]. At the same peptide concentration in methanol a monomeric form was observed almost exclusively [66]. Indeed, the dimerization constant for this slightly more polar solvent predicts a shift of the equilibrium in favor of dimers only at higher concentrations of about 5 mM [63]. In chloroform/methanol solutions a similar distribution of monomers and dimers was observed as in methanol [66].

CD studies of gramicidin in methanol indicated a reversal of the handedness upon binding of cations and a change in helical pitch that was dependent upon the type of cation bound [15,44,60]. Two-dimensional NMR studies showed that gramicidin in chloroform/methanol solution in the presence of Cs^+ forms a right-handed antiparallel double helical dimer with 7.2 amino acid residues per turn [54].

In the more polar solvent dimethylsulphoxide (DMSO) it can be calculated that, even at concentrations as high as 50 mM, more than 70% of gramicidin is present in a monomeric form [63]. A number of studies have been carried out on the conformation of gramicidin in this solvent [69,56,58-74,59,62,65]. While these studies are consistent with a monomeric conformation, controversies still exist about the secondary structure of the monomeric form . Several authors [56,58,62] proposed that an equilibrium is present in which there are rapid transitions from an unordered structure to an ordered one, the latter

being a helical structure consistent with a left-handed $\beta^{6.3}$ helix. Others proposed an LD-ribbon structure, whereas the most recent study [59] indicated a random coil behaviors with many rapidly interconverting conformations.

In trifluoroethanol (TFE), which is also highly polar, the conformation of gramicidin was proposed to be similar to that in DMSO [62]. Although the peptide does not behave exactly the same in these two solvent, as can be inferred for instance from differences in ion-binding [86,70], it is clear that in TFE gramicidin is preferably present in a monomeric form as well.

Gramicidin-Pyridine System:

In this section we present the first VCD and ir spectra of gramicidin (GA) in pyridine to illustrate its conformational behaviour in an organic solvent. As mentioned earlier, most studies have shown that GA exists in a monomeric conformation when in solution with polar organic solvents like DMSO, methanol and to a minor extent ethanol. However, questions remain about the secondary structure of this monomeric form. Thus, here we have applied VCD spectroscopy (a proven tool for elucidation of peptides' helical structures) to resolve the secondary structure of GA in pyridine solution; a polar solvent. Many solution conformational studies of GA had been conducted in organic solvents, this is perhaps the first study carried out in pyridine.

Absorption Spectra

Fig. 3-4 shows the ir absorption (bottom) and the VCD (top) spectrum of gramicidin dissolved in pyridine. The amide I band is characterized by a major peak with a maximum at 1633 cm^{-1} , a shoulder at 1646 cm^{-1} and a minor peak at 1685 cm^{-1}. These peaks have been assigned previously to specific structural conformations by several authors [36,61,64,65]. Sychev et al. [61] demonstrated that the main peak for GA monomers and dimers can be used to distinguish between this structures. The main peak position for monomers is at 1650 cm^{-1} , while that of dimeric form is at 1634 cm^{-1}. From their detailed study these workers ascribed characteristic absorption peaks to each of the four dimeric species form GA (see above). Our amide I band of GA in pyridine resembles very closely the band ascribed to species 3 of GA. This GA conformational species is thought to contain at equilibrium three different intertwined double helical structures, each with different numbers of residues per turn. There are left handed and anti-parallel in orientation. The predominant dimer of species 3 has 5.6 residues per turn

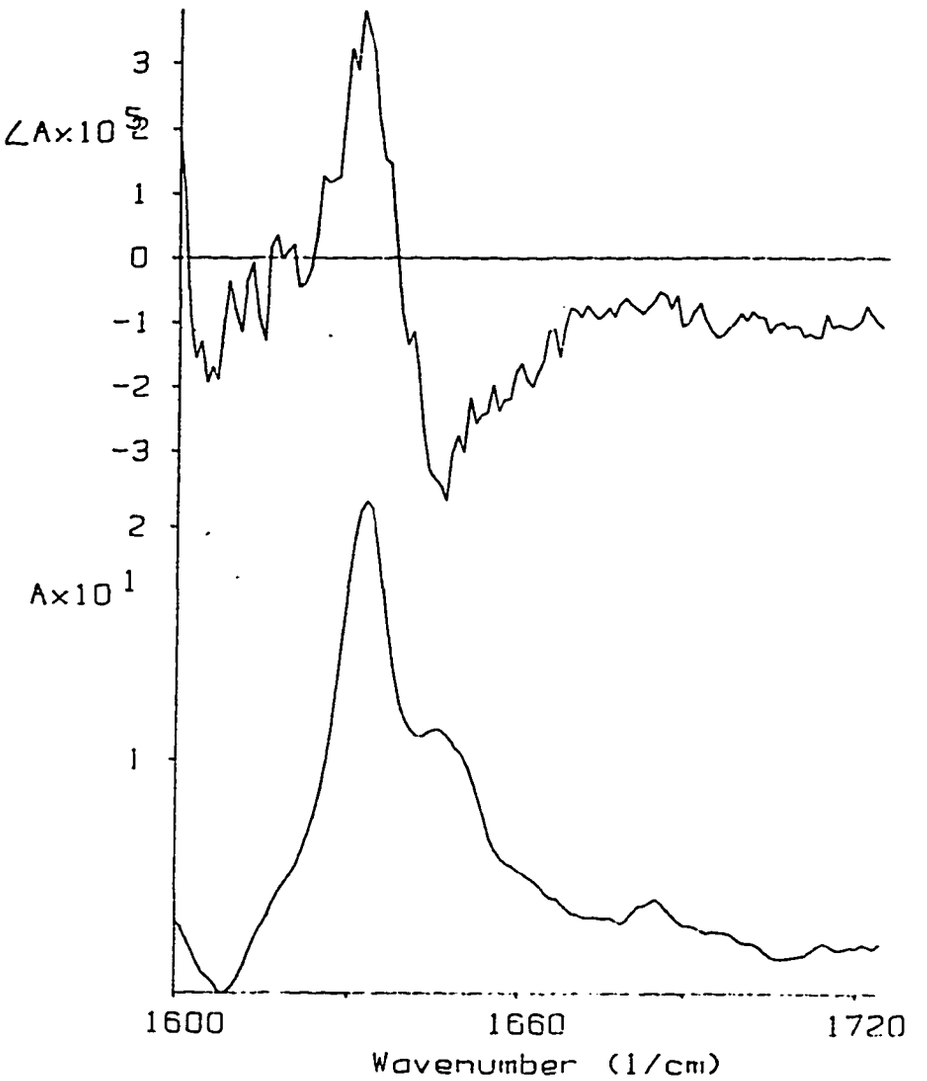

Figure 4. Gramicidin dissolved in pyridine (5mg/mL); 50μ pathlength;

and is designated $\uparrow\downarrow \pi\pi_{LD}^{5.6}$. The next abundant species is designated $\pi_{LD}^{4.4}\pi^{4.4}{}_{LD}$ and the third is $\pi_{LD}^{6.3}\pi^{6.3}{}_{LD}$. These are distributed as 0.75, 0.15 and 0.10 respectively.

Furthermore, Veatch et al [36] assigned a major peak at 1633 cm^{-1}, with a shoulder at 1650 cm^{-1}, and a resolved peak at 1680 cm^{-1} to species 3. In these studies [36,61] the structures of species 3 were "trapped" in dioxane to minimize interconversion among GA conformational species. Although pyridine is relatively more polar than dioxane, it appears to favor GA species 3.

VCD Spectra

The VCD spectrum exhibits a near-conservative positive single VCD couplet; i.e. a positive/negative VCD peaks from low to high wavenumbers of near equal amplitudes [89]. The zero crossing occurs at approximately 1632 cm^{-1}. This VCD pattern is opposite to that previously described for poly(β -benzyl-L-aspartate) (PBLA) and poly(*im*-benzyl-L-histidine) (PBLH) by Lal and Nafie [90] in that it is a positive couplet. PBLA and PBLH are model polypeptides, that are prototypical of left-handed α-helix. These polypeptides assumed a left handedness when they were dissolved in chloroform [90]. In their study, Lal and Nafie reported a left handed α-helix for a negative couplet. The negative VCD couplet occurs at 1660 cm^{-1}, while ours occurs at 1632 cm^{-1} and it is a positive coupplet. That our observed positive couplet is incident at around 1634cm^{-1}, strongly suggests that the pyridine solution mostly consisted of antiparallel double helical dimers, as oppose to monomers that would have occurred at 1650 cm^{-1}[61]. We ascribed left handedness to the observed VCD spectrum in figure 4. Also our calculated spectra supports our conclusion (see figure 8). Dihedral angles used in the computation of the calculated spectra was derived from a crystal of GA, that is an antiparallel left handed, double stranded $\beta^{5.6}$ helix. Furthermore, our observation is consistent with the findings of Sychev and coworkers' [61] (see above). Thus, we conclude that GA adopts an

antiparallel left handed, $\beta^{5.6}$ helical dimer in pyridine. The dimer has 5.6 residues per turn, and it is characterized by a positive VCD couplet, as indicated in figure 4.

B: VCD of Gramicidin in a Model Lipid Bilayer (DMPC)

Background [1,2]:

Already about a decade ago several lines of evidence reported that gramicidin in lipid vesicles was oriented with its C-terminus near the lipid/water interface and its N-terminus buried in the hydrophobic part of the bilayer, consistent with the channel conformation. This was first demonstrated independently by NMR on ^{19}F and ^{13}C-labeled gramicidin analogs and by fluorescence energy transfer measurements on gramicidin incorporated into dimyristolphophatidylcholine (DMPC) model membranes. Since then a variety of techniques have been applied to get more detailed insight into the orientation and conformation of gramicidin in bilayer systems. These techniques include CD [45,72,74,75], fluorescence [67,69,99], IR and Raman spectroscopy [65] high resolution NMR to monitor the interaction of gramicidin with different cations and solid state NMR [77-80]. Most of these studies were consistent with gramicidin being present in a $\beta^{6.3}$ helical conformation. Solid state NMR studies furthermore showed that the peptide is undergoing rapid reorientation about its long axis and that this axis is oriented parallel to the bilayer normal [78]. Recently, additional unambiguous and independent evidence reported a right-handed helix in SDS micelles and in DMPC bilayers is found [80]. This

was shown in an elegant study on chemical shift resonances of gramicidins that were ^{15}N-labeled at specific sites along the peptide backbone and incorporated into DMPC bilayers, oriented between glass plates [80].

Using different NMR techniques it is possible to characterize the structure and dynamics of the entire peptide backbone on an atomic level. So far, ^{2}H-NMR techniques have been used to study the orientation and dynamics of the $C_{\alpha}D$ bonds at specific sites along the backbone and of all ND bonds in hydrogen-exchanged peptides. Using ^{13}C-gramicidin, NMR information could be derived on the carbonyl groups of the backbone [78], while ^{15}N-NMR studies on the chemical shift [80], dipolar interactions and relaxation behavior yielded detailed information on the orientation and dynamics of different NH sites in the peptide backbone.

^{13}C-NMR data suggested a greater motional freedom of the channel near the C-terminus, based on differences in linewidth of the carbonyl resonances at different sites along the backbone [79]. ^{2}H-NMR measurements on the other hand, indicated that there was no substantial variation in the amplitude of molecular motions along the channel axis. A possible explanation for this discrepancy is that in the former study the interpretation of differences in linewidths may have been incorrect [2]. Also, based on differences in linewidth it was reported that the C-terminal part of the channel, but not the N-terminal part, is perturbed by addition of Na^{+} -ions [77]. However, the structural consequences of such perturbation can only be minor, since CD patterns of vesicle-bound gramicidin were found to be insensitive to the presence of cations [44,75,76]. In agreement with this recent X-ray measurements indicated that the pitch of the helix and the total channel length of gramicidin in a PC bilayer do not change on addition of cation [81].

Tryptophan side chains have been extensively investigated with NMR techniques. These side chains are important for the functional activity of gramicidin. Their damage by ultraviolet irradiation or chemical modification by formylation results in a loss of channel function. Using gramicidin containing perdeuterated tryptophan, it was demonstrated that these side chains are essentially immobile when the peptide was incorporated into bilayers with lysophosphatidyl choline (LPC) [84]. Results obtained in phosphatidylcholine (PC)

bilayers were difficult to interpret, because in these systems the entire molecule undergoes fast rotational motion leading to partial averaging of each of the NMR signals [84]. Detailed information on the orientation or dynamics of individual side chains is presently being derived from NMR measurements on gramicidins in which the individual tryptophans contain either a ^{15}N label [84] or ^{13}C labels at specific positions in the aromatic ring [85,86]. At present there is no consensus on the orientation of these residues in a PC bilayer. ^{13}C-NMR results [85] indicated that the orientations of the tryptophans are approximately similar to those proposed by Arseniev and coworkers [73]. Recent Raman spectroscopic data [87] suggested two possible models for the orientation of the tryptophan side chains, that both were different from those in Arseniev's model.

The fluorescence properties of tryptophan have also been used to investigate the orientation and dynamics of these residue in a lipid bilayer. By varying the temperature, pressure and viscosity of the surrounding medium, information could be obtained on the rotational motion of the tryptophans, the extent of inter- and intramolecular stacking-interactions, and on H-bonding of the tryptophan NH group with H-acceptors near the lipid headgroup [67,69]. Such H-bonding was proposed to be important for stabilization of the $\beta^{6.3}$ conformation and to be important for channel formation [67,68]. One obvious candidate to participate in H-bonding are lipid carbonyls. Meuledijks and coworkers [88] reported a change in permeability characteristics due to a weaker H-bond when using etherlipids. Also CD studies [45] suggested that there is a specific interaction between the lipid carbonyl and the carboxyterminus of the polypeptide, which may be important for stabilizing the membrane conformation. However, ^{13}C-NMR measurements showed similar characteristics of the peptide in ester and ether lipids [78,79], suggesting that the lack of H-bonding to the carbonyl does not result in significant structural changes.

The results and discrepancies mentioned above merit a further study of gramicidin in lipid bilayer via new spectroscopic methods. We choose VCD that can distinguish different conformational state of peptides. In the section that follows we present the first ever VCD spectra of GA in a DMPC in the presence of two separate aqueous solutions: K_2HPO_4 and Na_2HPO_4.

Results

Absorption Spectra

Fig. 3-5 shows the ir and VCD spectra of gramicidin-DMPC dispersed in 100 mM aqueous potassium bisphosphate (K_2HPO_4) buffer at pH 7.0. There is a single absorption peak with a maximum at ~1629 with a broad decreasing shoulder spanning ~1645 cm^{-1}. Although not shown here the FTIR spectrum of this solution resembles that observed by Bouchard et al. [1]. This structure is interpreted to be the $\beta^{6.3}$ conformer of GA in DMPC [1]. This is in agreement with several other studies [2,4,5].

VCD Spectra

The VCD spectrum exhibits a very weak negative/positive couplet, which has been described to be characteristic of a "random-coil" conformation, but which we (and other research groups [90]) have interpreted as the VCD spectrum of a left-handed, extended helix. Here the VCD peaks have a single zero-crossing at approximately 1629 cm^{-1}. In addition, there appears to be a single less intense negative peak positioned above the shoulder peak of the ir spectrum, which is absent from the gramicidin-pyridine's VCD spectrum. Fig. 3-6 is obtained from gramicidin-DMPC system that is solvated in 100 mM sodium bisphosphate buffer with a pH of 7.0. The ir and VCD spectra are virtually identical to Fig. 3-5. Since gramicidin is believed to be in the ion-channel conformer when associated with lipid (DMPC), it is reasonable that the spectra are identical.

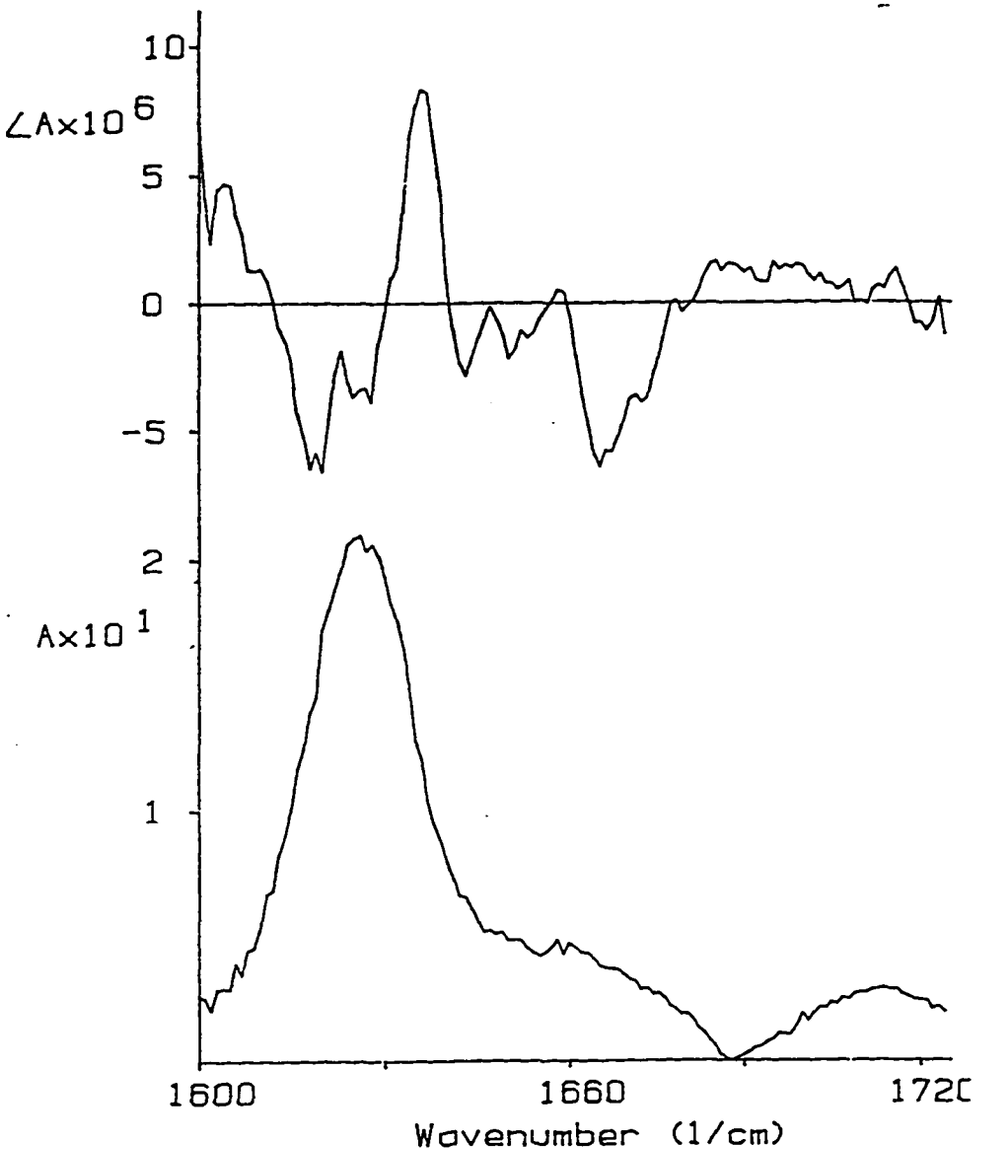

Figure 5. Presumed head-to-head $\beta^{6.3}$-helix gramicidin channel. Gramicidin (56mg)-DMPC (100mg) system hydrated with 100mM K_2HPO_4 buffer at pH 7.0; VCD (top) ;ir absorption (bottom) ; 50μ pathlength.

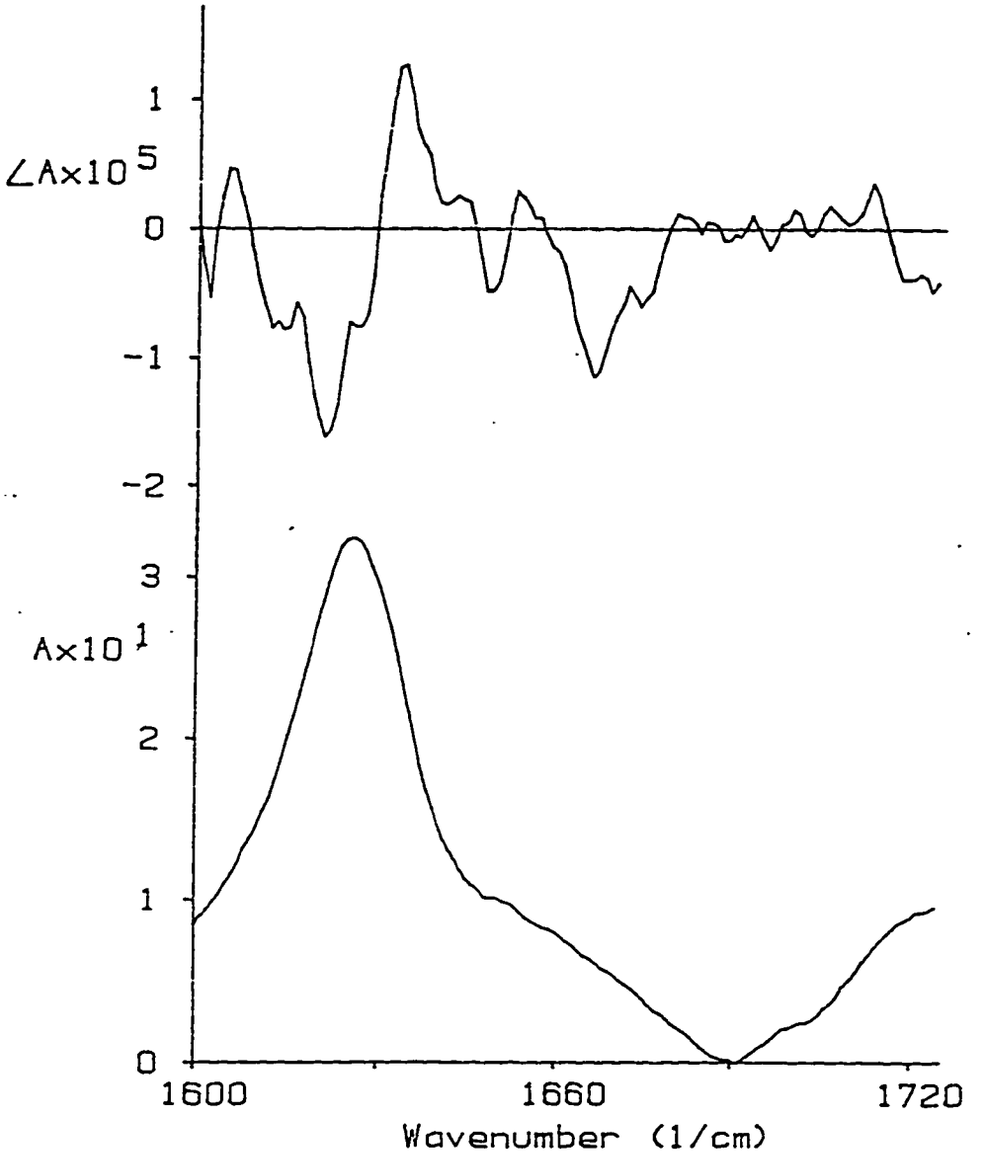

Figure 6. Presumed head-to-head $\beta^{6.3}$-helix gramicidin channel. Gramicidin(54mg)-DMPC(100mg) system hydrated in 100mM Na_2HPO_4 at pH 7.0; VCD (top); ir absorption (bottom); 50μ pathlegth.

C. Computational Procedures

Infrared absorption and VCD intensity calculations were carried out via the extended coupled oscillator (ECO) formalism, which is based on Tinoco's exciton description of the rotary power of polymers [24(ch.2)]. In this formalism, the rotational strengths for each of the *k* exciton components of an *n*-mer of coupled transitions can be written as [4(ch.2)].

$$R_k = -(\pi \nu_0 / c) \sum_{i=1}^{n} \sum_{j\neq i}^{n} C_{ik} C_{jk} (\mathbf{T_{ij}} \cdot \mu_i \times \mu_j) \qquad 3.1$$

Here, μ_i and μ_j are the interacting dipole moments, separated by vector T_{ij}, ν_0 is the frequency of the uncoupled transition, and *c* the velocity of light. The c_{ij} are the eigenvector components of the dipole-dipole interaction matrix V_{ij}.

$$V_{ij} = \frac{\vec{\mu}_i \cdot \vec{\mu}_j}{|T_{ij}|^3} - 3\frac{(\vec{\mu}_i \cdot \vec{T}_{ij})(\vec{\mu}_j \cdot \vec{T}_{ij})}{|T_{ij}|^5} \qquad 3.2$$

Each of the terms in the summation in eq 3.1 is equivalent to a coupled oscillator expression for a simple coupled dimer. The summation is over all pairwise interactions, weighted by the eigenvector coefficients. Inclusion of all coupling interactions is particularly important in peptide helices, where the coupling energy between carbonyl group *i* and *i*+3 is still relatively large [21(ch.2)].

The ECO expression in eq 2.1 above formally appears similar to the fixed charge equation derived by Schellman [17(ch.2)]. However, eq 3.1 is accurate within the exciton formalism and relies only on observable quantities, such as the dipole transition moment and geometric parameters.

The infrared absorption intensities can be obtained from the dipole strengths, *D*, defined by

$$\mathbf{D_k} = \sum_{i=1}^{n} c_{ik}^2 \, \mu_i^2 + 2 \sum_{i=1}^{n} \sum_{j>i}^{n} c_{ik} c_{ij} (\mu_i \cdot \mu_j) \qquad 3.3$$

The computations are carried out as follows. Structures for various GA conformations were generated using Hyperchem program (SciVision, Inc., Lexington, MA) running on a desktop computer equipped with a 90MHz Pentium processor. Hyperchem permits the creation of peptide structures using predetermined conformational angles for right- and left-handed α-helices, as well as for a number of other common structures. Alternatively, as in this case, the ϕ and ψ angles may be input manually to create less common structures, while the amino acid sequence is specified. No energy minimization of the structures was performed, since it is important for the following VCD calculations that the structures are the ones actually specified via the input parameters.

The Cartesian coordinates of all atoms of the peptides were fed into the ECO program, written in our laboratory, which selects the carbonyl C and O atoms, and attaches transition dipole moments along the C=O bond. The dipole transition moment for an amide I vibration was taken to be $\mu = 0.29$ D $= 0.29 \times 10^{-18}$ esu cm, in agreement with the work by Snir et al. [21(ch.2)] and our own previous peptide VCD data.

The rotational and dipole strengths were converted to spectra by overlaying Gaussian, Lorentzian, or mixed band shapes. In the results reported here, 100% Gaussian band shapes with a half-width (at half-heights) of 10 cm^{-1} were used. The resulting spectra are reported in absorbance units and normalized with respect to the number of residues in the computed structures.

Figures 7 through 13 show computed spectra of GA in different chemical environments. Figure 7 was derived from x-ray crystallographic studies of GA by Wallace and Ravikumar [49]. The GA crystals were complexed to Cs^+ in a methanolic solution in the abscence of any phospholipid. Torsional angles for L-residues are specified as ϕ = -149, ψ = 114, and those for D-residues are ϕ = 84, ψ = -89. Wallace and coworker describe this molecule to be a left-handed helical ion pore with 6.4 residues per turn. However, the VCD spectra computed from this data generates the only fit to our

GA-membrane results (fig. 5 and 6). This suggests that GA is proabably present in the DMPC bilayer as left-handed structure. In addition, figure 7 is identical to a previously calculated VCD spectra generated in our laboratory, to which we interpreted as an extended left-handed helical structure in the last chapter. On the other hand, these spectra (Fig.5 and 6) somewhat share patterns assigned to right handed helical structures by previous VCD studies [88-90] that were conducted in chloroform solutions. In comparison to the study of Wallace and Ravikumar [49], our two studies are similar in that GA is present in the ion-conducting conformer associated with cations; K^+ and Na^+ ions in our study, and Cs^- in theirs. However, a critical difference between these investigations is that our studies were conducted in solutions (e.g. GA embedded in a lipid membrane). That we assigned similar handedness complies with the idea that it is the overall secondary structure of GA that we are observing in both studies. Moreover, GA is known to assume a variety of conformations in solutions and in crystals; thus it is not surprising that both calculated (fig. 7) and solution VCD spectra (fig.5 and 6) are similar.

Figure 8 and 9 were computed from x-ray data generated from uncomplexed GA crystals by Langs[50]. The crystals were grown from benzene-ethanol azeotropes, a solution that can be considered to have similar polarity to pyrimidine used in our GA-solvent studies. In figure 8 the ϕ angle is -152 and ψ angle 110 for L-residues, while ϕ is -101 and ψ is -142 for D-residues. These calculated VCD spectra match our result in pyridine. These features are ascribed to left-handed helical structures. Langs [50] described this GA conformation to be a left-handed, antiparallel double-stranded helical dimer with 5.6 amino acid residues per turn. Figure 9 was generated from an idealized $\beta^{5.6}$ helix, and is proposed to be of left-handed helical sense as well. Both of these observations accede to the handedness predicted by computations and observed experimentally in our studies.

Figures 10 through 13 were generated from other models of double helix motifs of GA none of which fits our experimental computed data. Figure 10 and 11 were proposed by Chandrasekaran et al. [94] for double helical structures with approximately 5 and 7 residues per turn, respectively. They estimated the ϕ, ψ angles in the helix with 5 residues

per turn to be -135, 140 and 160, -120 for L- and D-amino acids, respectively, and for the 7 residues per turn helix to be -135, 165 and 140, -140, respectively. Lotz et al. [95] used parameters from model L, D-compounds to propose double helices with 5.6 residues per turn ϕ, ψ angles of -116, 141 and 159, -130; they also considered helices with 7.2 residues per turn, where the ϕ, ψ angles were -127, 146 and 154, -126. These are represented in figures 12 and 13. It is clear that none of the spectra generated from these values fit any of our data. This goes to the heart of the geometry sensitivity of degenerate extended coupled oscillator (DECO) formalism. Note that figures 10 through 13 show shift of amide I peak toward lower frequency, these are not in agreement with our experimental results.

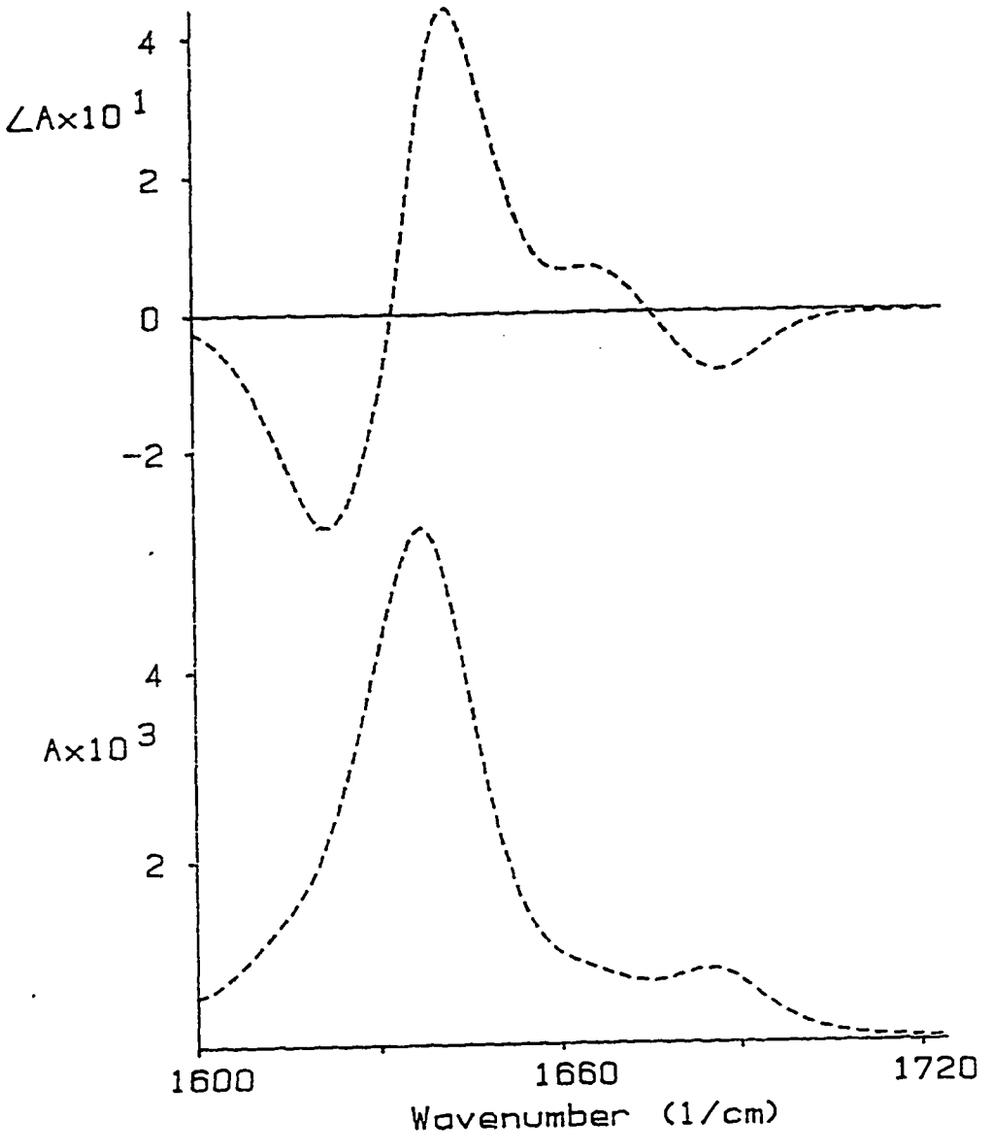

Figure 7. Presumed head-to-head $\beta^{6.3}$-helix gramicidin channel. For the observed spectra see figure 5 and 6. Calculated spectra of gramicidin crystal from x-ray crystallographic data. L-amino acid ; $\phi = -149$ $\psi = 114$ D-amino acid ; $\phi = 84$ $\psi = -89$

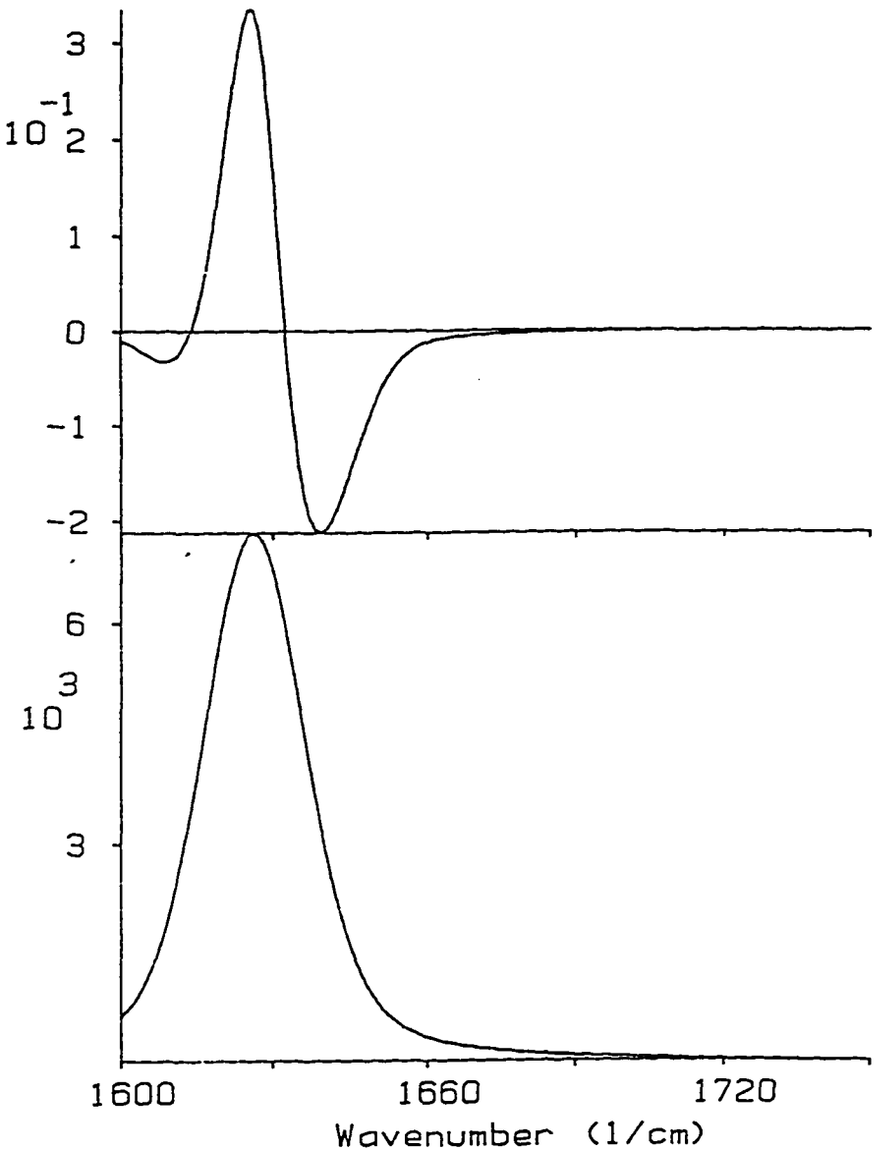

Figure 8. Presumed head-to-head $\beta^{5,6}$-helix gramicidin channel [49]. For the observed spectra see Figure 4. Calculated of gramicidin crystal from x-ray crytallographic data. L-amino acid; ϕ = 152 ψ = 110 D-amino acid; ϕ = -101 ψ = -142

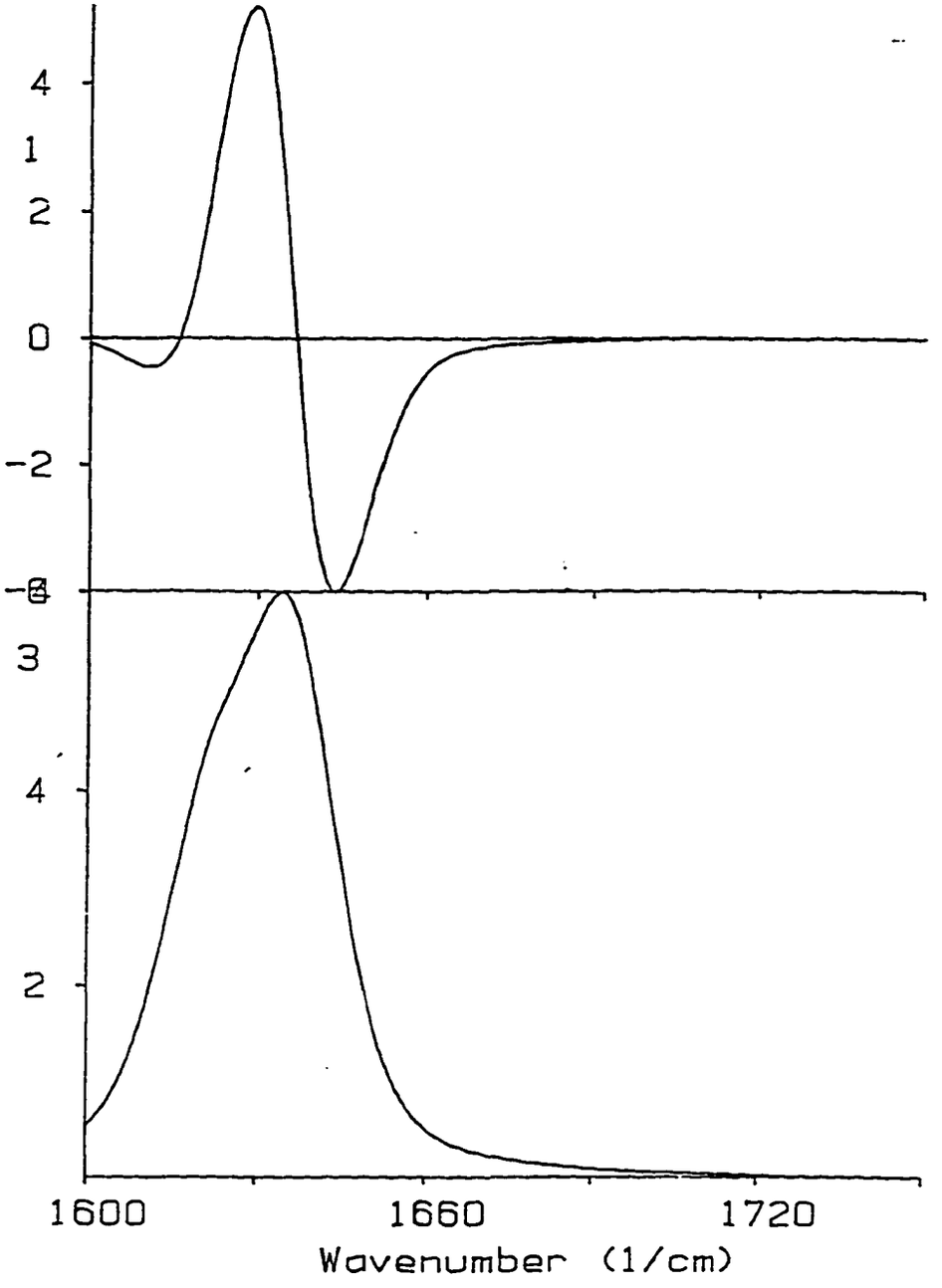

Figure 9. Calculated of gramicidin crystal from x-ray crytallographic data.
L-amino acid; ϕ = 141 D-amino acid; ϕ = 102
ψ = 116 ψ = -159

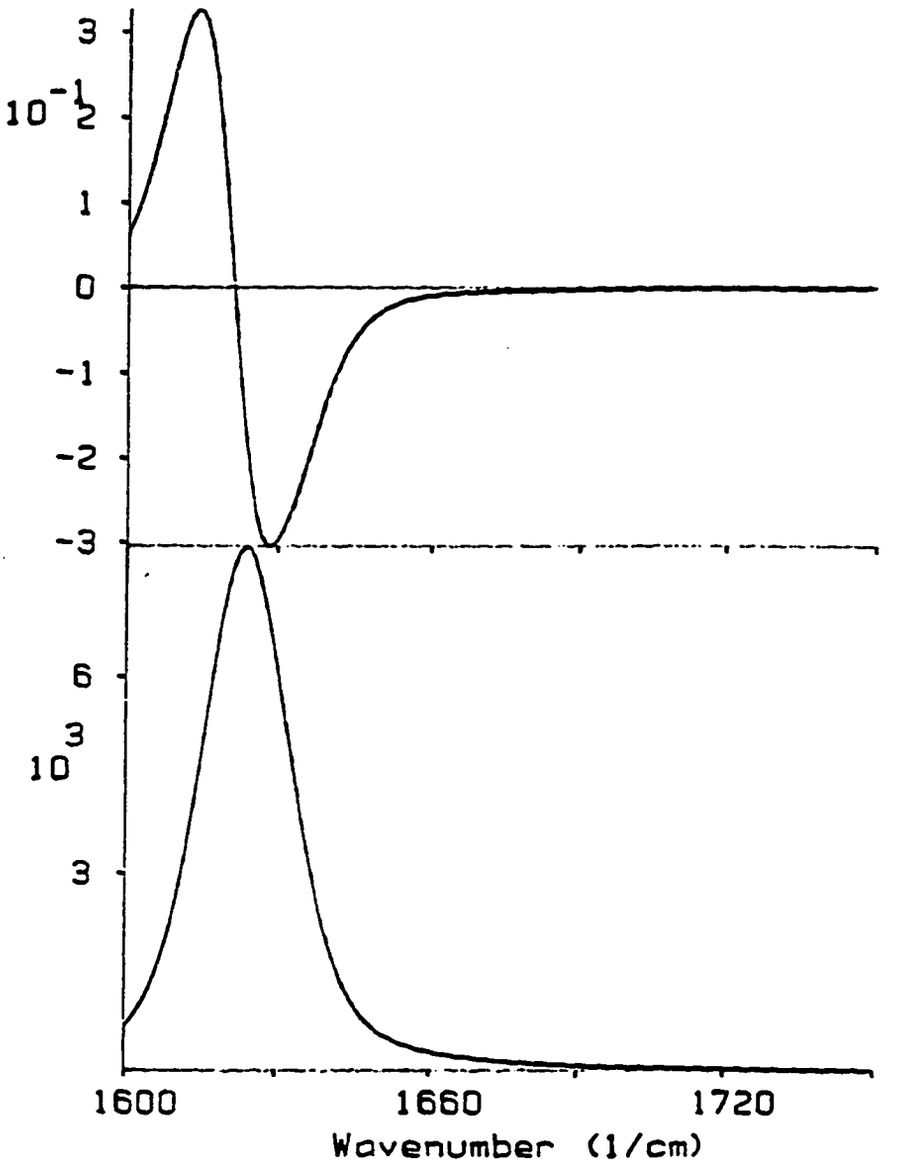

Figure 10. Calculated of gramicidin crystal from x-ray crytallographic data [94].
L-amino acid; ϕ = -135 D-amino acid; ϕ = 160
ψ = 140 ψ = -120

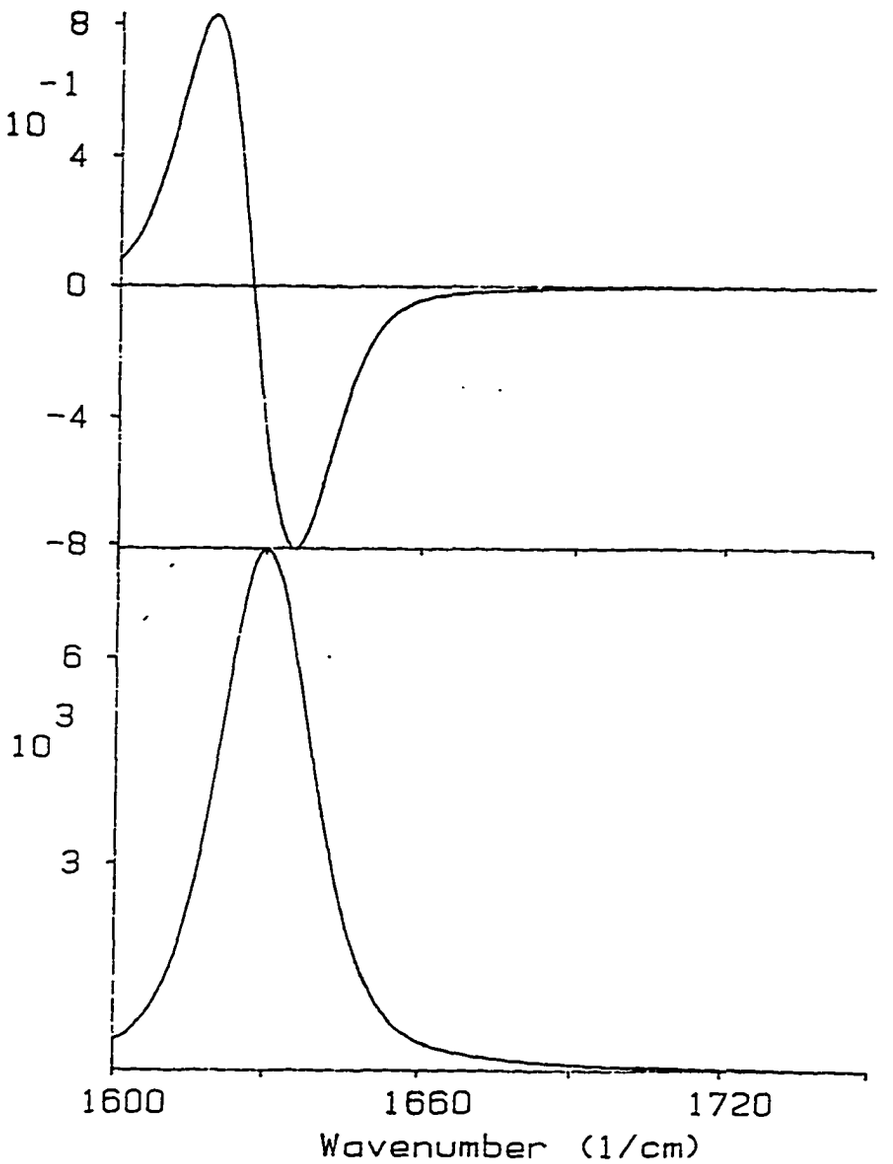

Figure 11. Calculated of gramicidin crystal from x-ray crytallographic data [94].
L-amino acid; ϕ = -135 D-amino acid; ϕ = 140
ψ = 165 ψ = -140

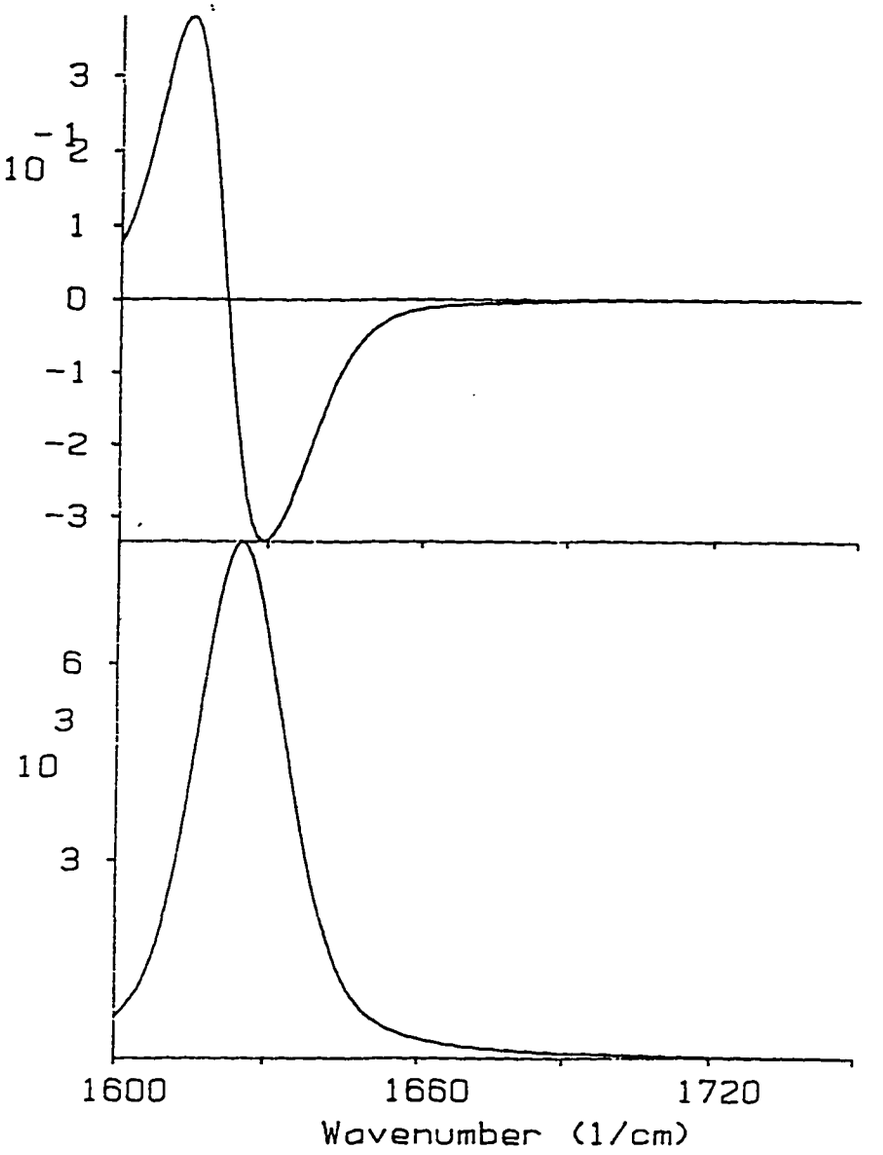

Figure 12. Calculated of gramicidin crystal from x-ray crytallographic data [95].
L-amino acid; ϕ = -116 D-amino acid; ϕ = 159
ψ = 141 ψ = -130

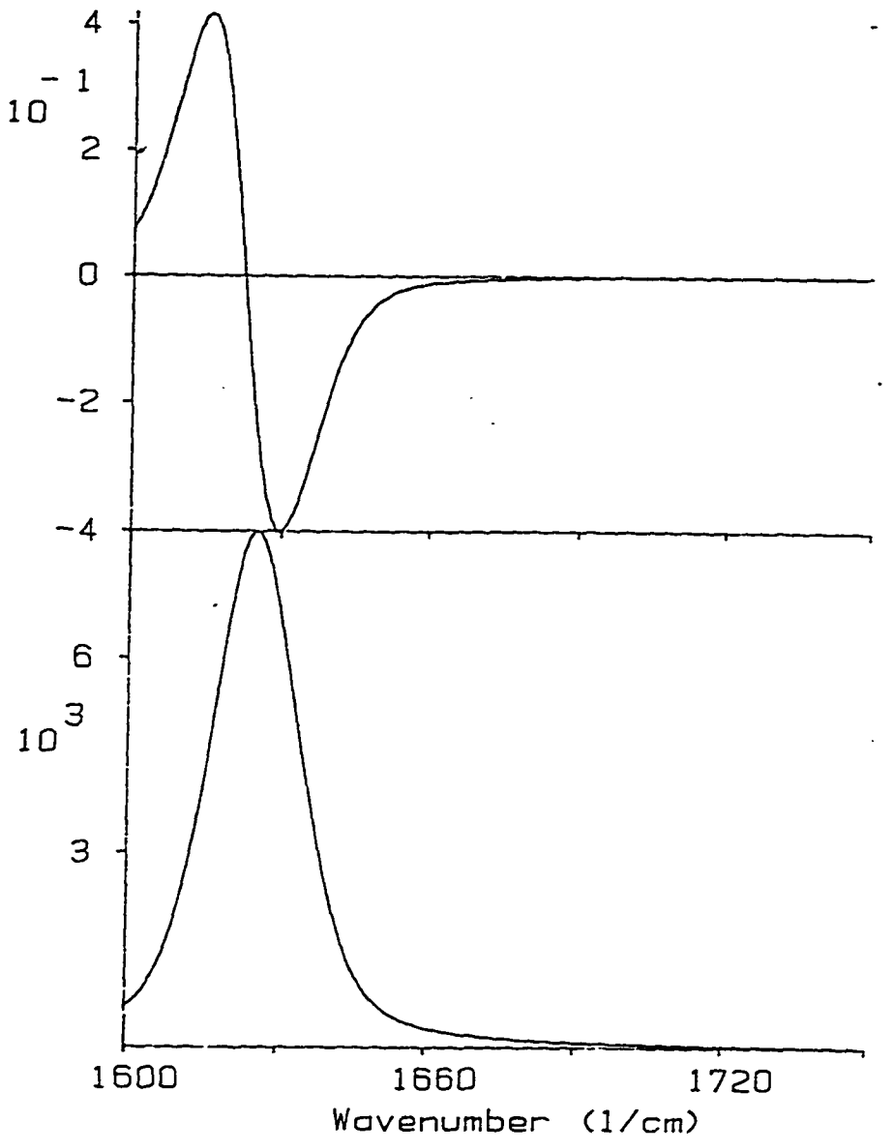

Figure 13. Calculated of gramicidin crystal from x-ray crytallographic data [95].
L-amino acid; ϕ = -127 D-amino acid; ϕ = 154
ψ = 146 ψ = -126

DISCUSSION

Our results are consistent with (and support) several other conformational studies of gramicidin in organic solvents and DMPC model membranes [60]. X-ray crystallographic studies of gramicidin have shown that gramicidin adopts different conformations in the presence and absence of DMPC. Moreover, it was suggested that gramicidin is present as the ion channel conformer when it associates with DMPC vesicles. These studies were spawned by the observations that gramicidin in "solution" adopts different conformers in the presence of DMPC. Hence, it became of interest to determine its crystal structure in the presence and absence of DMPC. It was suggested that gramicidin crystals formed with lipid may represent its conformation in organic solvent, whereas that formed with DMPC may represent its conformation in vesicles. One indication that the crystals without DMPC reflect the conformation in organic solvent is that crystals formed in the same manner with ions present are non-isomorphous[43,48], suggesting that they undergo a substantial change when they bind ions. Our results here are to a great extent in line with these findings, although we did not study the conformation of gramicidin with ions in organic solvents. Nonetheless, our results show that gramicidin adopts different conformers in pyridine and in DMPC in the presence of Na_2HPO_4 or K_2HPO_4 buffer.

Urry et al. [79] in 1972 were able to show with CD that gramicidin A occurs in a left-handed helical conformation in trifluoroethanol(TFE). Their findings have basis in the observation of a marked hypochroism and a circular dichroism with positive bands at 224 nm and 212 nm and a negative band at 194 nm. Earlier, it was mentioned that Bouchard et al. demonstrated with FTIR that gramicidin (when cosolubilize with TFE), incorporates into DMPC as a $\beta^{6.3}$-helix [1]. Combining the findings of these two groups one may infer that gramicidin forms a left-handed $\beta^{6.3}$-helix in DMPC. In support of this inference, our VCD spectra indicate the presence of an extended helical structure of gramicidin in the phospholipid bilayer system. The features of these spectra resemble those described for right-handed helical peptides in chloroform solutions [88,89,90], which is an experimental

condition different from ours. In fact such discrepancy should be expected, because these are two chemically different environments. Chloroform is a highly polar solvent, while the the interior of the DMPC bilayer is nonpolar. Bouchard et al. [1] and several other studies have demonstrated that GA does infact exist in contrasting conformations depending on the polarity of its environment (solvents or lipids). For example, GA assumes a random coil configuration when dissolved in DMSO. Although the data are not presented here, we were unable to observe a defined VCD spectra of GA in DMSO. This observation can be explained by the large dipole moments of this polar solvent, which inhibit the formation of intramolecular and intra-dimeric hydrogen bond, that are essential for the establishment of an ordered structure. Ordered structures have been observed in less polar solvents, such as methanol, ethanol and dioxane. Thus it appears that GA has extensive hydrogen bonding while in chloroform, which induced a right-handedness. Whereas, in TFE these hydrogen bonds are arranged differently and GA adopts a left-handed structure. Therefore, upon incorporation into DMPC (a nonopolar milieu) from TFE, a left-handed structure is maintained. Furthermore, hydrophobic interactions between the GA side groups within the bilayer are large enough to stabilize the handedness that was present in the TFE solution. A straight forward observation that may strengthen this latter assertion will be to observe GA conformation in a solvent of lesser polarity and confirm any conformational change that may take place. This is exactly what we did with the GA-pyrimidine study. Here, our findings contrast with the GA conformation indicated in the bilayer system, and it appears to be a non-extended left handed helical structure.

It is general knowledge that gramicidin behaves differently in organic solvents and lipid systems [2,60] because its conformation is solvent-dependent [60, 79]. Hence, it is known to adopt different conformations depending on the property of a particular organic solvent. Bouchard et al.[1] showed that gramicidin adopts $\beta^{6.3}$-helix conformer only in TFE, but not in methanol/chloroform (1:1 V/V), and ethanol. In addition, Urry et al., [79] employed NMR to show that gramicidin adopts different conformers in TFE and in DMSO. Therefore, our findings in this study are again in line with previous findings (fig. 3-4). Figure 3-4 suggests that gramicidin in pyridine adopts a left-handed helical

structure. Most importantly that this structure is not an extended helical conformer and that no ions are present suggests that the VCD spectra represents a GA channel that is functionally not conducting ions..

Comparison of fig. 3-4 with either fig. 3-5 or fig. 3-6 reveals another difference, apart from the inverted VCD signals. There appears to be a monosignate peak located above the minor (shoulder) peak of its ir absorption. If this peak is to be accepted as a VCD signal rather than instrumental noise, then it will be consistent with the signal of β-sheet same as a study of model polypeptide film [88] in the amide II region. Or, it is simply a spectral pattern characteristic of extended helical structures. Hence, our results seem to suggest that VCD is suitable for detecting more than one conformational motif, even in a lipid bilayer. As mentioned earlier, gramicidin is proposed to be a β-sheet that is rolled into a helical conformation [Urry 79], and many studies have supported this view [2].

A great many structural models have been described for GA, and consequently a wide array of torsional angles have been reported for its backbone configuration. Some of these were used for our computed structures. Of these only the torsional angles reported by Wallace and Ravikumar [49] and Langs [50] fits both our calculated and experimental data for GA-DMPC and pyrimidine solvated GA, respectively. Wallace and Ravikumar specified ϕ,ψ angles for L- and D-residues as -149,114 and 84,-89, respectively. From Lang those angles are ϕ,ψ = -152, 110 for L-residues, and for D-residues as ϕ,ψ = -101, 142. Thus, we proposed that GA is present in DMPC as an extended left-helical structure, whereas it is not as extended in pyridine, though it has identical handedness. This fits the functional configuration of GA, which is believed to be extended as it conducts ions. A critical point to note here is that there is plenty of Na^+ and K^+ in the buffer solutions within which our GA-DMPC studies were conducted. Thus, one can safely assume that the GA channel was conducting ions as these we investigated this system, and for this reason it was present in the extended conformation as opposed to when it was solvated in pyridine.

It is well accepted that the membrane-bound channel conformation is a pair of double helical structure arranged in a head to head fashion. Based on our computed data

alone, we are unable to reach such a conclusion. All of torsional angles used in our calculation as proposed by the studies above did not produce any fit to our results. Torsional angles from Lotz et al. [95] and Chandraskan and coworkers [94] generated VCD spectra that are incompatible with our observed spectra, though these workers had predicted right-handed helices. Moreover, Teng et al. [96] determined backbone torsion angles for the Ala3 of GA that is embedded in DMPC, by obtaining data for both the Gly2-Ala3 and Ala3-Leu4 peptide linkages via solid state NMR spectroscopy. They specified a pair of torsion angles for the Ala3; ϕ,ψ = -129, 153 and -129, 122, and concluded that these are consistent with a right-handed β-helix. However, implementation of these angles to calculate a VCD spectra, using ECO formalism, yielded a spectrum that is ascribed to left-handed helical structures. In addition, these also differ from our experimental data. Thus, it seems that the ECO formalism may at times predict structures that are different from the experimental result. The reason for this is not clear at the moment, except that this formalism is extremely sensitive to conformational angles, such that a slight deviation from the true values may lead to a prediction that is totally different from the observed.

Therefore, from this study we have provided experimental data, which are the first of this kind. Our data suggest that gramicidin is present in pyridine (a polar solvent), as a left-handed helical strucure. That this strucure is a dimer, and that is of a particular dimension (e.g. $\beta^{6.3}$ arranged in an head-to-head fashion) was inferred from other empirical and calculated determinations from ir studies from other laboratories that are comparable to our experimental conditions [36,61,64,65]. Also we are able to support this claim with our calculated data.

In addition, we are proposing that GA is present in the lipid bilayer as an extended left-handed helical dimer. From this, combined with the findings of Bouchard et al. [1], we infer that this dimer is arranged in a head-to-head configuration. Though not substantiated by ECO formalism, other studies support this interpretation. Worth noting, however, is that the calculated spectra generated from cation-complexed x-ray data (fig 7)

show GA to be present in the extended form, while that generated from uncomplexed data (fig 8) exhibit a simple left-handed helix.

CONCLUSION

From this study we are able to reach three important conclusions regarding the secondary structure of gramicidin in pyridine solution and in buffered DMPC, by applying VCD spectroscopic technique. First, our absorption spectrum of GA in pyridine resembles that obtained in ethanol from a study conducted by Sychev et al [61]. They concluded that GA exists mostly as a left handed, intertwined double helical structure with 5.6 residues per turn. We attribute the VCD spectrum in Fig. 4 to this structure. Our observation is supported by the VCD spectrum (fig. 8) computed from the torsional angles obtained from the crystallographic study by Langs [50], in which he concluded that GA was present as an antiparallel left handed, double helical structure, with 5.6 residues per turn. The GA crystals used in that study were grown from ethanolic solution similar to that used by Sychev and coworkers. Although pyridine is not as polar as ethanol, it is capable of forming hydrogen bonds with GA molecules. Such interactions are sufficient to induce conformations similar to that observed in ethanolic solution. Hence, we conclude that GA exists in pyridine as the intertwined antiparallel left handed, $\beta^{5.6}$-helix.

Secondly, the VCD spectrum of GA in a DMPC bilayer (figs. 5 and 6) suggests an extended, left handed, dimeric conformer that is arranged in a head-to-head configuration, which we interpreted as the $\beta^{6.3}$-helix. The $\beta^{6.3}$-helix has 6.3 residues per turn and is stabilized by intra- and intermolecular hydrogen bonds. Our interpretation agrees with the study by Bouchard et al. [1] and several others [34,35,37]. We were able to reproduce the FTIR spectrum of GA in DMPC, that was reported by Bouchard et al. [1], and our observed IR absorption spectrum in Figs. 5 and 6 resemble theirs. In addition, the calculated VCD spectrum in Fig. 7 provides the only fit to our experimental result. Dihedral angles used for the computation were obtained from a study by Wallace and Ravikumar [49]. In that study, GA was complexed with Cs^+ ion. They described the GA-Cs^+ crystal as a left handed, helical structure. Put in perspective, the GA-Cs^+ crystal chemical environment is similar to that of GA-DMPC complex in that these structures were bathed in monovalent cations, that are known to have affinity for GA ion channel.

We believe that the spectra shown in Figs. 5, 6 and the calculated spectrum in figure 7 are indicative of the left handed, head-to-head $\beta^{6.3}$ helix.

Finally, we have also shown that the DECO formalism is a very sensitive computational method. This fact is demonstrated in Figs 10 through 13. In these figures the zero crossings and peak maxima of the calculated VCD spectra are shifted to lower frequency and they are not in agreement with any of our experimental results. During our previous studies in chapter 2, we observed that simply changing the dihedral angles by as little as a few degrees is sufficient to reverse the pattern of a computed VCD couplet. Although DECO is a very sensitive formalism, it has its limitations. This is because this formalism only considers the dipole-dipole coupling, whereas in reality factors such as vibrational coupling of interacting dipoles (via the vibrational force fields) do have effects on the intensities of IR and VCD of experimental spectra. This can result in calculated intensities that are different from the observed.

In summary, our VCD spectra data suggest that GA, when co-solubilized with TFE, is inserted into DMPC bilayer as a left handed, extended $\beta^{6.3}$-helix, and that it adopts a left-handed intertwined $\beta^{5.6}$-helix in pyridine. Both of these structures are consistent with functional configurations of GA. The $\beta^{6.3}$ dimers are believed to undergo local extension as they conduct ions through the lipid bilyer. Thus, the spectra reported here for $\beta^{6.3}$-helix may well represent the saturated GA channels in the DMPC bilayer, as Na^+ and K^+ ions are conducted through them. Such a structure should be expected to be in an extended conformation. On the other hand, the pyridine solution is void of ions. Therefore, GA is not extended, but is simply a left handed, antiparallel double stranded $\beta^{5.6}$-helix. In the light of this discussion our results suggest that VCD is a tool with a potential for elucidation of different secondary conformations of defined polypeptides. Such conformations may be indicative of their chemical environment.

APPENDIX.

PROTOCOL FOR DMPC/GRAMICIDIN PREPARATION

1. In 1 mL of 2, 2, 2-trifluoroethanol, dissolve DMPC/gramicidin in 5:11 molar ratio (100mg DMPC/54mg gramicidin).
2. Incubate samples at 52 degrees centigrade for 4h. Intermittently shake the solution on a vortex several times during the incubation.
3. Evaporate the solvent by speedvac followed by lyophilization
4. Hydrate the sample with 2mL of 100mM sodium bisphosphate or potassium biphosphate (7.0pH) buffer prepared in D_2O.
5. Warm solution to 52° C and cool to 20°C. Vortex on the way up (50°C) and on the down (20°C).
6. Step 5 was repeated several times.
7. Obtain FTIR and VCD.

REFERENCE [1]

1. Bouchard, M. and Auger, M., 1993. Solvent History Dependence of Gramicidin-Lipid Interactions: A Raman and Infrared Spectroscopic Study. *Biophys. J.* 65:2484-2492.

Table 2-1
Dipole-Dipole Coupling Energies for [Poly-tyrosine]$_8$
phi angle = 52, psi angle = 53

V_{ij}	i = i	i = i+1	i = i+2	i = i+3	i = i+4	i = i+5	i = i+6	i = i+7
j = 1		14.2	-3.1	-11	-5.1	-1.8	-1.5	-1.2
j = 2			14.1	-3.1	-11	-5.1	-1.8	-1.5
j = 3				14.2	-3.1	-11	-5.1	-1.8
j = 4					14.2	-3.1	-11	-5.1
j = 5						14.2	-3.1	-11
j = 6							14.2	-3.1
j = 7								14.2
j = 8								

Table 2-2
Frequency, Intensity and Rotational Strength of Dipole Oscillators of theTyrosine Residues

Oscillator Number	Frequency cm^{-1}	Intensity $[esu\ cm]^2 \times 10^{38}$	Rotational Strength $[esu\ cm]^2 \times 10^{42}$
1	1685.27	0.028	0.129
2	1684.54	0.003	0.36
3	1661	1.639	-1.236
4	1652.42	85.821	14.504
5	1637.76	31.434	-4.971
6	1628.94	0.539	-2.53
7	1625.44	0.88	-4.741
8	1624.63	0.243	-1.19

Table 3-1

Dipole-dipole Coupling Energies (cm^{-1}) for Gramicidin Crystal From X-ray Crystallographic Data.
L-amino acid; phi angle = -149, psi angle = 114
D-amino acid; phi angle = 84, psi angle = -89

V_{ij}	i = i	i = i+1	i = i+2	i = i+3	i = i+4	i = i+5	i = i+6	i = i+7	i = i+8	i = i+9	i = i+10	i = i+11	i = i+12	i = i+13	i = i+14
j = 1		12.3	4.36	5.19	-2.77	-55.7	-5.33	-2.42	-2.86	-1.66	2.95	-0.5	-0.66	-0.6	0.4
j = 2			12.24	5.09	2.59	3.24	7.56	1.03	-0.46	0.01	0.38	0.64	-0.11	-0.11	-0.19
j = 3				14	3.44	3	2.13	2.42	-0.09	0.49	-0.07	0.34	0.108	0.19	-0.18
j = 4					12.24	5.09	2.59	3.24	7.56	1.03	-0.45	0.01	0.38	0.64	-0.11
j = 5						14	3.44	2.99	2.13	2.42	-0.1	0.47	-0.7	0.34	0.11
j = 6							12.24	5.09	2.59	3.24	7.56	1.03	-0.46	0.01	0.38
j = 7								14	3.44	3.99	2.13	2.42	-0.1	0.5	-0.07
j = 8									12.24	5.09	2.456	3.24	7.56	1.03	-0.46
j = 9										14.04	3.44	2.99	2.13	2.42	-0.1
j = 10											12.24	5.09	2.59	3.24	7.56
j = 11												14	3.44	2.99	2.13
j = 12													12.24	5.09	2.59
j = 13														14.04	0.44
j = 14															12.24
j = 15															

Table 3-2
Frequency Intensity and Rotational Strength of the Dipole Oscillators

Oscillator Number	Frequency cm^{-1}	Intensity $[esu\ cm]^2 \times 10^{38}$	Rotational Strength $[esu\ cm]^2 \times 10^{42}$
1	1715.7	21.05	-18.36
2	1691.19	11.28	7
3	1679.95	4.75	-4.42
4	1662.92	2.1	2.13
5	1656.93	92.99	94.43
6	1656.4	63.05	3.8
7	1652	14.39	-82.45
8	1645.01	22.89	24.27
9	1639.37	2.76	-22.81
10	1635.87	3.34	-5.97
11	1635.56	2.41	-3.43
12	1632.47	1.26	-6.94
13	1630.9	0.41	1.5
14	1625.98	15.85	0.61
15	1589.75	24.1	0.64

Table 3-3

Dipole-dipole Coupling Energies (cm^{-1}) for Gramicidin Crystal From X-ray Crystallographic Data.
L-amino acid; phi angle = -152, psi angle = 110
D-amino acid; phi angle = -101, psi angle = -142

V_{ij}	i = i	i = i+1	i = i+2	i = i+3	i = i+4	i = i+5	i = i+6	i =i+7	i = i+8	i = i+9	i = i+10	i = i+11	i = i+12	i = i+13	i = i+14
j = 1		2.8939	-1.4445	-4561	-0.0435	-0.2037	-0.063	-0.1049	0.0895	0.0162	-0.0156	0.0304	-0.0288	-0.0045	-0.0039
j = 2			3.6876	-3.3181	0.8737	-0.0655	0.2656	0.1316	0.0439	0.1038	-0.0197	0.0362	-0.003	0.0078	0.0077
j = 3				2.991	1.1991	0.6884	-0.0151	0.1558	-0.0471	-0.0125	0.2878	-0.0256	0.0341	0.0105	0.0021
j = 4					1.9515	0.8718	-0.3276	-0.2487	0.0238	-0.1531	0.775	-0.131	0.0011	0.0207	-0.0253
j = 5						2.9913	1.1992	0.6884	-0.0151	0.1558	-0.0471	-0.0125	0.0288	-0.0236	0.0341
j = 6							1.9515	0.8718	-0.3276	-0.2487	0.0238	-0.1531	0.0775	-0.0131	0.0011
j = 7								2.9914	1.1992	0.6884	-0.0151	0.1558	-0.0471	-0.0125	0.0288
j = 8									1.9512	0.8718	-0.3276	-0.2487	0.0238	-0.1531	0.0775
j = 9										2.9915	1.1991	0.6884	-0.0151	0.1558	-0.0471
j = 10											1.9514	0.8718	-0.3276	-0.2487	0.0238
j = 11												2.9913	1.1992	0.6884	-0.0151
j = 12													1.9515	0.8718	-0.2376
j = 13														2.9914	1.1992
j = 14															1.9514
j = 15															

Table 3-4
Frequency Intensity and Rotational Strength of the Dipole Oscillators

Oscillator Number	Frequency cm-1	Intensity [esu cm]2 x 10^{38}	Rotational Strength [esu cm]^2 x 10^{48}
1	1632.99	2.28	-9.68
2	1632.19	17.71	-98.59
3	1631.05	49.92	7.55
4	1630.42	15.2	35.53
5	1628.93	19.29	113.53
6	1627.16	3.26	-37.19
7	1625.91	9.99	58.55
8	1625.02	13.99	-71.27
9	1624.05	4.82	46
10	1623.17	19.91	-19.73
11	1622.79	31.91	-69.18
12	1622.75	21.66	60.77
13	1622.72	2.95	38.18
14	1622.33	8.69	-42.12
15	1618.45	6.78	-11.72

BIBLIOGRAPHY

CHAPTER ONE

1. F. Arago, Mém. Classe Sci. Math. Phys. Inst. Impér. France 12I, 93 (1811) (publ. 1812).
2. J. B. Biot, Ann. Chim. Physique (2) 4, 90 (1817); Mém. Acad. Roy. Sci. Inst. France (2), 2, 41 (1817) (publ. (1819).
3. L. Pasteur, Ann. Chim. Physique (3) 24, 442 (1848) (3) 28, 56 (1850); C. R. hebd. Séances Acad. Sci. 28, 477 (1849); 29, 297 (1849).
4. J. A. Le Bel, Bull. Soc. chim. France (2) 22, 337 (1874).
5. J. H. van't Hoff, Bull. Soc. chim. France (2) 23, 295 (1875).
6. W. Klyne, in "Determination of Organic Structures by Physical Methods," by E. A. Braude and F. C. Nachol. Academic Press, New York 1955.
7. K. Freudenber, Ber. dtsch. chem. Ges, 66, 177 (1933).
8. S. Bernstein, W. J. Kauzmann, and E. S. Wallis, J. org. Chemistry 6, 319 (1941).
9. J. H. Brewster, J. Amer. chem. Soc.. 81, 5475 (1959).
10. W. Kauzmann, F. B. Clough, and I. Tobias, Tetrahedron 13, 57 (1961).
11. E. Fischer, Ber, dtsch. chem. Ges. 24, 2683 (1891).
12. W. Kuhn, Z. physik. Chem. B 31, 23 (1936).
13. J. M. Bijvoet, A. F. Peerderman, and A. J. van Bommel, Nature (London) 168, 271 (1951).
14. J. B. Biot, Ann. Chim. Physique, 59, 206 (1860).
15. A. Cotton, Ann. Chim. Physique 8, 347 (1896).
16. cf. P. A. Levene and A. Rothen, in "Organic Chemistry," by H. Gilman, John Wiley, New York 1938, vol. 2, p. 1799.
17. H. Rudolph, J. opt. Soc. America 45, 50 (1955).
18. O. C. Rudolph and Sons, constructor, Caldwell, N. J.; M. Billardon and J. Badoz, C. R. hebd. Séances acad. Sci. 248, 2466 (1959); M. Grosjean, A. Lacam, and M. Legrand, Bull. Soc. chim. France 1959, 1495.

19. C. Djerassi, "Optical Rotary Dispersion,"McGraw Hill, New York 1960.
20. cf. W. Kuhn, Annual Rev. physic. Chem 9, 417 (1958).
21. M. Grosjean, and M. Legrand, C. R. hebd. Séances Acad. Sci. 251, 2150 (1960).
22. J. P. Mathieu, "Les Théories Moléculaires du Pouvoir Rotatoire Natural," Gauthier-Villars, Paris 1946.
23. J. G. Kirkwood, J. chem. Physics 5, 479 (1937).
24. W. Moffitt and A. Moscowitz, J. chem. Physics 30, 648 (1959).
25. Biot, J.-B., Mem. de l'Inst. 13, part 1, 218 (1812).
26. Arago, D.F.J., Mem. de l'Inst. 12, part 1, 93 (1811).
27. Biot, J.-B., Me. de l'Inst. 2:41, 136 (1817).
28. Haidinger, W., Ann. Phys. 70, 531 (1847).
29. Pasteur, L., Ann. Chim. 24, 457 (1848).
30. Cotton, A., Compt. Rend. 120, 989, 1044 (1895).
31. Kuhn, W., Trans, Faraday Soc. 26, 293 (1930).
32. Moffitt, W., Woodward, R.B., Moscowitz, A., Klyne, W., and Djerassi, C., J. Amer. Chem. Soc. 83, 4013 (1961).
33. Landau, L.D., Lifshitz, E.M., and Pitaevskii, L.P., "Electrodynamics of Continuous Media," Pergamon Press (1984).
34. Barron, L.D., "Molcular Light Scattering and Optical Activity," Cambridge (1982), and references therein.
35. Diem, M., "Analytical Applications of Circular Dichroism," (Purdie, N. and Brittain, eds.) 1994, vol. 14, chapter 4.
36. Greenfield, N. & Fasman, G.D. (1969) Biochemistry 8, 4108-4116.
37. Tiffany, M.L. & Krimm, S. (1968) Biopolymers 6, 1379-1382.
38. Tiffany, M.L. & Krimm, S. (1969) Biopolymers 8, 347-359.
39. Krimm, S. & Mark, J.E. (1968) Proc. Natl. Acad. Sci. USA 60, 1122-1129.
40. Hiltner, W.A., Hopfiner, A.J. & Walton, A.G. (1972) J. Am. Chem. Soc. 94, 4324.
41. Ruegg, M., Metzger, V.& Susi, H. (1975) Biopolymers 14, 1465-1471.
42. Lippert, J.L., Tyminski, D. & Desmeules, P.J. (1975) J. Am. Chem. Soc. 98, 7075

43. Peticolas, W.L., Cutrera, T., Rodgers, G.R. (1980) in Biomolecular Structure, Conformation, Function and Evolution, Vol. 2, Srinivasan, R., Ed., Pergamon Press, New York, pp. 45.
44. Williams, R.W. & Dunker, A.K. (1981) J. Mol. Biol. 152, 783-813.
45. Susi, H. & Byler, D.M. (1983) Biochem. Biophys. Res. Comm. 115, 391-397.
46. Yang, W.J., Griffiths, P.R., Byler, D.M. & Susi, H. (1985) Appl. Spectrosc. 39, 282.
47. Byler, D.M. & Susi, M. (1986) Biopolymers 25, 469-487.
48. Davies, M., Doctoral Dissertation, 1987, C.U.N.Y.
49. a) Holzwarth, G., Hsu, E.C., Mosher, H.S., et al., J. Amer. Chem. Soc. 96 (1974)
51. b) Faulkner, T.R., Moscowitz, A., Holzwarth, G., et al., J. Amer. Chem. Soc. 96 (1974) 252.
52. Nafie, L.A., Cheng, J.C. and Stephens, P.J., J. Amer. Chem. Soc. 97 (1975) 3842.
53. Snir, J., Frankel, R.A. and Schellman, J.A., Biopolymers, 14 (1975) 173.
54. Velluz, L., Legrand, M. and Grosjean, M., Optical Circular Dichroism: Principles, Measurements and Applications, Verlag Chemie - Academic Press New York (1986).
55. Cadwell, J.D., and Erying, H.,: The Theory Optical Activity; Wiley -Interscience, New-york, London, Sydney, Toronto, 1971.

CHAPTER TWO

1. Creighton, T. E. (1984) *Proteins: Structures and Molecular Principles*, W. H. Freeman and Co., New York.
2. Deutsche, C. W., & Moscowitz, A. (1968) *J. Chem. Phys. 49*, 3257.
3. Deutsche, C. W., & Moscowitz, A. (1970) *J. Chem. Phys. 53*, 2630.
4. Dickerson, R. F., & Geis, I. (1969) *The Structure and Action of Proteins*, Harper & Row, Publishers, New York.
5. Diem, M., Roberts, G. M., Lee, O., & Barlow, A. (1988) *Appl. Spectrosc. 42*, 20.

6. Dukor, R. K., & Keiderling, T. A., (1991) *J. Pept. Protein Res.* 38(3), 198-203.
7. Greenfield, N. J., & Fasman, G. D. (1969) *Biochemistry 8*, 4108.
8. Gulotta, M., Goss, D. J., & Diem, M. (1989) *Biopolymers 28*, 2047.
9. Holzwarth, G., & Doty, P. (1965) *J. Am. Chem. Soc. 87*, 218.
10. Keiderling, T. A. (1990) in *Practical Fourier Transform Infrared Spectroscopy*, pp 203-283, Academic Press, New York,
11. Lee, O., Roberts, G. M., & Diem, M. (1989) *Biopolymers 29*, 1759.
12. Lipp, E. D., & Nafie, L. A. (1985) *Biopolymers 24*, 799.
13. Miyazawa, T., & Blout, E. R. (1961) *J. Am. Chem. Soc. 83*, 712.
14. Moore, W. H., & Krimm, S. (1976) *Biopolymers 15*, 2439.
15. Paterlini, G. M., Freedman, T. B., & Nafie, L. A. (1986) *Biopolymers 25*, 1751.
16. Roberts, G. M., Lee, O., Calienni, J., & Diem, M. (1988) *J. Am. Chem. Soc. 110*, 1749.
17. Schellman, J. (1973) *J. Chem. Phys. 58*, 2882.
18. Schellman, J., & Becktel, W. J. (1983) *Biopolymers 22*, 171.
19. Schulz, G. E., & Schirmer, R. H. (1979) *Principles of Protein Structure* (Cantor, C.R., Ed.) Springer-Verlag, New York.
20. Sengupta, P. K., & Krimm, S. (1987) *Biopolymers 26*, S99.
21. Snir, J., Frankel, R. A., & Schellman, J. A. (1975) *Biopolymers 14*, 173.
22. Still, C. (1989) MacroModel Version 2.5, Columbia University, New York.
23. Tiffany, M. L., & Krimm, S. (1968) *Biopolymers 6*, 1379.
24. Tinoco, I. (1963) *Radiat. Res. 20*, 133.
25. Wen, K. J., & Woody, R. W. (1975) *Biopolymers 14*, 1827.
26. Yasui, S. C., & Keiderling, T. A. (1986a) *Biopolymers 25*, 5.
27. Yasui, S. C., & Keiderling, T. A. (1986b) *J. Am. Chem. Soc. 108*, 5576.
28. Zhong, W., Gulotta, M., Goss, D. J., & Diem, M. (1990) *Biochemistry 29*, 7485.
29. Chen, X.G., Bormmet, Lemmon, R., Asher, S.A., Diem, M.: Proceedings of the 13th international conference on Raman spectroscopy, Wurzburg, Germany, 1992; 88

CHAPTER THREE

1. Bouchard, M. and Auger, M., (1993) Biophys. J., 65: 2484-2494.
2. Killian, J. A. (1992) Biochim. Biophys. Acta., 1113: 391-425.
3. Voet, E. and Voet, G. V. (1990), by John Wiley and Sons, Inc., (Chapter 18).
4. LoGrasso, P., Moll III and Gross, T., (1988) Biophys. J. 54: 259-267.
5. Killian, J. Prassad, K., et al., (1988b) Biochim. Biophys. Acta. 943: 535-540.
6. Wallace, B. A. (1983) Biopolymers. 22: 397-402.
7. Urry, D. W. (1984) Proc. Natl. Acad. Sci. USA 68: 1907-1911.
8. Tournois, H., Killian, J., et al., (1987) Biochim. Biophys. Acta. 905: 222-226.
9. Lee, D, Durrani, A. and Chapman (1984) Biochim. Biophys. Acta. 769: 49-56.
11. Naik, V. M. and Krimm, S. (1986) Biophys. J. 49: 1131-1154.
12. Davies, M., Baruner, H., et al. (1990) Biophys. Res. Commun. 168: 85-90.
13. Lipmann, F. (1971) Science 173: 875-884.
14. Lipmann, F. (1980) Adv. Microb. Phys. 21: 227-266.
15. Kurahashi, K, (1981) in Antibiotics IV (Corcoran, J. W., ed.) pp. 325-352, Springer Verlag, New York.
16. Akashi, K. and Kurahashi, K. (1977) Biochem. Biophys. Res. Commun. 77: 259-267.
17. Kubota, K. (1987) Biochem. Biophys. Res. Commun. 144: 203-209.
18. Kemp, G., Jacobson, K. A., and Wenner, C. E. (1972) Biochemi. Biophys. Acta 255: 493-501.
19. Ristow, H., Pschorn, W., et al. (1979) Nature 280: 165-166.
20. Hold, J. G. (ed.) (1984) in Berley's manual of systemic bacteriology, pp. 356-374, Williams and Wilkens, London.
21. Koeppe, II.R.E., Paczkowski, J. A. and Whaley, W. L. (1985) Biochemistry 24,: 2822-2826.
22. Young, M. and Mandelstam, J. (1979) Adv. Microbiol. Physiol. 20, 103-162.
23. Demain, A. L. and Piret, J. M. (1979) Proc. FEBS Meet. 55: 183-188.
24. Ristow, H. , C=Schazschneider, B., Bauer, K., et al. (1975) Biochim. Biophys. Acta